

Politecnico di Torino

École polytechnique fédérale de Lausanne

Master Course in Civil Engineering



EPFL

Master Thesis:

Life Cycle Assessment of Maillart's Bridges

Giulia Pirro

Professors:

C. Fivet and C. De Wolf

Supervisor:

R. Ceravolo

Academic Year 2018/2019

Abstract

Robert Maillart's contribution to the community of civil engineers and, most of all, his crucial role in the evolution of the structural art are undeniable. He was able to merge not only mechanical efficiency with innovative solutions but also aesthetic expression as a real artist, always balancing his choices with limited resources both in terms of construction materials and costs.

Following these three key parameters he succeeded in producing structures which can be considered a very good combination of structural performance and sustainability. The actual goal is to understand to what extent Maillart's bridges are indeed sustainable in addition to be efficient and elegant. That is why performing a Life Cycle Assessment (LCA) of his bridges is a valid quantitative confirmation of his achievements. The followed procedure is, thus, based on the computation of construction materials volumes. Starting from the original drawings [1], elaborating them as 3D model, the contribution of concrete and steel is computed. Then, the volume of masonry is also calculated and, where present, the timber for the scaffolding. The goal is to compute the Global Warming Potential (GWP) of each bridge, to normalise them per deck area and to be able to compare them according to different strategies. The amount of equivalent carbon dioxide ($\text{kg CO}_2\text{e}$) is computed as a linear combination of each structural material quantity (SMQ) with a relative Embodied Carbon Coefficient (ECC) [2].

Moreover, considering their structural scheme, their foundation soils and all the geometrical parameters of the decks and arches, it is possible to gather different bridges and to find relationships according to the similarities of emissions of each class. The main results are found in the structural and soil properties. First, in the correlation between GWP only due to steel with respect to the total one of each bridge and the amount of steel for each static scheme. Then, in the average values among two macro groups of terrains which make the bridges to assume similar GWPs within these macro classes themselves.

Summary

ABSTRACT	2
SUMMARY.....	3
NOTATIONS.....	5
INTRODUCTION	6
Motivations	6
Problem statement	6
Life Cycle Assessment.....	7
Literature Review	9
Maillart's legacy.....	11
CATALOGUE: MAILLART'S BRIDGES	19
Stauffacher Bridge.....	27
Zuoz Bridge.....	30
Steinach Bridge	34
Tavanasa Bridge	38
Aarburg Bridge.....	42
Marignier Bridge	46
Flienglibach Bridge	49
Ziggenbach Bridge.....	53
Schrärbach Bridge.....	56
Lorraine Bridge	60
Salginatobel Bridge	64
Schwandbach Bridge	68
Felsegg Bridge.....	72
Birs Bridge	75
Vessy Bridge	79
PARALLEL CATALOGUE: NON MAILLART'S BRIDGES	82
Langwieser Bridge by Schürch	82

Tamina Bridge by LAP	85
ANALYSIS.....	88
Elaboration of data.....	88
Maillart vs other engineers	107
GWP compared with car emissions and trees	109
CONCLUSIONS.....	114
APPENDIX	119
INDEXES.....	122
Tables.....	122
Figures	124
Equations.....	127
REFERENCES	128

Notations

ECC	–	Embodied Carbon Coefficient
CO ₂	–	Carbon dioxide
CO ₂ e	–	Equivalent Carbon dioxide
GHG	–	Greenhouse Gases
GWP	–	Global Warming Potential
KBOB	–	Coordination Conference of the Building and Property Organs of Public Builders. Translated form the German acronym of “Koordinationskonferenz der Bau - und Liegenschaftsorgane der öffentlichen Bauherren”
LCA	–	Life Cycle Assessment
LCI	–	Life Cycle Inventory
LCIA	–	Life Cycle Impact Assessment
SMQ	–	Structural Material Quantity

Introduction

Motivations

When it comes to bridges, it is always difficult to distinguish the structural and the architectural role of engineering. Their philosophical and social meaning increase their importance and could give them additional symbolic significance. However, the great innovations rise in the combinations of the two aspects in the discipline of structural art: Maillart was one example of that and a prove that a single professional role who is able to merge these two sides, gave more results than the application of the ideas of two separates mind.

His work was the expression of the pure essence of engineering seen as the making of things that did not previously exist. As a designer he succeeded in seeing forms as the means of controlling the forces of nature. Following simple principles, he gave birth to unprecedented visual power, he increased material efficiency, and decreased cost for construction and maintenance [3]: his structures are a very clever synthesis of all the requirements fulfilled by a “good” structure: economy of material, cost-saving efficiency, a well-conceived procedure for construction and remarkable durability over time [4]. Thus, the additional meaning to this research, is to check if his qualities as engineer could also be an inspiration for sustainable engineering through life cycle assessment (LCA). In fact, this method allows to calculate the environmental impact of buildings.

Problem statement

The numerical goal of the master project is to compute the Global Warming Potential (GWP) of 15 different bridges designed by Robert Maillart and compare them according to environmental footprint. Looking at his structures, it is undeniable that his bridges are among the most efficient in the world, thus performing an LCA represents the possibility to quantify this awareness and to prove it quantitatively. The use of a minimal amount of materials and costs, as well as a maximum aesthetic expression possible are the three key aspects in order to achieve the necessary balance within not only a “good” structure in engineering terms, but also a sustainable one in environmental terms. That is why the analysis is not confined only to his bridges, but it is also extended to two other bridges designed by different engineers. These extra structures are able to give additional support to the thesis above-mentioned, starting from their differences with Maillart's bridges. In fact, they turn out to be counter examples in terms of sustainability. The first one (Langwieser Bridge) was designed in the same period of Maillart's work and therefore built with the same technological, theoretical and computational tools he had. The second one (Tamina Bridge) was designed in 2017 with present tools and different technological conditions, but the same materials of construction. The comparison with 15 Maillart bridges is, indeed, an opportunity to understand his qualities as engineer with respect to other people.

Life Cycle Assessment

The first important aspect is defining LCA and the scopes for which it is used. There are many different parts which could be included in LCA, but the considered one, used in this project is related to the calculation of the Global Warming Potential (GWP). The present interest is just the computation of the environmental impact of a structure in terms of emissions of harmful gases during its entire life, including the production and construction stage, the operating one and the end of life. In fact, according to the definitions of International Standards [5], this part of LCA leads to an evaluation of the environmental impact of a product system, starting from the evaluation of the inputs and the outputs. It is a method which considers the whole product's life cycle in order to understand the environmental aspects and potential environmental aspects. That is why it is possible to define it as a cradle-to-grave model. All stages of life are taken into account: raw material acquisition, production, use, end-of-life treatment, recycling and final disposal. Moreover, in the same standards [5], the process is divided into 4 steps:

1. the goal and scope definition phase,
2. the inventory analysis phase,
3. the impact assessment phase, and
4. the interpretation phase.

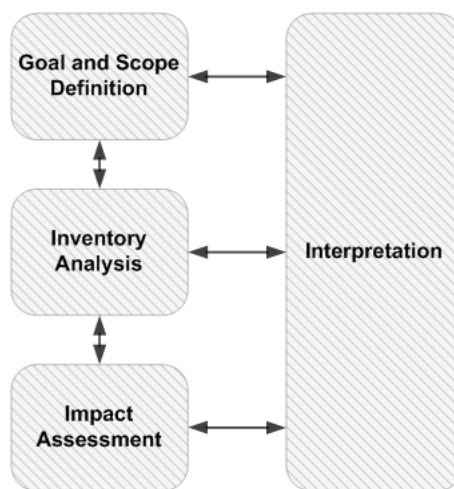


Figure 1. Steps of LCA [5]

The first phase which is the scope includes system boundary and level of detail. The depth of LCA can differ considerably depending on the goal of an LCA. The second phase, so the life cycle inventory (LCI) analysis phase is an inventory of input/output data with regards to the system being studied. It involves the collection of the data necessary to meet the goals of the defined study. The life cycle impact assessment (LCIA) phase is the third phase of the LCA. Its purpose is to provide additional information to help assess a product system's LCI results and to better understand their environmental significance. Life cycle interpretation is the final phase of the LCA procedure. It consists in the summary and discussion of the results of the LCI and the LCIA.

It is the basis for conclusions, recommendations and decision-making in accordance with the goal and scope definition [5] .

According to the aim of the entire project, the first aspect is to find reliable values which express the effective environmental impact of each structure and, more particularly, the embodied carbon emissions. The embodied carbon corresponds to the emitted greenhouse gas (GHG) related to the embodied energy of a physical entity and to the carbon it emits or absorbs during non-operational life stages, expressed in carbon dioxide equivalents (CO₂e) [6]. The cradle-to-gate embodied energy, on the other hand, is the quantity of energy required by all activities associated with the production of a material. So, there is an important difference between the embodied energy and the embodied carbon: the first one is thus measured in joule and it considers the energy needed from extracting the material to the final manufacture of the product. The second one is measured in kilograms of carbon dioxide equivalent and it takes into account the fuel used while the material is being processed, but also the carbon emitted and/or absorbed during that phase [7]. In this sense, it is possible to use the following formula, since it offers a simple method to achieve the goal of calculating the cradle-to-gate emissions of bridges.

$$GWP = \sum_{i=1}^n ECC_i \cdot SMQ_i$$

Equation 1. Cradle-to-gate GWP [8]

Where

GWP = Global Warming Potential (kg of CO₂e)

ECC = Embodied Carbon Coefficient (kg of CO₂e per kg of material)

SMQ = Structural Material Quantity (kg)

The formula gives directly the kg of CO₂e by multiplying each structural material quantity (SMQ in kg of material) with the corresponding embodied carbon coefficient (ECC in kg of CO₂e per kg of material). Through these only two key variables, excluding the operational emissions, the GWP of a structure can be directly computed [8]. So, the needed quantities are masses and coefficients. While the masses have to be extracted from plans or bills of quantities, the coefficients can be found in databases. The coefficients are expressed as kg of carbon dioxide equivalent per kg of materials and they are related to a cradle-to-gate process of the material so from its production to its extinction. Moreover, it is necessary to underline that CO₂ is only one of the six main greenhouses limited by the Kyoto protocol, but for simplicity the mass of each gas emitted is translated into its equivalent in carbon dioxide. In this way the total impact can be expressed in one number, also often called the carbon footprint. The GWP was indeed developed to allow comparisons of the global warming impacts of different gases. Specifically, it is a measure of how much energy the emissions of 1 ton

of a gas will absorb over a given period of time, relative to the emissions of 1 ton of carbon dioxide (CO₂). The time period usually used for GWPs is 100 years [9]. GWPs provide a common unit of measure, which allows analysts to add up emissions estimates of different gases (e.g. to compile a national GHG inventory) and allows policymakers to compare emissions reduction opportunities across sectors and gases. CO₂, by definition, has a GWP of 1 regardless of the time period used, because it is the gas being used as the reference [9].

Starting from this theoretical definition, it is also necessary to specify some differences which are performed in the present analysis. The first aspect to highlight is the assumption related to the ECC. As mentioned before, these coefficients are taken from specific databases, but they are related to the present time. Thus, the computational process leads to a value which corresponds to the embodied carbon of the bridge if the bridge itself would have been built today. So, the CO_{2e} is not the actual embodied carbon of the bridge, effectively produced for its construction in the 20th century.

Therefore, another aspect to underline is the fact that the final computed values of GWP of different bridges cannot be compared as they are. In fact, each structure is different from the others, so it is essential to perform a normalisation procedure in order to make the data comparable. In particular, each LCA is done by studying a unit. This unit is the result of the normalisation itself, performed according to different geometric parameters, in this case: deck surface, span, rise, length and width.

Literature Review

Unfortunately, it is not common to perform LCAs in bridges. Some interesting literature about it is summarised in the second chapter of Dequidt's thesis [10] and in Du's doctoral thesis [11].

In the first mentioned thesis, the described documents are the followings:

1. C. Zhang. *Environmental evaluation of FRP in UK highway bridge deck replacement applications based on a comparative LCA study* [12];
2. J. Hammervold et al. *Environmental life-cycle assessment of bridges* [13];
3. Z. Lounis et al. *Towards sustainable design of highway bridges* [14];
4. L. Bouhaya, L. Le Roy, and A. Feraille-Fresnet. *Simplified environmental study on innovative bridge structure* [15];
5. H. Gervásio and L.S. Da Silva. *Comparative life-cycle analysis of steel-concrete composite bridges* [16];
6. D. Collings. *An environmental comparison of bridge forms* [17];
7. MEEDDM. *Analyse du cycle de vie d'un pont en béton* [18];
8. K. Steele. *Environmental sustainability for bridge management* [19];

9. G. A. Keoleian, A. Kendall, J. E. Dettling, V. M. Smith, R. F. Chandler, M.D. Lepech, and V. C. Li. *Life cycle modelling of concrete bridge design: Comparison of engineered cementitious composite link slabs and conventional steel expansion joints* [20];
10. Martin. *Concrete bridges in sustainable development* [21];
11. Y. Itoh et al. *Using CO₂ emission quantities in bridge life cycle analysis* [22];
12. Horvath et al. *Steel versus steel-reinforced concrete bridges: Environmental assessment* [23];
13. J. Widman. *Environmental impact assessment of steel bridges* [24].

These articles and papers are related to 45 different bridges with several construction materials (concrete, steel, steel-concrete composite, wood and bricks) and different situations. The values of GWP are distinguished if related only to deck replacement or to the entire bridge. The conclusion given in the thesis is that material production is the most polluting life cycle phase, followed by maintenance, transportation distances and traffic disruption. The author focuses also on the fact that timber and concrete offer relative environmentally performing solutions, compared to steel and steel-concrete composite alternatives, so it is highlighted the importance of material design and construction methods improvement.

In the second above-mentioned doctoral thesis [11] the goal is to highlight that the environmental performance can be influenced by different designs of bridges. It underlines also that LCAs have the potential to help the process of decisions between different options to select the most environmentally optimal design. So, the literature review is focused on identifying the major structural and life-cycle scenario contributors.

1. G. Du, M. Safi, L. Pettersson, R. Karoumi. *Life cycle assessment as a decision support tool for bridge procurement: environmental impact comparison among five design proposal* [25];
2. M. Safi, G. Du, R. Karoumi and H. Sundquist. *Holistic approach to sustainable bridge procurement considering LCC, LCA, User-cost and Aesthetics* [26];
3. G. Du, L. Pettersson and R. Karoumi. *Life cycle environmental impact of two commonly used short span bridges in Sweden* [27];
4. G. Du and R. Karoumi. *Environmental life cycle assessment comparison between two bridge types: reinforced concrete bridge and steel composite bridge* [28];
5. G. Du and R. Karoumi. *Environmental comparison of two bridge alternative designs* [29];
6. G. Du. A literature review of life cycle assessment for bridge infrastructure [30].

However, apart from those two collections of references, the current practice is more focused on buildings than infrastructures. Moreover, current bridges are mainly designed from an economic, technical, and safety point of way, while considerations of their environmental performance are rarely integrated into designing process [11]. Even if for buildings it is not common at all, some additional problems make the analysis of infrastructures even rarer. The difficulty is created by two main reasons: the first one is that bridges have almost null emissions during the operational phase, as opposed to most buildings. Plus, they create a shorter path for cars or vehicles, so they reduce other kinds of emissions which are very not straightforward to quantify [7].

Maillart's legacy



Figure 2. Schwandbach Bridge [31]



Figure 3. Salginatobel Bridge's scaffolding [31]

The innovations of Maillart's design procedures and theories cover lots of different disciplines. His approach and his way of thinking about bridges is not only from a single point of view but within a holistic prospective.

The first aspect that must be considered is the constraints that he had to face: his bridges were public structures, and so he was forced to set his ideas within a public landscape. The second special condition for Maillart's work was his exclusive commitment to concrete. These two aspects required a balance among many conflicting objectives. Maillart strove for minimum use of materials and for minimum cost. Thus, he gradually developed a distinctive style: light, straight, and exposed, with few curves, and a minimum of decoration [32]. Moreover, Maillart frequently argued in favour of reinforced concrete for structures in Switzerland since all that was

needed was to transport cement and steel reinforcement on site where gravel, sand, water and wood for scaffolding were already present.

But thinking about the general legacy it is possible to say that Maillart's great contribution to bridge design was that, while he kept within the traditional discipline of engineering, he continually played with the forms in order to achieve maximum aesthetic expression [3].

However, what makes his work different can be found also in the comparison with the present method of bridges design. A classical design procedure today based on structural analysis would not therefore naturally result in his forms. Contemporary engineers assume that if a structure cannot be rigorously analysed, then it cannot be built [33]. However, Maillart's methods contrast greatly with this method discovered by calculation for designing structures [34]. He did not compute his bridges analytically by checking them and optimising them, but he almost only used graphic statics. For example, it is possible to observe that there is very little chance that such an analytically based design process could lead to a structure where the role of a stiffening member is played by the deck while the arch remains thin. Therefore, it is perhaps lucky that the kind of analytical tools suitable for an analysis like this were not available for Maillart. Even though saying that, means that something wrong is related to his way of design, the opposite is indeed true: his methods permitted him to optimise his design as much as possible, to maximise the savings in materials, to reduce building costs and to achieve very long-lasting structures. It will not be difficult to prove that the longer a structure's life, the greater the savings in terms of resources and costs and so, the more sustainable the design has been. A clear structural behaviour is one of the best ways to achieve both reliability and sustainability [4].

Influences

During Maillart's education it is possible to find different personalities who influenced his future works. The first one was given by **Carl Culmann** who brought to Zürich, in 1855, the idea that structural calculations could be made graphically. He is considered the founder of graphic statics. Thanks to his legacy Maillart learnt at ETH the habit of connecting force diagram to design forms, since he attended lectures with the direct successors of him [35]. In fact, the courses on building construction was under the architect **Benjamin Recordon** who was Maillart's professor. Starting from his theories, Maillart was able to develop an innovative approach to use graphical tools, different from his teachers: in the two successive editions of Karl Culmann's founding treaty graphic statics is primarily conceived as the central tool of mechanical analysis for structures. But structural analysis mainly takes place when all the geometric features of the structure have already been done. For Maillart, it becomes a design tool in the sense that it helps define the geometry (morphogenesis) at a very early stage [36]. Another great lesson was taught by **Wilhelm Ritter** who influenced Maillart during all his life especially as the technical foundation of deck-stiffened arches, is to a large extent, the work of Ritter. Moreover, he unceasingly confronted his students with the fact that the creation of structures is both an aesthetic and a scientific enterprise [3]. Then, Wilhelm Ritter anticipated the creation of a course on reinforced concrete by giving his students a basic grounding in it. A similar merit can be found in **von Emperger** who

explained exactly the behaviour of Maillart's three-hinged bridges. When cracks in concrete occurred, the cracked sections can rotate, as if they had hinges. This is why building three hinges into a concrete arch would eliminate the cracking by allowing the arch to expand or contract freely under temperature changes or small settlements in the foundations, without adding any stresses to the materials [32].

Graphic Statics

One of the most important aspects making Maillart a great and innovative engineer, not stuck in the tradition but always looking for progress, is his revolutionary design method: he thought that it was necessary the bridge calculations employed elementary mathematics with no calculations at all [32]. In fact, he always tried to use approximations or simplified structural mechanisms and combined them as tools to achieve a structural typology. The simplicity of the mathematical model gives him the freedom and opportunity to minimise costs, to integrate parts of the work together with the same aim and consider the various aspects of the design without getting caught up in analytical complexity to resolve the problem. The reduction of costs differentiates his structures from those of other engineers [4].

He achieved this innovative technique through the application of graphic statics from the perspective of morphogenesis, since from what it is currently known no one had ever done anything similar before him. His use of graphic statics was to create forms and considering parameters such as geometrical patterns, the status of the materials and the structural consequences of deformations under stress in some of his structures. As already mentioned in his education he was trained to use graphic statics to analyse bridges, so he perfectly knew the power of this tool. Therefore, this approach goes beyond Culmann and Ritter's conception of graphic statics as a science intended for structural analysis because it became a method used to actually draw the bridge [35]. Maillart went further by using analogical methods to set out the structural scheme of load bearing using graphic statics. In this perspective, the tool becomes a tool of morphogenesis instead of an analytical one.

Graphic statics have been used as a heuristic method for morphogenesis and as a powerful tool for equilibrating the structure with the aim of placing materials in the right position within a structural system. The material is not used in places where it is superfluous but only placed along the loads' paths. The concrete is mainly used in compression, sometimes in traction, and only bent incidentally. Since concrete works best in compression the system is very efficient and his structures very economical. Since it was also used as an assembly method, it made the structures as efficient as possible. Moreover, there is no doubt about the behaviour of the whole structure since it has been drawn to fulfil a given structural behaviour. All this serves to make the structure reliable [34]. The challenge in the geometrical organisation of concrete is to equilibrate the stresses. If the material is placed around the thrust lines, it is indeed possible to manage the group of possible thrust lines depending on various loading cases. A well-designed concrete geometry avoids tensile stresses and guarantees relatively long-lasting structures [37]. Maillart was thinking in terms of struts and ties, considering especially concrete as struts. However, if concrete is primarily considered as a material to be placed along the loading path in compression it means that it remains a kind of moulded stone. That is why reinforcement steel are

essential to be placed along the traction path. Their combination is a kind of strut-and-tie design long before the term existed [34]. Graphic statics as a morphogenesis tool still holds a promising future. Depending on the considered material, choosing correctly to put them only in traction or in compression makes them as most efficient as possible. Maillart's graphic methods for geometrical definition could help to design a durable and reliable structure with advantages comparable to contemporary goals of sustainable design.

Efficiency, elegance and economy

However, he was not only innovative merely as a structural engineer, he revolutionised also the relationship between the artistic aspect of the structure and its mechanical properties. Maillart was much more than just an aesthetic visionary. He was a modern figure and a talented engineer, who showed that bridges could be pure expressions of the engineering ideals – cost and efficiency – while remaining works of art [38]. For the first comparison and the most explicitly quantitative, that of efficiency, Maillart use two measures: one the “boldness ratio” and the other the amount of concrete. The boldness ratio expresses the flatness of the arch, that is the ratio of span squared over rise. The flatter the arch, the smaller the rise and hence the bolder the design. But in the modern structuring of an environment, efficiency and elegance are merely aspects of the same design seen from the perspectives of science and of art; and that the essence of engineering lies in the integration of the two by the connecting link of economy. Maillart's primary concerns were efficiency of materials, safety of the entire system, and the endurance against the environment. But each of these measurable qualities had to meet a dual requirement which is cost. Thus, these three aspects of bridge design that would guide his own work: the empirical proof of efficiency by load test, the social ethic of minimum cost, and the visual elegance possible in efficient and economical design [32]. Artistic sensitivity, broad construction experience and deep technical proficiency. In the modern art of structural engineering, these three qualities must go hand in hand. From one point of view, he won design and construction contracts because his structures were reasonably priced but on the other hand because Maillart paid so much attention to the appearance of his bridges, he saw no need for the input of an architect to complete his designs [33] even without advanced techniques Maillart's bridges, by virtue of their lightness and panoramic settings, are in many cases considered works of structural art. The origin of his behaviour is found in his education: as already mentioned he studied under Wilhelm Ritter (1847-1906), who instilled in him the idea that engineers are not simply the stewards of the technical aspect of construction but also hold responsibility for the aesthetic manifestation of a structure. Maillart's holistic approach to bridge design – the combination of structural efficiency, economy and visual impact – was the inspiration for his work. He showed that an engineer should never consider these criteria mutually exclusive, and to balance them properly is to create works of structural art [38]. Therefore, Maillart resolved the conflict between minimum materials and minimum cost by designing forms in which the construction procedure permitted very light scaffolding. The bottom curved slab become not only an integral part of the final hollow-box arch, but also a part of the construction support for the vertical walls and horizontal roadway. In this way, the scaffold needed to carry only the thin arch, which was slightly less than 30 percent of the total concrete dead weight. Thus, by making the lower slab as light as possible. Maillart significantly

reduced the scaffolding, which is a major part of construction cost [32]. While not every bridge built by Maillart is a masterpiece, it is the evolution and the visible progress in his ideals that is exemplary. He was always critical of his work, continually refining his designs to improve both their structural efficiency and aesthetic impact.

Shapes with concrete

The last, but not less important factor that must be considered is that Maillart had a deep understanding of the working of concrete depending on the way in which it was loaded so he was able to use reinforced concrete into new, appropriated and innovative forms [35]. Concrete is a complex material, but, even without a deep theoretical knowledge, Robert Maillart used his own formulas. Furthermore, designing is not calculating, and it was not common then to theorise about the form that concrete structures should have in order to respect the intrinsic characteristics of the behaviour of this material which was not well known. While many of his contemporaries supported the idea that reinforced concrete structures should simply mirror the characteristically heavy masonry designs of the past, Maillart believed that the shape of a structure and its ability to carry loads carrying are directly linked to the material [33]. The dominant science of structures was the theory of elasticity. It led to the development of systems to secure the resistance of concrete beams, as shown by Hennebique's system involving the development of steel reinforcing stirrups. The technology suggested by Hennebique came from empirical observations and from translating wood, metal or masonry technologies into concrete executions. But Robert Maillart produced a series of remarkable bridges that are not easy to interpret as a collection of beams, columns and arches. He realised that the use of concrete would necessitate both a structural and aesthetic departure from masonry arch bridges. The leading principle was always to meet requirements concerning structural efficiency and reliability and to meet the need to build with geometrical rules they are as simple as possible [37]. Maillart's fundamental idea was that the structure should be liberated from mathematical analysis; but, at the same time it should be disciplined by the results of physical testing and visual observation. The ideas continue to guide Maillart, and can be summarized in three principles: first, structural strength is derived from form rather than from materials. Second, field and test experience take priority over theoretical and mathematical analysis. Third, maximum quality goes together with minimum materials. When Maillart expressed for the first time a coherent set of ideas about structural design he said that: theory is dangerous, numbers are merely guides, codes are restrictive, full-scale testing is crucial, and safety can be guaranteed. His basic idea was that reinforced concrete is so unpredictable that only from direct observation of the material in action can good designs result.

Structural schemes of bridges

The combination of the previous mentioned aspects of Maillart's legacy are at the base to understand his design ideas. His structures are, indeed, the combination of all the influences received during his education, and his will to peruse the principles of efficiency, elegance and economy. Even if Maillart's ideas on analysis remained

constant, his ideas on design continuously evolved. Among all of his bridges two major ideas had taken shape over the previous third of a century in his career as a structural engineer: the deck-stiffened idea and the three-hinged idea [32]. However, apart from these two main classes it can be also found that there are other two additional families. Every of these is described below [37].

1) **Three-hinged arch bridges and massive classical arch bridges**

Maillart's three-hinged bridges and massive classical bridges are the translation of masonry bridges into concrete ones. They are the heirs of massive masonry bridges where the dead load is dominant and live loads are almost disregarded. Where the bridge dead loads were from heavy solid stone, and the live loads were from people, horse carts, and snow, the dead load determined from making. In fact, published documents give no indication that Maillart considered the live loads in the derivation of his structural forms for any of his bridges built between 1899 and 1913 [32].

In these kinds of bridges thrust lines are used to define the average geometry. When it comes to the final geometry arrangement, arcs of a circle and eventually parabolas were chosen to match the average geometry itself [37]. As far as this structural scheme is concerned it is possible to say also that the series of three hinges enabled the trajectories of thrust lines to be defined according to the distribution of bending stresses. They will be largest in the midway between the hinges (at the quarter spans), and zero at the springing and crown because the hinges allow free rotation without any stresses due to bending. Therefore, to reduce live load bending stresses, the designer needs to increase the arch section towards the quarter spans [32]. Thus, for the series of Maillart's early three-hinged arch bridges designed in the spirit of heavy masonry bridges the arch becomes thinnest around the hinges and thickens further away from them. Moreover, relying on regular geometry such as the circle or parabola even if they had no relation to a funicular configuration, simplified evaluations of load distributions enabling thrust lines to be drawn. That is why the arch of a massive arch made of concrete is mostly an arch of a circle [37]. Loadings also indicate the geometries to be given to the hinges. Initially, lead sheets served as hinges. From the Salginatobel Bridge the system of concrete hinges was made from crossing bars [35].

With the evolution of his artistic experience Maillart's later bridges change much, up to a point in which they are only composed of straight lines, but before this final stage, in his later three-hinged works he started to increase the importance of live loads which leads to bigger widths and height of the arch, except around the hinges. Moreover, the connection between both curves of each half-bridge were broken and the form slightly ogival. The geometrical rule remains the same: two arcs of a circle with increasing radii while getting close to the support or straight lines [37]. Tavanasa Bridge led eventually to a series of three-hinged arch bridges that today are works of art [39].

2) **Deck arch bridges and deck-stiffened arch bridges**

Deck arch-bridges (both stiffened and not) are the translation of inverted suspension bridges into a concrete arrangement. They are the complementary association of a funicular arch with a rigid deck fulfilling the role of a stiffening girder for the arch. This is the perfect inversion of the principles of a

suspension bridge, as suggested by W. Ritter [34]. A significant portion of the bending moments due to traffic loads may be assigned to the stiff deck beam but the essence of his method lay in a first assumption that the arch does not bend under live load. More precisely, Maillart assumed that the arch stresses due to live-load bending were so small that they could be neglected. Therefore, the stiffening girder carried all the live-load bending. The second assumption was that this girder bending had to be numerically equal to that which the arch would have had to take were it unstiffened. Under these two assumptions, Maillart made a structural analysis to determine the forces in both the arch and the girder. Finally, on the basis of that analysis, he computed both the concrete compression stresses in the arch and the reinforcing steel required in the girder [32]. The reference loading case remained dead loads in which the funicular arch supports permanent loads by compression only, and a rigid deck acting as a girder, is against live loads. So, the geometrical issue of the middle line is simplified since there is a specific device supposed to sustain bending forces caused by variations induced by live loads [37]. The whole deck section, including the parapet walls, would act as a stiff beam. When it is integrated with the rest of the structure it reduces the bending forces in the arch, allowing it to be much thinner and lighter. Maillart's approach was to superimpose elementary structural mechanisms to build the complete structural response for the final arrangement. However, he ignored the interactions between various elements [35]. In the case of his stiffened arch bridges, geometrical considerations lead almost to a regular thickness in the whole trajectory of the thrust line even if there was always a considerable freedom in selecting geometrical and stiffness parameters [37]. Those bridges can even be divided in straight or curved deck-stiffened arch bridges. In particular, with his curved deck-stiffened arch form, Maillart once again proved the forefront of his profession by elegantly solving the problem of how to combine curved roads with bridges [38].

In the present time for short and medium-span bridges, frame systems are typically more suitable than deck-stiffened arches. While, appropriately modified, arch systems still offer interesting opportunities for long-span curved bridges and post-tensioning of the deck beam. They, indeed, permit an increase in the spacing of columns or cross walls [40].

3) **Continuous girder bridges**

The continuous girder bridges come from situations where the span is viewed as a beam [37]. This case is typical for the railway structures and for his last designed bridges. Maillart, in the last period of his career, stopped, indeed, to design arch bridges to experiment his theories in straight bridges. For them, the only possible structural schemes are the present and the following one. Both lead to a correct distribution of the loads. In fact, the traffic and dead loads are not transferred to the soil through the arch but through straight columns which support the girder bridge. This also means that the span must be rigid and hard enough to bear properly these loads.

4) **Rigid Frame Bridges**

In this structural scheme the deck acts like a continuous beam but the structural behaviour remains practically independent of the geometry [37]. In medium-span bridges very stiff response to live loads

can be achieved by longitudinally fixing the ends of the deck beam. This technique improves response to anti symmetric loads too. In long-span bridges end supports are fixed, and the deck and arch are appropriately connected at midspan. Moreover, it is possible also to use a frame system with inclined columns, somewhat like Ziggensbach Bridge. The frame system responds to live loads in a similar way as the deck-stiffened arch [40].

Catalogue: Maillart's bridges

Description

The first part starts with description of each bridge, a brief analysis of the history and of the design process that lead Maillart to specific choices. The structures are analysed in a chronological order. This part also aims to underline the innovations and the differences of each specific structure with respect to the previous ones.

The initial part contains also all the necessary properties used to understand the structural behaviour of the bridge. In particular, it is reported the structural scheme which can be distinguished as follows:

Structural classification:

- Three hinged arches
- Massive Classical Arch bridges
- Deck arch bridges
- Deck-Stiffened arch bridges
- Rigid frame bridges
- Continuous girder bridges

Then all the geometrical properties are defined:

Geometrical properties:

- Span
- Length
- Width
- Rise
- Ratio between Span and Ratio

Finally, the foundation soil is reported in order to understand the kind of foundations used.

Environmental aspects:

- Foundation soil

The described classification is also useful for the computational process and so to understand if there is a correlation between specific aspects of the structures (as the ones reported above) and the GWP. The data about the foundation soil is found in the Swiss geotechnical map [41]. There, it is possible to find a legend in which every colour is associated with a different kind of soil. The French version of it, is reported below.

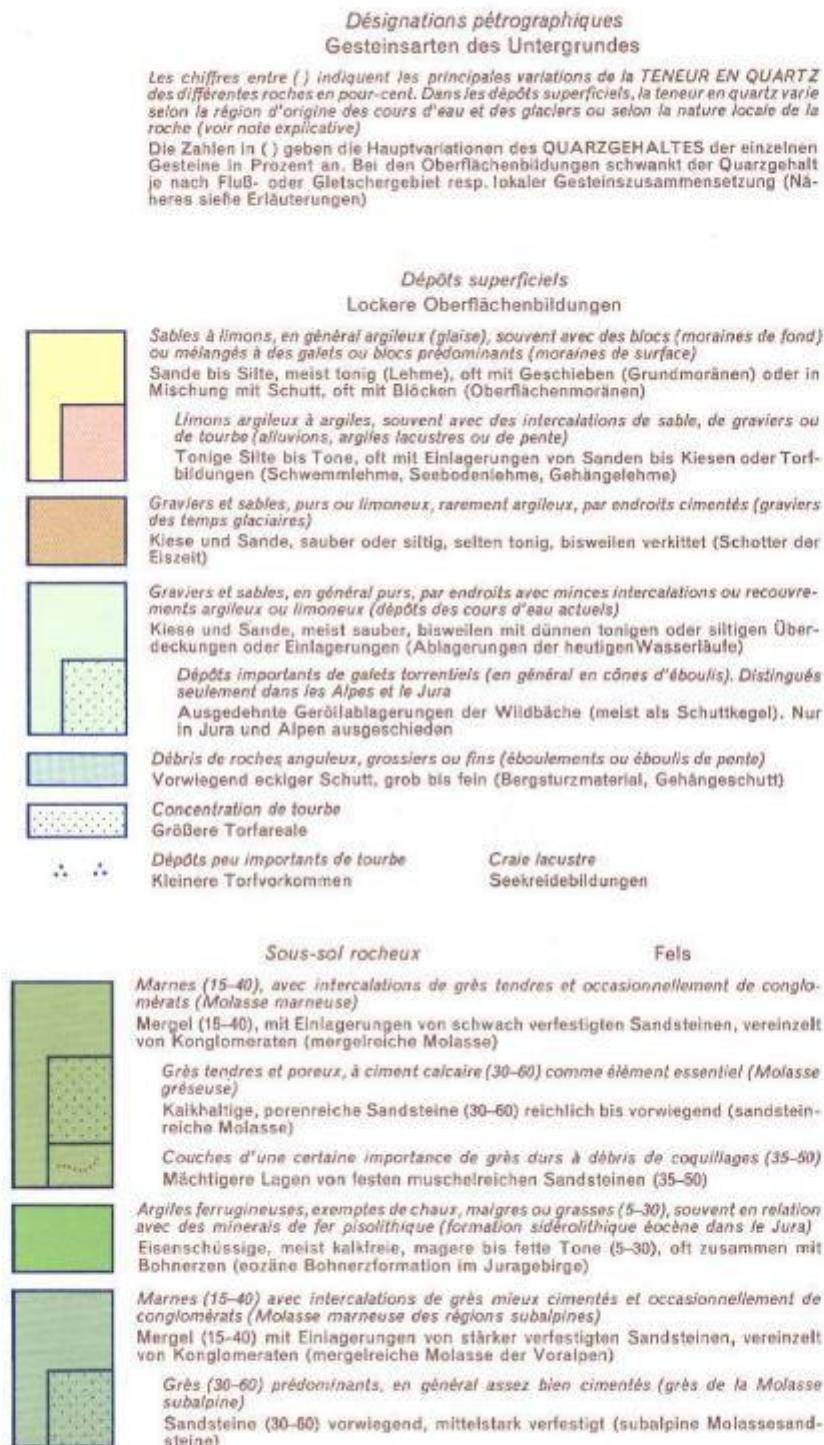


Figure 4. Legend of the geotechnical map of Switzerland, page 1 [41]



Figure 5. Legend of the geotechnical map of Switzerland, page 2 [41]

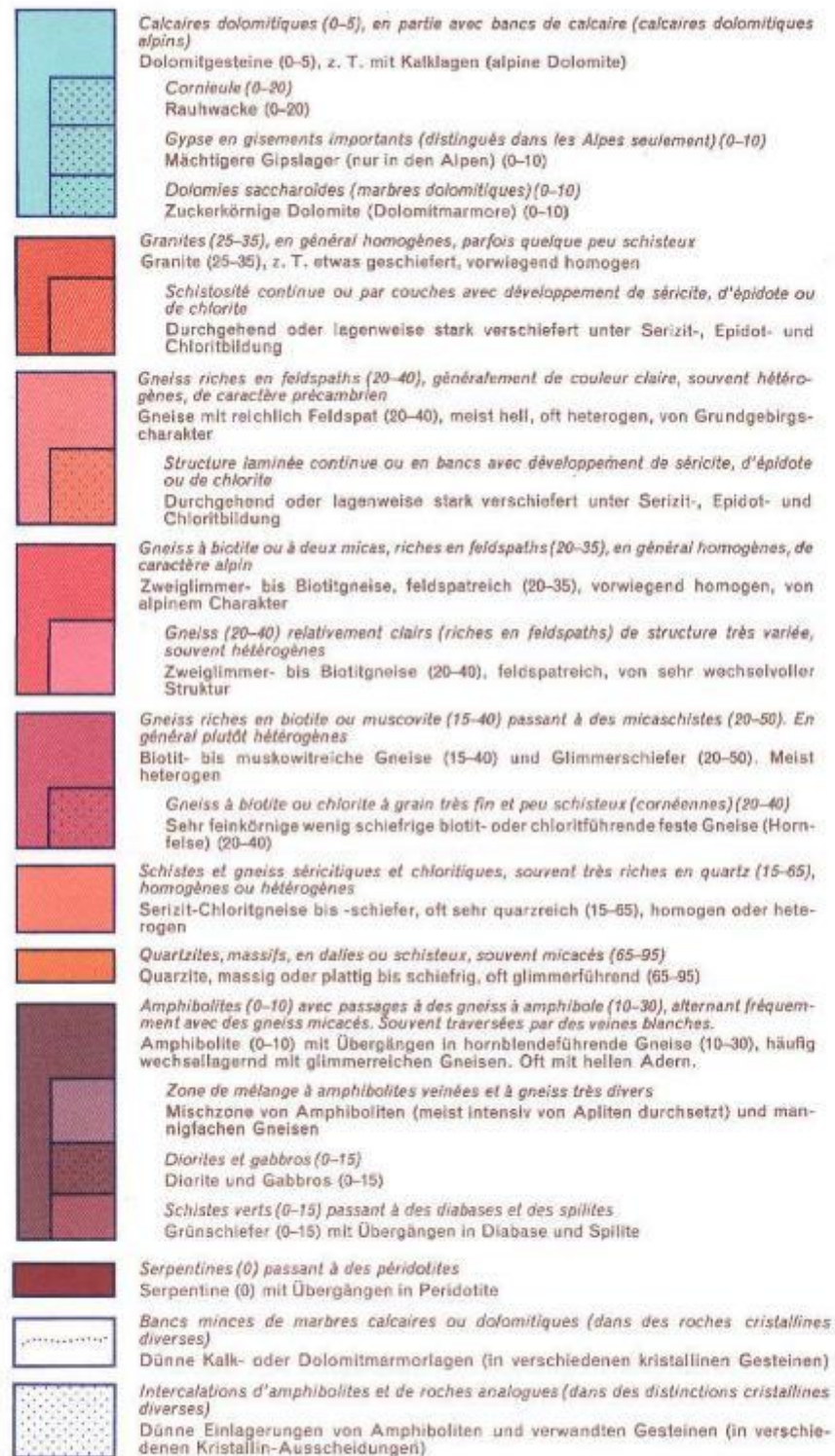


Figure 6. Legend of the geotechnical map of Switzerland, page 3 [41]

Signes	Zeichen
	<i>Les signes sont remplis pour les exploitations de pierre, d'argile, de gravier et de sable d'une certaine importance (p. ex. extraction mécanique, installation fixe de concassage ou de traitement)</i> Für Steinbrüche, Ton-, Kies- und Sandgewinnung Zeichen gefüllt: bedeutendere Anlagen (z. B. mit Schotterwerk, Aufbereitung, wesentlicherem Abbau usw.)
○	<i>Gravières et sablières dans des dépôts de gravier et dans des moraines</i> Kies- und Sandgruben in Schottern und in Moränen
●●●●●	<i>Concentration de gravières</i> Kiesgrubenareale
○	<i>Exploitations de gravier et de sable dans des cours d'eau et des lacs (petits points: exploitation sans station fixe)</i> Kies- und Sandgewinnung aus Gewässern (kleine Punkte: Areal in Seen)
◇	<i>Exploitations de matériaux d'éboulis et d'éboulements</i> Abbau von Gehängeschutt und Bergsturzmaterial
△	<i>Carrières pour pierres brutes ou concassées</i> Steinbrüche für Bruchsteine und Schotter
▽	<i>Carrières de pierre dure pour l'empierrement des routes et des chemins de fer</i> Steinbrüche in Hartgestein für Straße und Bahn
▽	<i>Production importante de pavés (pour routes et pour caniveaux)</i> Wichtige Erzeugung von Pflaster- und Schalensteinen
△	<i>Carrières fournissant principalement de la pierre de taille et de sculpture</i> Steinbrüche für Hausteinzwecke und Bildhauerei
◇	<i>Exploitations d'ardoise</i> Gewinnung von Dach- und Tafelschiefer
◇	<i>Exploitations de dalles</i> Gewinnung von Platten
^	<i>Carrières bien connues de pierre de taille et d'ardoise abandonnées</i> Bekanntere aufgelassene Haustein- und Schieferausbeutungen
x	<i>Gisements de tufs calcaires (en général exploitations abandonnées)</i> Vorkommen von Kalktuff (meist früher ausgebeutet)
▽	<i>Gisements de pierre ollaire</i> Vorkommen von Ofen- (Gilt-) Stein
□	<i>Extraction de glaise et d'argile pour tuileries</i> Gewinnung von Ton (Mergel, Lehm) für Ziegelei
⊥	<i>Tuileries</i> Ziegeleien
▽	<i>Extraction de roche pour la fabrication de ciment</i> Gewinnung von Gestein für Zementfabrikation
⏏	<i>Usines de ciment</i> Zementfabriken
△	<i>Exploitations de gypse (plâtrières)</i> Ausbeutung von Gipsstein
T	<i>Fabrication de produits en plâtre</i> Fabrikation von Gipsprodukten
x	<i>Affleurements peu importants de roches gypseuses</i> Kleinere Aufschlüsse in Gipsstein
◇	<i>Exploitation de roche destinée à l'industrie chimique et à la métallurgie</i> Gewinnung von Gestein für chemische Industrie und Metallurgie
□	<i>Exploitation de quartz filonien</i> Gewinnung von Gangquarz
◇	<i>Exploitation de roche pour la fabrication d'engrais</i> Gewinnung von Gestein für Düngzwecke

Figure 7. Legend of the geotechnical map of Switzerland, page 4 [41]

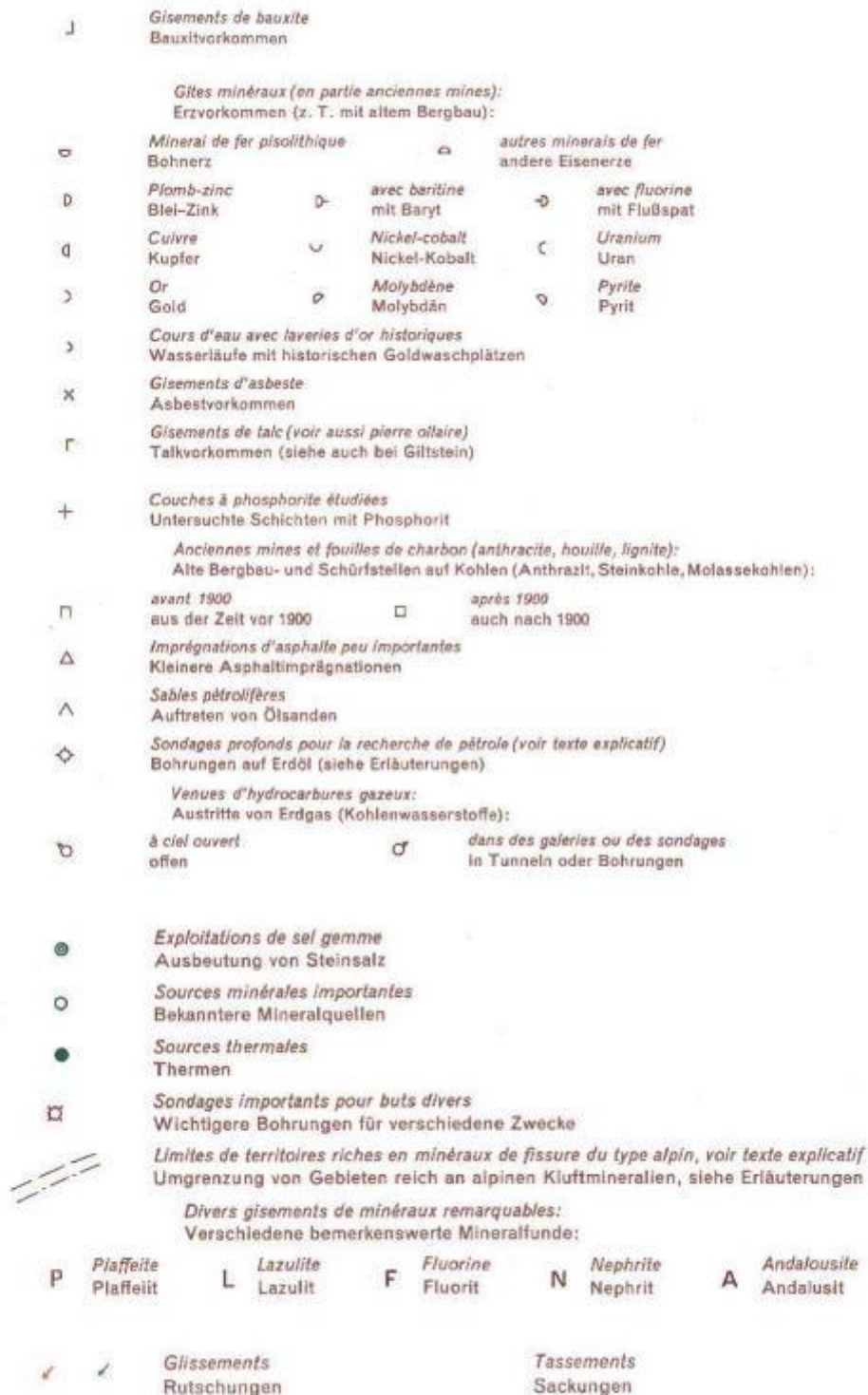


Figure 8. Legend of the geotechnical map of Switzerland, page 5 [41]

Volumes

The aspects of the computation of volumes that are common to all the selected bridges are explained in this section. There are, indeed, some characteristic which are the same for all of them and some other which are specified in the relative section of each bridge.

The cubic meters of concrete and steel are directly computed from the original drawings [1]. In almost every case it is chosen to build a 3D model and to use CAD tools to compute the total volume itself. The errors originating from this process are the ones that occur when the starting point is a paper document which is transformed into a digital version of it. In particular, the common aspects which can lead to mistakes are scale and graphical errors related to the quality of the detail of the scan and to the thickness of the line. Other assumptions are related also to the conversion of specific parts of the structure into equivalent curved lines which implies some geometrical transformations by the software which can be wrong. This process is common to almost all the structures because most of them are arch bridges so at least the bottom part is a curve.

Another hypothesis is done according to the density of concrete. The available documents, indeed, are presenting the structural analysis and to the spread of stresses, but a detailed characterisation of the material properties is not included. Thus, the density of concrete, essential to compute its mass, is simply assumed according to plausible and reliable values. In specific cases this number changes, but the choices and the reasons are specified in the relative section of the bridge in question. The same considerations are related to density of steel which is assumed as the one typical for reinforced bars. In particular, for a coherence reason, the density of each material is assumed as the one reported in the KBOB table [2] where the ECC coefficients are taken too.

	Concrete	Steel
Density [kg/m ³]	2 300	7 860

Table 1. Densities of concrete and steel

The computation of the GWP, as well as the computation of volume, includes the contribution of the scaffolding too. Drawings [1] of the scaffolding are available, so the quantity of timber is computed from them in the same way as for the quantity of the bridge materials themselves, through 3D models. Sometimes, additional data on the iron used for the scaffolding foundation and screws used in the connections are present, but it is chosen not to include them in the scope of the final GWP computation as in common practice. Moreover, an important assumption that must be mentioned is that the scaffolding is supposed to be used only once for the bridge in question, and not reused on future bridges. None of their parts or elements are assumed to be used in more than one occasion. This is highlighted for two reasons: the first one is to explain the role of the engineer in charge of the design of the scaffolding and the other one is a geometrical reason. It is well known that for some projects Coray was the engineer in charge for the design of the scaffolding. Moreover, it is also known that for two of his different projects in Fribourg, Coray used the same scaffolding. However, he never did the same with the ones done in collaboration with Maillart [42]. Saying this only proves that between

two different structures there were no common scaffolding elements, but Maillart's approach was always dictated by economic considerations. This resulted in very light arches and minimum scaffolding costs. Thus, it should also be mentioned that Maillart always considered the composite action of the concrete arch and scaffolding to resist construction loads resulting from casting of the deck. Furthermore, for wide bridge decks, he usually subdivided the arch into a series of two or more parallel, narrow arches so that the scaffolding could be shifted later and thus be used several times [32]. Where this happened, a variation of the GWP related to that practice is described. Therefore, sometimes the architect of the city or Maillart himself was in charge or decided to cover the concrete structure using masonry walls. Their volume is included in the final value of the GWP, even though they do not have any load-bearing functions, as they add mass to the entire structure.

Analysis

The coefficients for the computation of the embodied carbon, the ECCs, are taken from the KBOB database [2], which gives data for the present Swiss market. In fact, the values of these coefficients are related to the technological tools used to produce all the activities associated with the production of a material itself. Referring to present coefficients means that the current production of energy, technological level and development of the tools is used instead of those relative to the first decades of the 20th century. While the coefficients should have been linked to the period of construction of the analysed bridges, there are no available detailed tables and information about past coefficients. Thus, the environmental impact is calculated as if the bridges were built today. In the KBOB tables, there is a distinction between GHG emissions related to production and to disposal of each component, but in LCA, the overall value should be considered. The embodied emissions in the construction and use phase are neglected, and the production and end-of-life emissions are summed up. Since detailed descriptions of materials are not available, some assumptions are done in order to find similar materials and, among them, the worst option to be on the conservative side. They are assumed as following:

	ID	ECC
Building construction concrete (without rebars)	01.002	0.099
Reinforcement steel	06.003	0.682
Solid spruce/pine/larch, chamber-dried, planed	07.011	0.143
Clay brick	02.001	0.258

Table 2. ECC used to compute the GWP

The coefficient related to timber is chosen by exclusion since data for the used wood, as for the other materials are not available. First, all the coefficients related to panels are excluded because scaffoldings are not built with these elements. Then, among the six different remained categories of solid timber it is chosen the one that has the highest coefficient to be, as above-mentioned, on the safe side.

Stauffacher Bridge

Place	Year	Span	Width	Length	Rise	Ratio
Zürich	1899	39.60 m	4 m	40 m	3.70 m	10.7
Unreinforced three-hinged arch bridge						
Breccias ¹ and conglomerates, strongly cemented sandstones, partly with schistose structure with deposits of phyllites.						

Table 3. Characteristics of Stauffacher Bridge [1]



Figure 9. Stauffacher Bridge [43]



Figure 10. Geo-localisation of Stauffacher Bridge to define its foundation soil [41]

¹ Breccias are a type of clastic sedimentary rocks which are composed of angular or subangular, randomly oriented clasts of other sedimentary rocks [52]

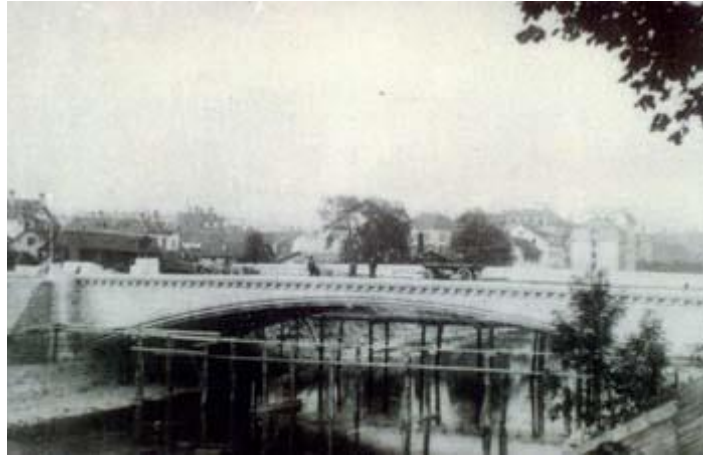


Figure 11. Scaffolding of Stauffacher Bridge [44]

Description

The Stauffacher bridge was the first project in which Maillart won the design competition. In fact, until that moment he only had supervised the construction of one bridge, built in Pampigny. Even if this last-mentioned bridge is considered his first bridge, it was in the Stauffacher project that his signature started to emerge. It is important to underline that the design process consisted on four different alternatives: the first one was a steel girder, the second a two-span steel arch bridge, the third a one-span steel arch bridge and the fourth a two-span masonry arch bridge.

The entire project was reviewed by Ritter who set out some criteria upon which the final choice was made: follow not only usefulness and carrying capacity but also aesthetic considerations [45]. Ritter was against single-span bridges and he recommended a three-hinged concrete arch with steel hinges at the crown and at each of the abutments [32]. Maillart decided to follow Ritter's suggestions and designed his first three-hinged concrete arch bridge, without reinforcement. It was cheaper than any other proposed, so he won. However, the Zürich city architect, Gustav Gull, was chosen as well to design a masonry façade to conceal the concrete structure completely [32]. Concrete was not seen as a material to be externally shown yet. The problem related to the masonry side walls, apart from the aesthetical one, was linked to the fact that both them, add weight without reducing stresses or carrying any load. Therefore, this aspect continued to highlight the attitude that structure and decoration are separate as it was during the past.

Volumes

Stauffacher bridge is made only on concrete so the computation of volume, as well as the global warming potential, does not include the contribution of steel rebars. However, it is important to consider the contribution of the scaffolding. Therefore, as mentioned in the description, the architect of the city was in charge to cover the concrete structure. He decided to use masonry walls to cover it, so its volume is computed separately.

As for the all other bridges the drawings are available from the original documents [1] stored in the ETH Archives, in Zurich. The boundaries of the structure are shown in the following figure (Figure 12) produced to compute the volumes.



Figure 12. Representation of the 3D model of Stauffacher Bridge

	Volume [m ³]	Density [kg/m ³]	Mass [t]
Concrete	407.0	2 300	936.0
Masonry	25.0	900	22.5
Timber	30.4	465	14.1

Table 4. Computed quantities of Stauffacher's Bridge

Analysis

	ID	ECC
Building construction concrete (without rebars)	01.002	0.099
Clay brick	02.001	0.258
Solid spruce/pine/larch, chamber-dried, planed	07.011	0.143

Table 5. Coefficients for Stauffacher's GWP

Multiplying the correspondent coefficient values with the above-computed material quantities it is possible to find the result of carbon emissions of Stauffacher bridge.

$$\begin{aligned} \text{GWP} &= 0.099 \text{ CO}_2\text{e/kg} \cdot 936 \cdot 10^3 \text{ kg} + 0.258 \text{ CO}_2\text{e/kg} \cdot 22.5 \cdot 10^3 \text{ kg} + 0.143 \text{ CO}_2\text{e/kg} \cdot 14.1 \cdot 10^3 \text{ kg} \\ &= 10^5 \text{ kg CO}_2\text{e} \end{aligned}$$

Equation 2. Computation of Stauffacher's GWP

Zuoz Bridge

[illegible]

Table 6. Characteristics of Zuoz Bridge [1]



Figure 13. Zuoze Bridge [43]

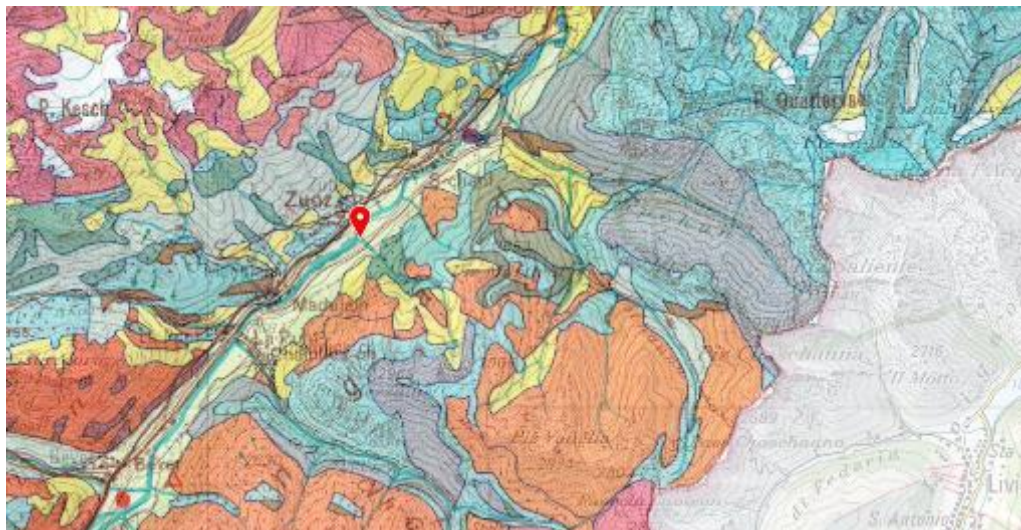


Figure 14. Geo-localisation of Zuoz Bridge to define its foundation soil [41]

Description

Zuoz Bridge was one of the bridges in which Maillart succeeded in experimenting something new. The major contributions of this bridge are two: the innovative design of the scaffolding and the different structural concept of the cross section. He proposed a concrete box girder (for the arch profile), the first one ever built. The form is a three-hinged U-shape arch which has become monolithic by its connection with the longitudinal walls bearing the deck [34].

The innovation of the scaffolding consisted on the legacy inherited by the Solis bridge (a 42-meter-span masonry arch on the Rhätische Bahn line between Thusis and Tiefschäpfer). The arch was divided into three layers, only the first of which needed to be carried by the wood scaffold. Once that the initial layer was complete, it could itself act as a thin support and carry the remaining two layers. In that way the scaffold could be much lighter, since it had to bear only one-third of the entire arch weight [32]. Thus, Maillart's idea was to build only the bottom curved slab and once it had hardened, the longitudinal walls and the roadway deck were cast. The procedure reduced scaffold costs but introduced major uncertainties.

Moreover, in the cross section he tried to integrate elements which previously were considered only separated. In particular, in his new structural concept the arched slab, the longitudinal walls, and the roadway slab together form the arch [45]. In a conventional arch bridge, the weight of the roadway is transferred by columns to the arch. It, indeed, must be relatively thick to keep the bending stresses low under the loads resulting from bridge traffic. In Maillart's design, though, the roadway deck and arch were connected by three vertical walls, forming two hollow boxes running under the roadway. The integration of parts which were never considered together before, produced a lighter, cheaper and more elegant structure, but it gave also computational difficulties. The load would be carried by all three parts of the hollow box, so the arch would not have to bear the load alone, it could be much thinner. Moreover, incorporating the bridge's arch and roadway minimised the amount of concrete needed [33]. It was therefore possible to design these components separately, integrate them into a section where their contributions strengthen each other [36]. However, Zuoz bridge was in keeping with the spirit of massive bridges even if was hollowed out, and therefore a simple arc of circle was used for the bottom line of the arch [37].

Ritter was in charge to approve the project and only after a quite long period of time he recommended that the design could be approved with no further change. The problem was related to the distribution of stresses: Maillart assumed an evenly distribution of stresses over the cross section, but this assumption is correct at the crown and at the quarter spans, while it is incorrect at the abutment hinges. However, even today it is not an easy computational and analytical problem that is why Maillart could not convince his doubters with mathematical arguments. Fortunately, Ritter recognised that good design did not necessarily require rigorous analysis, so he supported Maillart's project [32]. It was a physical success while being a mathematical mystery.

The bridge was completed in 1901 and passed a full-scale load test. The test program was performed by Ritter, the district engineer, the building superintendent and Maillart, and it gave positive results, so it confirmed the quality of the project itself.

Over the following two years, however, cracks appeared in the vertical walls near the bridge's abutments. The cracks resulted from the gradual drying of the structure. This defect did not threaten the bridge's safety, but it motivated Maillart to correct the flaw when he designed his first masterpiece: Tavanasa Bridge [33]. When Maillart was asked to inspect those cracks, his report concluded that the cracks had no impact on the structural integrity of the bridge. The arch's internal forces are in fact concentrated at the abutment hinges where the cracks occurred. This meant that the longitudinal walls, at the location of the cracks, were in fact structurally useless. Their use at the abutments was just a feature that dated back to antiquity, it recalled the circular masonry bridges of the Romans [38].

Volumes

Zuoz bridge is made with reinforced concrete, but since it was the first design in which Maillart included reinforcement steel, there are no data available about the detailed distribution of the rebars themselves. Thus, it is necessary to follow another strategy to compute the effect on the GWP of steel. Considering its structural scheme (hollow-box three hinged arch), it is possible to assume that the amount of rebars is the same as the other structures built, more or less, on the same way. For every one of the hollow-box three hinged arches, the ratio between the mass of steel and the volume of concrete is computed. This ratio is very useful in the bridge construction field, also in present days, because it relates two different materials in a unique value, without considering the actual placement of the rebars. In fact, an alternative is to refer to the percentage of steel in a concrete cross section, but since in a different part of the bridge the distribution is different as well, it is better to refer to the previous value which can give a general overview of the entire structure without distinguish cross section by cross section. For a three hinged arch the ratio should be between 50 and 100. In the analysed structures, the average value equals 62.2. This same value is used for the computation of the steel amount of Zuoz Bridge. Moreover, as already mentioned in the description, it is important to consider the contribution of the scaffolding because of its innovative design.



Figure 15. Scaffolding of Zuoz Bridge [46]

As for the all other bridges the drawings are available from the original documents [1] from which the boundaries of the structure are shown (Figure 16).

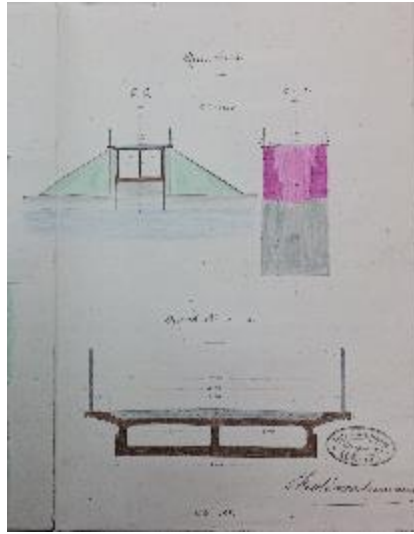


Figure 16. Cross sections of Zuoz Bridge

	Volume [m ³]	Density [kg/m ³]	Mass [t]
Concrete	115.8	2 300	266.0
Steel	$62.2 \cdot 115.8 = 0.9$	7 860	7.2
Timber	19.7	465	9.2

Table 7. Computed quantities of Zuoz's Bridge

Analysis

	ID	ECC
Building construction concrete (without rebars)	01.002	0.099
Reinforcement Steel	06.003	0.682
Solid spruce/pine/larch, chamber-dried, planed	07.011	0.143

Table 8. Coefficients for Zuoz's GWP

Multiplying the correspondent coefficient values with the above-computed material quantities it is possible to find the result of carbon emissions of Zuoz bridge.

$$\begin{aligned} \text{GWP} &= 0.099 \text{ CO}_2\text{e/kg} \cdot 266 \cdot 10^3 \text{ kg} + 0.682 \text{ CO}_2\text{e/kg} \cdot 7.2 \cdot 10^3 \text{ kg} + 0.143 \text{ CO}_2\text{e/kg} \cdot 9.2 \cdot 10^3 \text{ kg} \\ &= 3.26 \cdot 10^4 \text{ kg CO}_2\text{e} \end{aligned}$$

Equation 3. Computation of Zuoz's GWP

Steinach Bridge

Place	Year	Span	Width	Length	Rise	Ratio
Saint Gallen	1903	29.15 m	10 m	36.78 m	6.28 m	4.6
Concrete-block arch bridge						
Breccias and conglomerates, strongly cemented sandstones, partly with schistose structure with deposits of phyllites.						

Table 9. Characteristics of Steinach Bridge [1]



Figure 17. Steinach Bridge [43]



Figure 18. Steinach Bridge [43]



Figure 19. Geo-localisation of Steinach Bridge to define its foundation soil [41]

Description

Steinach bridge was designed and built in 1903, in Saint Gallen. It was built entirely of concrete blocks; even the facing blocks were concrete, with broken natural stone surfaces cast in to give a masonry like façade [32]. It was meant to be a classic bridge both in the aesthetic aspect and in the structural one, without any particular point of innovation, but perfectly in line with the past tradition. However, there is an interesting part in this geometry: it is not the usual arch bridge with one big span, and a straight deck which meets the below arch in the crown, but it has a different configuration. In fact, the deck is supported by 4 small arches (with a span of 4.23 m and a rise of 1.76 m) which are again supported by the central and principal arch. The span/rise ratio is 2.4 which means that they are very close to a semicircle. This geometry reminds classical time and tradition, but their position breaks the expected harmony: they are not placed symmetrically with respect to the crown, but three on one side and one on the other one. The final visual effect is, then, much more dynamic.

Volumes

In this situation the density of concrete is not assumed the same of the other bridges, because according to the design of the structure, it was built with concrete blocks which have a different weight and, in the analysis part, a different coefficient too. The values related to the density itself and to the ECC are taken from the KBOB list [2] where each material (in this case cement block) has a different coefficient and a relative density. Moreover, Steinach bridge is made only of this kind of unreinforced concrete blocks so the GWP does not include the contribution of steel rebars, though it comprises the scaffolding.

As for the all other bridges the drawings are available from the original documents [1] stored in the ETH Archives, in Zurich from which the boundaries of the structure are shown (Figure 21 and Figure 20) and used to compute the volumes.

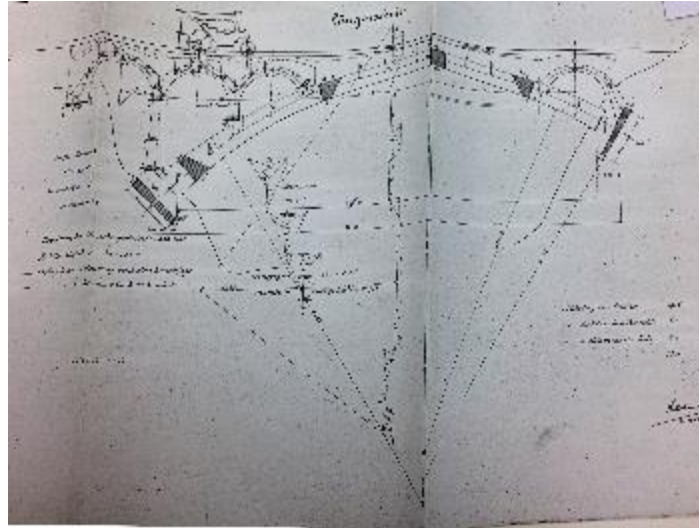


Figure 20. Longitudinal view of Steinach Bridge

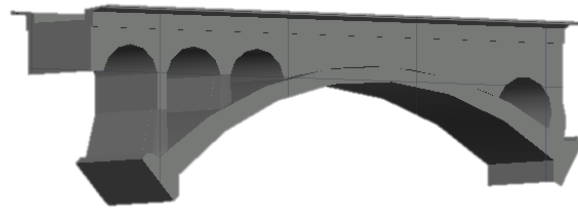


Figure 21. Representation of the 3D model of Steinach Bridge

	Volume [m ³]	Density [kg/m ³]	Mass [t]
Concrete	1061.2	1700	1 804.0
Timber	96.6	465	44.9

Table 10. Computed quantities of Steinach's Bridge

Analysis

The coefficients chosen for the computation of the embodied carbon, are the ones of KBOB [2], but in this case a different assumption is done for concrete. Since it was not the traditional cast one, but concrete blocks are used, the followings are selected:

	ID	ECC
Cement block	02.007	0.129
Solid spruce/pine/larch, chamber-dried, planed	07.011	0.143

Table 11. Coefficients for Steinach's GWP

Multiplying the correspondent coefficient values with the above-computed material quantities it is possible to find the result of carbon emissions of Steinach bridge.

$$\text{GWP} = 0.129 \text{ CO}_2\text{e/kg} \cdot 1804 \cdot 10^3 \text{ kg} + 0.143 \text{ CO}_2\text{e/kg} \cdot 44.9 \cdot 10^3 \text{ kg} = 2.39 \cdot 10^5 \text{ kg CO}_2\text{e}$$

Equation 4. Computation of Steinach's GWP

Tavanasa Bridge

Place	Year	Span	Width	Length	Rise	Ratio
Tavanoas	1906	51.25 m	3.60 m	57 m	5.70 m	9
Hollow box 3 hinged arch						
Conglomerates, few or quite cemented, always with banks of gravel and marl.						

Table 12. Characteristics of Tavanasa Bridge [1]



Figure 22. Tavanasa Bridge [44]



Figure 23. Geo-localisation of Tavanasa Bridge to define its foundation soil [41]



Figure 24. Scaffolding of Tavanasa Bridge [46]

Description

The Tavanasa Bridge was designed by Maillart in 1906 and at the time of the bridge's completion, with a main span of more than 51 m, it was the longest reinforced concrete bridge in Switzerland, and 3rd largest in the world [38]. Unfortunately, in September 1927, a landslide swept down and tore out the 1905 Tavanasa bridge over the upper Rhine River. The most daring Swiss bridge of its time was reduced to a pile of debris on the left bank [32].

The total opening at Tavanasa was 51 meters, which forced Maillart to choose between two very much shorter spans of about 25 meters each, or one span almost 30 percent longer than Stauffacher [32]. He chose to design the Tavanasa Bridge without embellishment – simply mirroring the flow of forces documented at Zuoz. The structure was made even lighter than the Zuoz Bridge by removing the longitudinal walls at the abutments [38]. The decision to remove those longitudinal walls was dictated by the fact that they were not essential because they carried no load [33]. In this way he tried to learn from his previous errors. He simply eliminated material in the longitudinal walls near the abutments, where cracks had arisen in Zuoz [32]. Without the spandrel walls it was achieved a technically superior form and a visually new [3].

In the other direction lateral walls were hollowed near to the supporting hinges, close to a thrust line that was almost parabolic [37]. Maillart had, indeed, decided to eliminate the central longitudinal wall and increase the deck span in the transverse direction. This made necessary to increase the deck thickness too. Then, the walls served as part of the overall arch. Whereas the deck carried essentially truck loads only, the overall arch carried essentially dead loads only. Therefore, the reduced walls meant reduced dead loads and reduced stresses [32].

Moreover, Maillart made use of funicular polygons to calculate the thrust lines in the structure, but its geometry remains very classic: a circular underside for his arch [34].

So, the result was completely in line with his guiding principles: beautiful, functional and inexpensive [33].

The disaster of the destruction of the bridge provided a unique opportunity to test the materials in a relatively old bridge. Mirko Roš, after making the tests, concluded that the bridge was well built and had been in good condition after twenty-two years of service in harsh climate [32].

Volumes

Tavanasa bridge is made on reinforced concrete so the GWP must include the contribution of steel rebars and, as for the other bridges, the scaffolding too. In this case, as sometimes happens for steel rebars, there is a detailed table with all the dimensions of the timber elements used for the scaffolding. Thus, the volume is computed from that list and not from a 3D model as usual.

Moreover, additional data on the iron used for the scaffolding foundation and screws used in the connections are available but, they are not added in the mass of the whole bridge.

Mass of iron = 344 kg

Mass of screws = 1400 kg

As for the all other bridges the drawings are available from the original documents [1] stored in the ETH Archives, in Zurich. The boundaries of the structure are shown in the following figure (Figure 25) produced to compute the volumes.

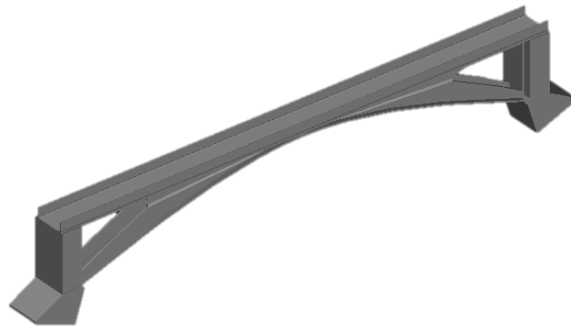


Figure 25. Representation of the 3D model of Tavanasa Bridge

	Volume [m ³]	Density [kg/m ³]	Mass [t]
Concrete	364.2	2 300	837.7
Steel	0.8	7 860	6.3
Timber	93.4	465	43.4

Table 13. Computed quantities of Tavanasa's Bridge

Analysis

	ID	ECC
Building construction concrete (without rebars)	01.002	0.099
Reinforcement Steel	06.003	0.682
Solid spruce/pine/larch, chamber-dried, planed	07.011	0.143

Table 14. Coefficients for Tavanasa's GWP

Multiplying the correspondent values with the above-computed material quantities it is possible to find the result of carbon emissions of Tavanasa bridge.

$$\begin{aligned} \text{GWP} &= 0.099 \text{ CO}_2\text{e/kg} \cdot 837.7 \cdot 10^3 \text{ kg} + 0.682 \text{ CO}_2\text{e/kg} \cdot 6.3 \cdot 10^3 \text{ kg} + 0.143 \text{ CO}_2\text{e/kg} \cdot 43.4 \cdot 10^3 \text{ kg} \\ &= 1.03 \cdot 10^5 \text{ kg CO}_2\text{e} \end{aligned}$$

Equation 5. Computation of Tavanasa's GWP

Aarburg Bridge

Place	Year	Span	Width	Length	Rise	Ratio
Olten	1912	67.80 m	5.30 m	71.92 m	6.95 m	9.8
Deck Arch bridge						
Gravels and sands with light covering or clay-silt interlaying (deposits of current watercourses).						

Table 15. Characteristics of Aarburg Bridge [1]



Figure 26. Aarburg Bridge when it was originally built [47]



Figure 27. Aarburg Bridge at present time [43]



Figure 28. Geo-localisation of Aarburg Bridge to define its foundation soil [41]

Description

In 1911, Maillart experimented again with a new form through the winning of a competition for a concrete bridge which lead him to the deck-stiffened arches [32]. This work, after Tavanasa, was the Maillart's only pre-war arch bridge that revealed its concrete arch structural form. The three main structural members – deck, columns, and arch – were clearly visible; but unlike the Tavanasa bridge, they were designed to perform their structural functions separately. In fact, although Aarburg bridge had the appearance of Maillart's later deck-stiffened arch bridges where the straight deck has a deep parapet wall, it lacked the internal reinforcement of later bridges [32]. At Aarburg the deck and the arch were not working as a combined structure, as the arch was thick (800mm-1.02m) and carried all the load. The concrete arch of this bridge supported very thin concrete columns, which in turn supported both the 5-meter-wide longitudinally ribbed deck and the two solid 1.25-meter-high concrete parapets. The arch was the longest span (67.80 meters) built by Maillart up to that time and had the highest ratio of span to rise (9.75) of any of the cast concrete bridges ever built by his firm. The bridge has a visually striking location, this is why the canton engineer insisted on a handsome structure. In particular the bridge had to be an arch and must have a single span, a pillar in midstream would have been aesthetically displeasing [32].

The required one span lead Maillart to take the conservative line of designing and produce a relatively heavy hinge less arch big enough to carry both the entire dead weight and the complete live load. Thus, the Aarburg bridge marked a break away from his earlier practice, from Zuoz to Tavanasa, in which he had designed the deck, walls, and arch to carry the loads as one unit. On the other hand, Maillart designed extraordinary thin columns (20 cm x 25 cm) to carry the deck loads of the arch. Visually, these elegant columns contrasted strongly with the comparatively thick solid arch (form 80 cm to 100 cm) and the deep parapet (125 cm).

The overall effect was one of two strong members – one straight and one curved – joined by very delicate vertical lines. These verticals were mere struts (only compressed elements) designed to carry vertical loads and they were not intended to stiffen either the top of bottom members against bending. Unfortunately, these

thin elements deteriorated over time because of water leaking from the faulty drainage system on the deck. This problem gradually caused concrete over the reinforcing steel to crack off, through freezing and thawing, and it led to expose the steel to rust [32]. Cracks appeared on the underside of the deck beams near the column heads, showing that the deck was moving downwards relative to the arch. So Maillart realised that to avoid cracking, deck and arch would have to work together [48].

Volumes

As for all other bridges the drawings are available from the original documents [1] stored in the ETH Archives, in Zurich. The boundaries of the structure are shown in the following figures (Figure 29 and Figure 30) produced to compute the volumes.

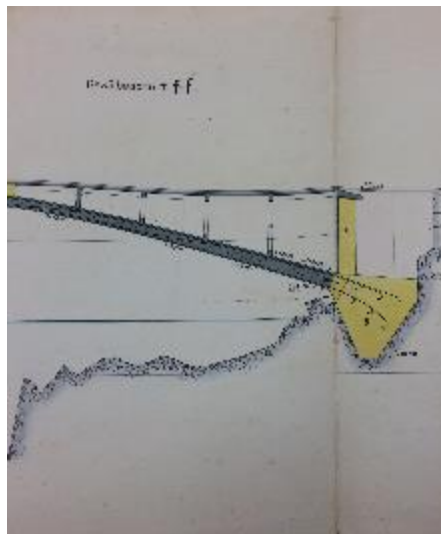


Figure 29. Part of the transversal section of Aarburg Bridge

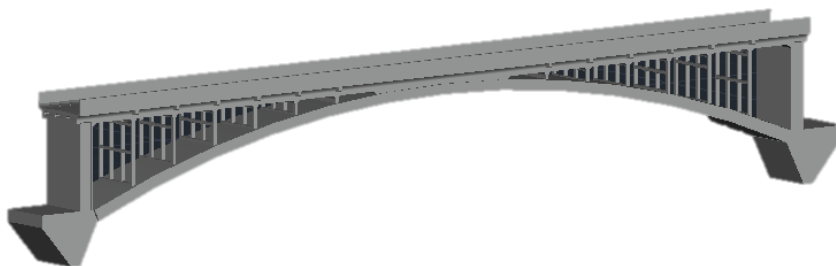


Figure 30. Representation of the 3D model of Aarburg Bridge

	Volume [m ³]	Density [kg/m ³]	Mass [t]
Concrete	776.5	2 300	1785.9
Steel	5.9	7 860	46.7
Timber	64.1	465	29.8

Table 16. Computed quantities of Aarburg Bridge

Analysis

	ID	ECC
Building construction concrete (without rebars)	01.002	0.099
Reinforcement Steel	06.003	0.682
Solid spruce/pine/larch, chamber-dried, planed	07.011	0.143

Table 17. Coefficients for Aarburg's GWP

Multiplying the correspondent coefficients values with the above-computed material quantities it is possible to find the result of carbon emissions of Aarburg bridge.

$$\text{GWP} = 0.099 \text{ CO}_2\text{e/kg} \cdot 1785.9 \cdot 10^3 \text{ kg} + 0.682 \text{ CO}_2\text{e/kg} \cdot 46.7 \cdot 10^3 \text{ kg} + 0.143 \text{ CO}_2\text{e/kg} \cdot 29.82 \cdot 10^3 \text{ kg} = 2.13 \cdot 10^5 \text{ kg CO}_2\text{e}$$

Equation 6. Computation of Aarburg's GWP

Marignier Bridge

Place	Year	Span	Width	Length	Rise	Ratio
Marignier	1920	20.44 m	7.70 m	66.90 m	2.33 m	8.8
Deck Arch Bridge						
Gravels and sands with light covering or clay-silt interlaying (deposits of current watercourses).						

Table 18. Characteristics of Marignier Bridge [1]



Figure 31. Marignier Bridge [43]

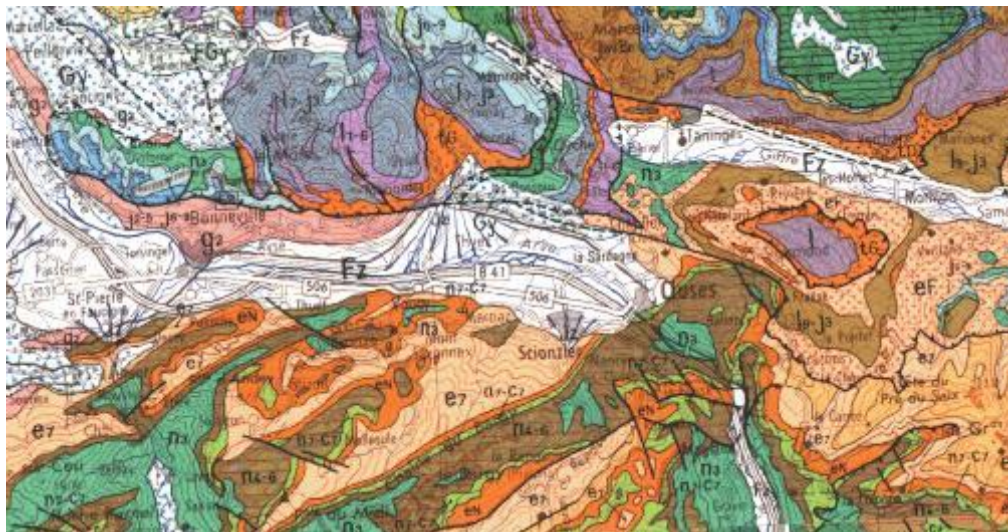


Figure 32. Geo-localisation of Marignier Bridge to define its foundation soil [49]

Description

Marignier Bridge was designed in 1920. The inspiration and the analysis of the bridge was given to Maillart by someone else's 1911 plans [32]. It is the only analysed structure which is not in Switzerland. However, even if it is in France, the distance with the border is such that there are not significative distinctions in relevant aspects linked to the environment. In particular, the most important factor that could be significantly different country to country is the soil. In the geotechnical plan of France [49] it is found that the foundations lie on gravels and sands with light covering or clay-silt interlaying (deposits of current watercourses). Thus, in this case, the terrain is the same as Aarburg and Zuoz, and the dislocation does not influence structural characteristics. Moreover, Marignier was the first bridge to be made of 3 consecutive arches.

Given the span (almost 67 m) Maillart decided to divide it into 3 equivalent segments, even if he had already designed Aarburg bridge in Olten as a deck arch bridge with a similar total length (66.90 m) and a unique supporting arch.

Volumes

For this bridge, also masonry has to be considered. In fact, as for Stauffacher Bridge, in Marignier Bridge the entire structure is covered by bricks which mask the concrete structure behind.

As for the all other bridges the drawings are available from the original documents [1] stored in the ETH Archives, in Zurich. The boundaries of the structure are shown in the following figure (Figure 33) produced to compute the volumes.

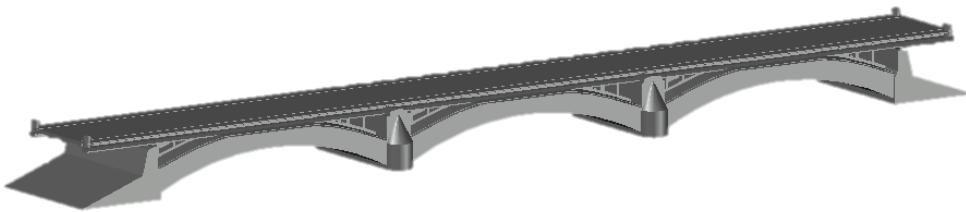


Figure 33. Representation of the 3D model of Marignier Bridge

	Volume [m ³]	Density [kg/m ³]	Mass [t]
Concrete	1509.8	2 300	3472.5
Steel	20.8	7 860	163.5
Timber	80.1	465	37.2
Masonry	25.2	900	22.7

Table 19. Computed quantities of Marignier Bridge

Analysis

	ID	ECC
Building construction concrete (without rebars)	01.002	0.099
Reinforcement Steel	06.003	0.682
Solid spruce/pine/larch, chamber-dried, planed	07.011	0.143
Clay brick	02.001	0.258

Table 20. Coefficients for Marignier's GWP

Multiplying the correspondent coefficient values with the above-computed material quantities it is possible to find the result of carbon emissions of Marignier bridge.

$$\text{GWP} = 0.099 \text{ CO}_2\text{e/kg} \cdot 3472.5 \cdot 10^3 \text{ kg} + 0.682 \text{ CO}_2\text{e/kg} \cdot 163.5 \cdot 10^3 \text{ kg} + 0.143 \text{ CO}_2\text{e/kg} \cdot 37.2 \cdot 10^3 \text{ kg} + 0.258 \text{ CO}_2\text{e/kg} \cdot 22.7 \cdot 10^3 \text{ kg} = 4.66 \cdot 10^5 \text{ kg CO}_2\text{e}$$

Equation 7. Computation of Marignier's GWP

Flienglibach Bridge

Place	Year	Span	Width	Length	Rise	Ratio
Innerthal	1923	38.70 m	4.60 m	40.76 m	5.17 m	7.5
Deck Arch bridge						
Dolomitic limestone						

Table 21. Characteristics of Flienglibach Bridge [1]



Figure 34. Flienglibach Bridge [43]



Figure 35. Geo-localisation of Flienglibach Bridge to define its foundation soil [41]



Figure 36. Scaffolding of Flienglibach Bridge [46]

Description

After Marignier Bridge, over the following 10 years, Maillart concentrated on refining the visual appearance of the deck-stiffened arch and started to think about the effects of live loads. He did that thanks to a new bridge necessary to cross the Flienglibach watercourse, which flows into Lake Wägital (Wägitalersee). The lake is a pumped storage reservoir for a hydro-electric power plant, formed by the construction of the Schräh Dam at Innerthal between 1922 and 1924. It is encircled by the Seestrasse road, which crosses the many brooks and streams that feed into the lake. The new design for Flienglibach Bridge was almost a visual refinement of his 1912 hinge-less arch bridge over the Aare River in Aarburg, Aargau canton, which had vertical and thin columns supporting the deck from the arch [48].

Up to that moment he had only taken account of dead loads (only the weight of the bridges themselves) since the used technology lead him to design safe and resistant structures neglecting any other effect. However, theoretically an arch bridge is like an inverted cable where the tension in the cable balances the weight. But, once the arch's form is fixed to fit the dead load, it cannot be changed even if live loads will cause the arch to bend [33]. Thus, the arch must be strong and thick enough to resist the bending. For aesthetic reasons, however, Maillart wanted thinner arches. His solution was to connect the arch to the roadway deck with walls. Because the arch and deck must then bend together, the forces that cause bending moment would be distributed between the arch and deck in proportion to their relative stiffness. If the deck is much stiffer than the arch the bending moment would be almost completely on the deck and the effect on the arch would be negligible. In this way, Maillart justified making the arch as thin as possible. The technique was to stiffen the deck of the Flienglibach Bridge by adding more reinforcing steel [33].

These new principles lead to a new deck-stiffened from the Flienglibach bridge. The idea consisted of designing a stiff longitudinal parapet that serves as a straight deck-girder and was connected through slender transverse cross walls to a thin arch below the deck. The stiff parapet prevented the arch from bending under heavy traffic loads. And it permitted the use of an arch as thin as can be accurately built. This did not mean that the transverse walls were the essential connectors of the deck and the arch; Maillart clearly stated in the patent that the connection was by the longitudinal walls. Flienglibach bridge contained the seed for the deck-

stiffened concept; first, by its technical rationale of connecting the deck and the arch together to save materials; and second, by its visual suggestion of that connection by transverse rather than by longitudinal walls [32].

Unfortunately, the bridge began to suffer frost damage soon after completion and it was discovered that the its concrete was inferior in terms of chemical composition because not frost-resistant. But Maillart's design was not a fault. However, a reparation was needed. So, around 1933, the frost damage was fixed using sprayed concrete, and longitudinal reinforced concrete walls were added to both sides of the bridge, closing the openings between deck and arch. Unlikely in 1969, Maillart's bridge over the Flienglibach was replaced by a wider bridge of much plainer design: a horizontal concrete deck supported by two piers [48].

Volumes

For this bridge the quantity of steel is more easily to be found because it is not computed from drawings, but directly from the so called "Eisenliste". The list is part of the whole available project [1] and it shows the position, the length and the mass of each steel rebars and respectively the total quantities. In fact, the final used value is the total mass of steel. This number is, then, converted to the volume through the density in order to be able to subtract the steel volume itself from the total volume (computed from the drawings as usual) to have the concrete cubic meters.

As for the all other bridges the drawings are available from the original documents [1] stored in the ETH Archives, in Zurich. The boundaries of the structure are shown in the following figure (Figure 37) produced to compute the volumes.



Figure 37. Representation of the 3D model of Flienglibach Bridge

	Volume [m ³]	Density [kg/m ³]	Mass [t]
Concrete	215.1	2 300	494.8
Steel	2.1	7 860	16.5
Timber	36.8	465	17.1

Table 22. Computed quantities of Flienglibach Bridge

Analysis

	ID	ECC
Building construction concrete (without rebars)	01.002	0.099
Reinforcement Steel	06.003	0.682
Solid spruce/pine/larch, chamber-dried, planed	07.011	0.143

Table 23. Coefficients for Flienglibach's GWP

Multiplying the correspondent coefficients values with the above-computed material quantities it is possible to find the result of carbon emissions of Flienglibach bridge.

$$\text{GWP} = 0.099 \text{ CO}_2\text{e/kg} \cdot 494.8 \cdot 10^3 \text{ kg} + 0.682 \text{ CO}_2\text{e/kg} \cdot 16.5 \cdot 10^3 \text{ kg} + 0.143 \text{ CO}_2\text{e/kg} \cdot 17.1 \cdot 10^3 \text{ kg} = 6.27 \cdot 10^4 \text{ kg CO}_2\text{e}$$

Equation 8. Computation of Flienglibach's GWP

Ziggenbach Bridge

Place	Year	Span	Width	Length	Rise	Ratio
Innerthal	1924	20 m	5.30 m	37.50 m	4.70 m	4.3
Deck Arch Bridge						
Dolomitic limestone						

Table 24. Characteristics of Ziggenbach Bridge [1]



Figure 38. Ziggenbach Bridge [43]

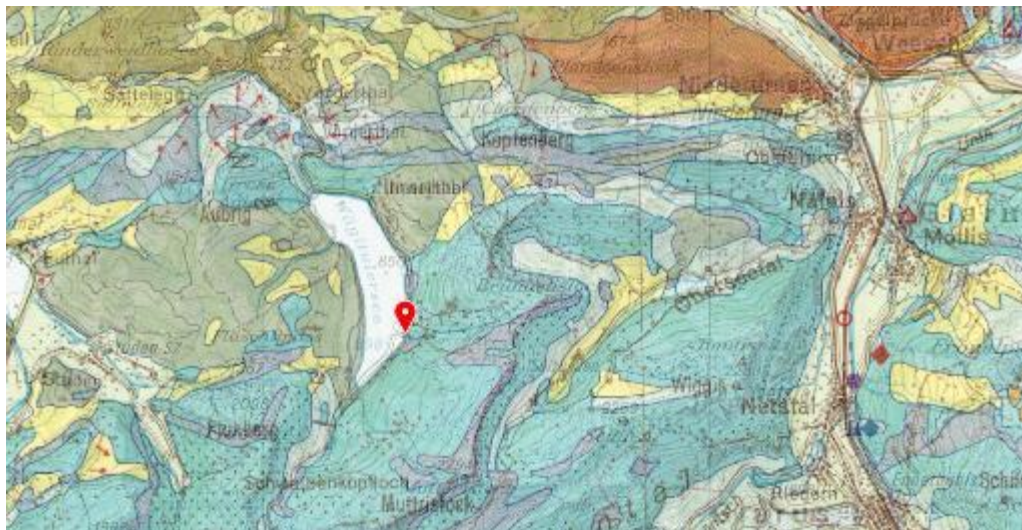


Figure 39. Geo-localisation of Ziggenbach Bridge to define its foundation soil [41]

Description

Ziggenbach Bridge was another grate experiment of Robert Maillart. It was his first attempt at a curved bridge. However, the approach was rather crude. The deck is not smoothly curved but polygonal in plan to allow for the 25m radius of curvature. In contrast, the arch is straight in plan [38]. At midspan, arch and deck merge. Because of the short span of the arch no intermediate cross walls connecting deck and arch were necessary. The arch acts like a frame with slightly curved, inclined columns supporting the central part of the bridge deck. The Ziggenbach Bridge was treated like a plane system. Maillart did not investigate how the concentrated moments resulting from the kinks of the deck beams would be carried. Instead, he simply increased traffic loads by one-third to account for secondary effects due to the deck curvature. So, as he has already done before, he did not design with precise loads, computed by a detailed process, but he assumed a conventional value which was able to carry even unpredicted effects [40].

Volumes

As for Flienglibach Bridge, the quantity of steel is not computed from drawings, but directly from the so called "Eisenliste" which is part of the whole available project [1]. This list shows the position, the length and the mass of each steel rebars and respectively the total quantities. The final given value is the total mass of steel. It is converted to the volume through the density and its value is subtracted from the total volume (computed from the drawings as usual) to have the concrete cubic meters.

The problem for this bridge is in the scaffolding. Among the original documents there are not pieces of information about the design of it, so it is not possible to compute directly the volume and the mass.

As for the all other bridges the drawings are available from the original documents [1] stored in the ETH Archives, in Zurich. The boundaries of the structure are shown in the following figure (Figure 40) produced to compute the volumes.



Figure 40. Representation of the 3D model of Ziggenbach Bridge

	Volume [m ³]	Density [kg/m ³]	Mass [t]
Concrete	175.3	2 300	403.2
Steel	1.3	7 860	10.5
Timber	N/A	465	N/A

Table 25. Computed quantities of Ziggenschach Bridge

Analysis

	ID	ECC
Building construction concrete (without rebars)	01.002	0.099
Reinforcement Steel	06.003	0.682
Solid spruce/pine/larch, chamber-dried, planed	07.011	0.143

Table 26. Coefficients for Ziggenschach's GWP

Multiplying the correspondent coefficient values with the above-computed material quantities it is possible to find the result of carbon emissions of Ziggenschach bridge.

Since data about scaffoldings are not available it is computed the ratio between the GWP of the previous structures with and without the contribution of timber. It is found that it increases the kg of equivalent CO₂ of a 4%. Then, it is chosen to add this percentage to the available result in order to have numbers with similar meaning and close enough to be compared.

$$\text{GWP} = 1.04(0.099 \text{ CO}_2\text{e/kg} \cdot 403.2 \cdot 10^3 \text{ kg} + 0.682 \text{ CO}_2\text{e/kg} \cdot 10.5 \cdot 10^3 \text{ kg}) = 4.90 \cdot 10^4 \text{ kg CO}_2\text{e}$$

Equation 9. Computation of Ziggenschach's GWP

Schrärbach Bridge

Place	Year	Span	Width	Length	Rise	Ratio
Innerthal	1924	28.80 m	3.90 m	30 m	4 m	7.2
Deck arch bridge						
Dolomitic limestone						

Table 27. Characteristics of Schrärbach Bridge [1]



Figure 41. Schrärbach Bridge [43]



Figure 42. Geo-localisation of Schrärbach Bridge to define its foundation soil [41]

Description

Schrärbach is the following experiment of deck arch bridge after Flienglibach and Ziggenbach. It was designed in the same location of Flienglibach, to cross another watercourse which flows into Lake Wägital (Wägitalersee). The difference of this structure with respect to the abovementioned other twos is in the thickness of the arch. The un-stiffened traditional arch at Stauffacher spanning 39.6 m required a 72 cm thick arch at the crown, while the deck-stiffened arches spanning 39.7 m at Flienglibach, and 28.8 m at Schrärbach, were designed with arches only 25 cm and 18 cm thick respectively. This innovation lead Maillart to pursue the optimization aim of materials and to save money in the scaffolding too. However, the thinness of the Schrärbach arch was obscured when decorative non-structural horizontal cross-walls were added soon after construction. Their function was only to mirror the aesthetic trends in bridges design at the time [38]. The innovation which lies in this architectural choice is that it is chose to cover the static structure with concrete walls instead of using masonry as it has already been done for previous bridges. Even if, on one hand, the traditional trend was respected in the shape, on the other hand it was given space to the use of a new and still unconventional material as reinforced concrete.

Volumes

As for Flienglibach and Ziggenbach Bridge, the quantity of steel is not computed from drawings, but directly from the so called "Eisenliste" which is part of the whole available project [1]. The list is organised always at the same way, so it shows the position, the length and the mass of each steel rebars and respectively the total quantities. In fact, the final used value is the total mass of steel. This number is converted to the volume through the density and subtracted from the total volume (computed from the drawings as usual) to have the concrete cubic meters.

The problem for this bridge, as for the Ziggenbach Bridge, is in the scaffolding. Among the original documents [1] there are not pieces of information about the design of it, so it is not possible to compute directly its volume and the mass.

As for the all other bridges the drawings are available from the original documents [1] stored in the ETH Archives, in Zurich. The boundaries of the structure are shown in the following figures (Figure 43 and Figure 44) produced to compute the volumes.

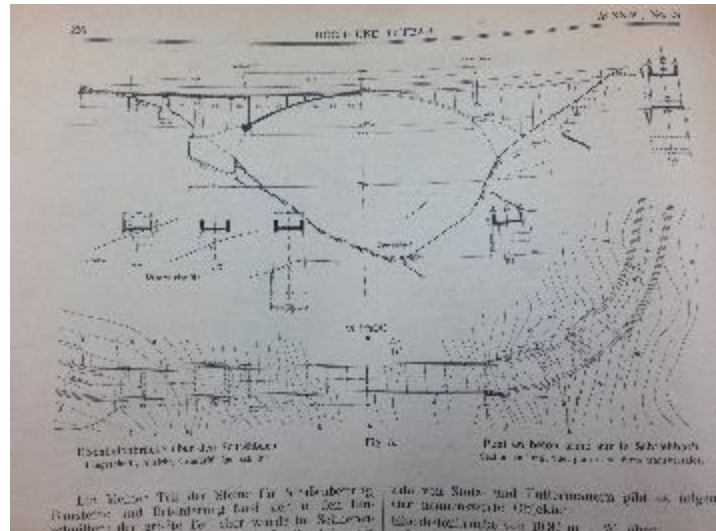


Figure 43. Bidimensional drawings of Schrähbach Bridge



Figure 44. Representation of the 3D model of Schrähbach Bridge

	Volume [m ³]	Density [kg/m ³]	Mass [t]
Concrete	81.4	2 300	187.2
Steel	0.4	7 860	3.3
Timber	N/A	465	N/A

Table 28. Computed quantities of Schrähbach Bridge

Analysis

	ID	ECC
Building construction concrete (without rebars)	01.002	0.099
Reinforcement Steel	06.003	0.682
Solid spruce/pine/larch, chamber-dried, planed	07.011	0.143

Table 29. Coefficients for Schrähbach's GWP

Multiplying the correspondent coefficient values with the above-computed material quantities it is possible to find the result of carbon emissions of Schrähbach bridge.

As for the previous bridge, since data about scaffoldings are not available it is chosen to add the 4% to the available result in order to have numbers with similar meaning and close enough to be compared.

$$\text{GWP} = 1.04(0.099 \text{ CO}_2\text{e/kg} \cdot 187.2 \cdot 10^3 \text{ kg} + 0.682 \text{ CO}_2\text{e/kg} \cdot 3.3 \cdot 10^3 \text{ kg}) = 2.16 \cdot 10^4 \text{ kg CO}_2\text{e}$$

Equation 10. Computation of Schrähbach's GWP

Lorraine Bridge

Place	Year	Span	Width	Length	Rise	Ratio
Bern	1930	82 m	21.40 m	178 m	31 m	2.6
Concrete-block arch bridge						
Breccias and conglomerates, strongly cemented sandstones, partly with schistose structure with deposits of phyllites.						

Table 30. Characteristics of Lorraine Bridge [1]



Figure 45. Lorraine Bridge [43]

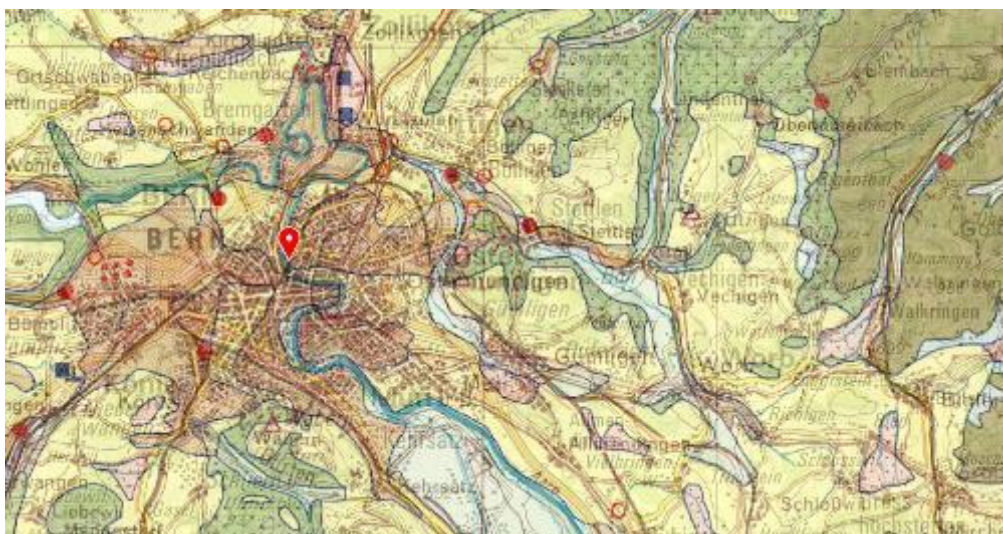


Figure 46. Geo-localisation of Lorraine Bridge to define its foundation soil [41]

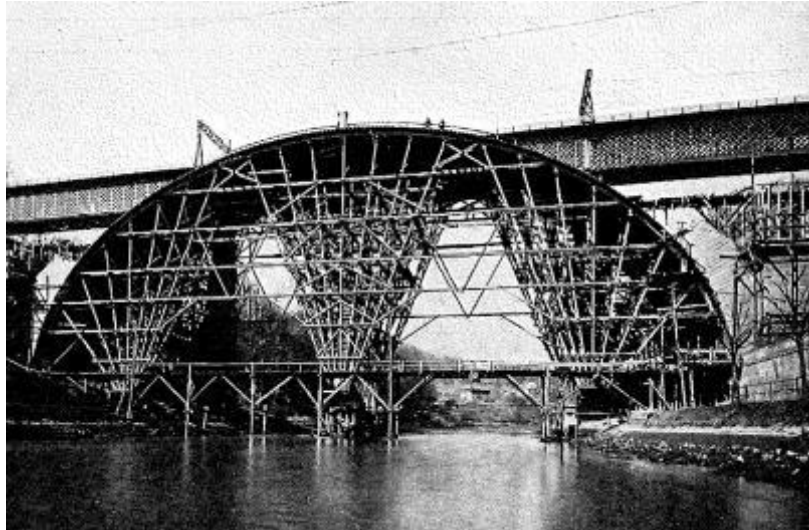


Figure 47. Scaffolding of Lorraine Bridge [50]

Description

Lorraine Bridge was one of the biggest structures designed by Maillart. The entire length of the bridge (178 m) includes a central arch whose span is 82 m and two smaller and symmetrical arches on the sides. These two small arches are semicircles since they have 17 m as span, 8.5 m as rise and a span/rise ratio perfectly equal to 2. Their position is essential to increase the development of the deck and to make it properly connecting the two sides of the river. Even considering only the central arch, its length is almost 20 m longer than the longest project up to that moment (Aarburg Bridge) so the final product was and is still nowadays massive and imponent. Maillart regarded the Lorraine Bridge as a commercial success, one of his “*beaux morceaux*”.

The form was traditional, but his means were original and economical. He built the central width of the arch first, directly on the scaffold. Once completed, that block arch, since it was built with the blocks in crenulated arrangement, it was also able to support the bands of blocks placed on either side. Following this new procedure, Maillart could make a much lighter scaffold that had only to support the central band [32]. This technique was essential to guarantee a reduction of costs due to the size of the entire structure.

However, the importance of the bridge was double. In fact, Maillart experimented again new techniques to optimize material performances, including the timber of the scaffolding even in a traditional shape. This project separated the period before Lorraine and the period after it. With the end of Lorraine, no other bridge project would come to him, partly because of the depression and partly because he would never again submit a nineteenth-century design for a major bridge competition. Only during the twenties his reestablishment had meant doing traditional works like Lorraine [32].

Volumes

In this situation the density of concrete is not assumed the same of the other bridges, because according to the design of the structure, it was built with concrete blocks which have a different weight and, in the analysis part, a different coefficient too. The values related to the density itself and to the ECC are taken from the KBOB list [2] where each material (in this case cement block) has a different coefficient and a relative density.

Moreover, Lorraine bridge, is made only on concrete blocks as well as Steinach Bridge. In both cases the construction technique is the same as masonry blocks which do not need reinforcement to bear loads, so the GWP does not include the contribution of steel rebars, but it comprises the scaffolding, designed as already mentioned in the description part.

As for the all other bridges the drawings are available from the original documents [1] stored in the ETH Archives, in Zurich. The boundaries of the structure are shown in the following figures (Figure 48 and Figure 49) produced to compute the volumes.

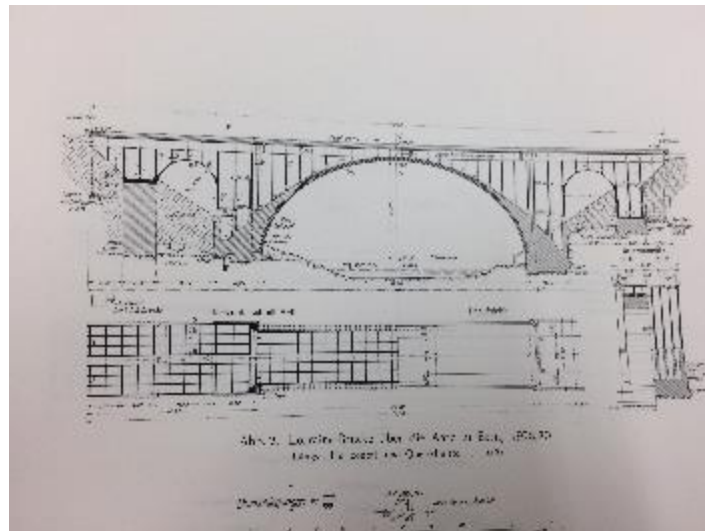


Figure 48. Bidimensional drawings of Lorraine Bridge



Figure 49. Representation of the 3D model of Lorraine Bridge

	Volume [m ³]	Density [kg/m ³]	Mass [t]
Concrete	15 229.1	1700	25 889.5
Timber	323.2	465	150.3

Table 31. Computed quantities of Lorraine Bridge

Analysis

	ID	ECC
Cement block	02.007	0.129
Solid spruce/pine/larch, chamber-dried, planed	07.011	0.143

Table 32. Coefficients for Lorraine's GWP

Multiplying the correspondent coefficient values with the above-computed material quantities it is possible to find the result of carbon emissions of Lorraine bridge.

$$\text{GWP} = 0.129 \text{ CO}_2\text{e/kg} \cdot 25889.5 \cdot 10^3 \text{ kg} + 0.143 \text{ CO}_2\text{e/kg} \cdot 150.3 \cdot 10^3 \text{ kg} = 3.36 \cdot 10^6 \text{ kg CO}_2\text{e}$$

Equation 11. Computation of Lorraine's GWP

Salginatobel Bridge

Place	Year	Span	Width	Length	Rise	Ratio
Schiers	1930	90 m	4.36 m	90 m	14 m	6.4
Hollow box 3 hinged arch						
Limestone often with marly interleaves						

Table 33. Characteristics of Salginatobel Bridge [1]



Figure 50. Salginatobel Bridge [43]



Figure 51. Geo-localisation of Salginatobel Bridge to define its foundation soil [41]



Figure 52. Scaffolding of Salginatobel Bridge [46]

Description

With Salginatobel bridge Maillart produced a revolutionary structure: he broke with the tradition and gave birth to an innovative structure. The Lorraine was the last of Maillart's masonry-like bridge, while the Salginatobel was the first of his thoroughly concrete bridge. In the Lorraine there is almost no trace of twentieth century. As Maillart himself said, the design of Lorraine reflected Bern's Nydegg bridge of 1844 while in the Salgina crossing, he broke definitively with nineteenth-century ideas of design [32]. The design was based on the hollow-box arch of the destroyed Tavanasa Bridge, but with refinements [33]. The reference loading case was the dead load, but due to its length and height the deck could not be supported only by its contact at the centre with the supporting arch and at both sides by abutments. So additional supports were needed. Thus, a rectangular frame made of columns and beams supporting the deck was used following a parabolic transition curve. This decision was dictated by the goal to connect the central section with the supports and meanwhile to stay close to the thrust line and limit bending. In fact, even if a parabola was used as a purely graphic means, disconnected with any structural logic linked to funiculars and thrust line, Maillart found that it was the best solution. Then exactly a parabola with a horizontal directrix was used [37].

However, after the presentation of Maillart's first project, Roš recommended a series of relatively minor modifications, all in the direction of more materials, mostly steel reinforcement. Maillart defended his design but agreed to add the additional steel provided the canton would pay the extra costs. The idea of the three-hinged arch centres on its ability to adjust to the small but measurable movements in the mountain because an arch without hinges will crack as the foundation moves. The problem found at Salgina was that these hinges, especially at the foundations, had to be strong enough to carry the entire bridge load into the supports, but flexible enough to permit rotation and thus prevent other parts of the arch form cracking. In fact, Salginatobel bridge was also the first time in which Maillart used a concrete hinge in one of his bridge, instead of a steel one. Tavanasa and the other early three-hinged bridges all had soft metal plates between two concrete surfaces, while Stauffacher had cast steel hinges [32].

As a fundamental key parameter, he also continued to choose economics whose importance was considered always as valid as safety and elegance. That is why he won the competition for the contract because his design

was the least expensive of the 19 submitted [33]. In order to improve structural efficiency, it was thought to reduce material. This led to saving costs, but also to a reduction of tensile cracking of the concrete and an improvement of durability of the bridge. In fact, it went without requiring repairs for 45 years after its completion [38]. Even if, Maillart criticised his own masterpiece, regretting his decision to round the underside of the arch near the bridge's crown because it was seen as an unnecessary reference to an older style, this bridge highlights the simplicity of Maillart's reasoning and computations. The few algebraic calculi remain basic and all the other computations were graphical and simply based on the manipulation of orientations and lengths of vectors [51].

Volumes

As for the all other bridges the drawings are available from the original documents [1] stored in the ETH Archives, in Zurich. The boundaries of the structure are shown in the following figure (Figure 53) which is also used to compute the volumes.

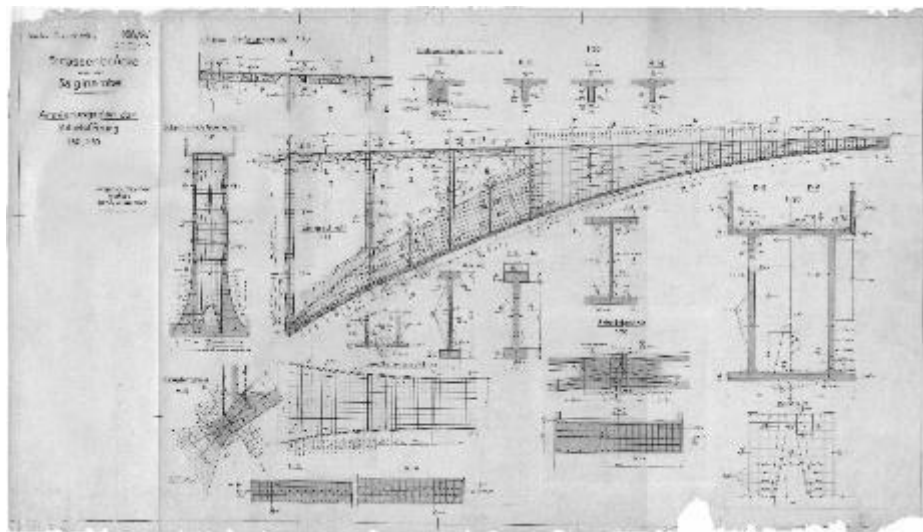


Figure 53. Representation of the plan of Salginatobel Bridge

	Volume [m ³]	Density [kg/m ³]	Mass [t]
Concrete	240.4	2 300	552.9
Steel	1.8	7 860	14.3
Timber	102.9	465	47.8

Table 34. Computed quantities of Salginatobel Bridge

Analysis

	ID	ECC
Building construction concrete (without rebars)	01.002	0.099
Reinforcement Steel	06.003	0.682
Solid spruce/pine/larch, chamber-dried, planed	07.011	0.143

Table 35. Coefficients for Salginatobel's GWP

Multiplying the correspondent coefficient values with the above-computed material quantities it is possible to find the result of carbon emissions of Salginatobel bridge.

$$\text{GWP} = 0.099 \text{ CO}_2\text{e/kg} \cdot 552.9 \cdot 10^3 \text{ kg} + 0.682 \text{ CO}_2\text{e/kg} \cdot 14.3 \cdot 10^3 \text{ kg} + 0.143 \text{ CO}_2\text{e/kg} \cdot 47.8 \cdot 10^3 \text{ kg} = 7.14 \cdot 10^4 \text{ kg CO}_2\text{e}$$

Equation 12. Computation of Salginatobel's GWP

Schwandbach Bridge

Place	Year	Span	Width	Length	Rise	Ratio
Hinterfultigen	1933	37.40 m	4.90 m	55.65 m	6 m	6.2
Deck Stiffened arch						
Marl with intercalations or conglomerates of soft sandstone (terrestrial and porous with limestone cement as an essential element)						

Table 36. Characteristics of Schwandbach Bridge [1]



Figure 54. Schwandbach Bridge [43]



Figure 55. Geo-localisation of Schwandbach Bridge to define its foundation soil [41]

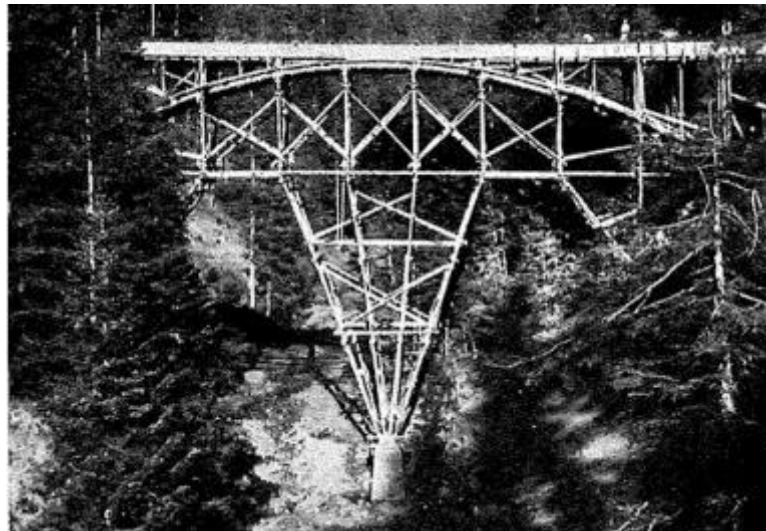


Figure 56. Scaffolding of Schwandbach Bridge [46]

Description

This structure is considered one of the greatest concrete bridges of the century. With the Schwandbach Bridge, Maillart was able to capture the technical excellence of his previous deck-stiffened arch bridges and to modify the form to suit the constraints of a curved road. He created a structurally efficient and cost sensitive work of structural art [38]. The reason why it is no doubt that this is Maillart's most significant work and perhaps the most beautiful concrete bridge ever built lied in the fact that it is a pure structural shape composed in nature. It achieved a perfect balance: nowhere too much, nowhere too little [39]. On some of the deck-stiffened bridges built between 1925 and 1932, he still used closed masonry like concrete walls for the approaches. But on the Schwandbach all traces of past forms and of masonry materials were gone [32].

He formed the structure on an elliptic ground plan, giving the Schwandbach its doubly curved appearance and allowing the roadway to cross the ravine smoothly with no sharp transitions as it was in Zigggenbach [32]. The bridge was shaped according to the thrust line for permanent loading. Its design could be justified by the expedient construction method alone. Moreover, the slim segmented arch requires only very light scaffolding and is thereafter capable of carrying the vertical wall supports and the much heavier stiffening girder without further scaffolding [39]. According to Maillart's calculations, curving of the arch axis in plan in the same sense as the deck would have a favourable effect.

Another evident principle at the base of the design process is the unexpected asymmetry, starting from the deck beam which has an asymmetrical cross section. Therefore, the arch is not symmetric about midspan too. The additional interesting aspect is that the arch is polygonal so, it is essentially a structure of straight members. Maillart had taken the idea of a form, first displayed in the 1923 Flienglibach bridge, and then in the Valtschielbach, and developed its design into the masterpieces of this bridge [32]. The polygonal arch joins the deck beam only over the central 2.8 m of the span so that these two structural members appear almost always as separate and continuous elements [40].

Volumes

As already happened for other bridges, the quantity of steel is not computed from drawings, but directly from the so called “Eisenliste” which is part of the whole available project [1]. It shows the position, the length and the mass of each steel rebars and respectively the total quantities. In fact, the final used value is the total mass of steel: then, it is converted to the volume through the density in order to be able to subtract the steel volume itself from the total volume (computed from the drawings as usual) to have the concrete cubic meters.

As for the all other bridges the drawings are available from the original documents [1] stored in the ETH Archives, in Zurich. The boundaries of the structure are shown in the following figures (Figure 58) produced to compute the volumes.

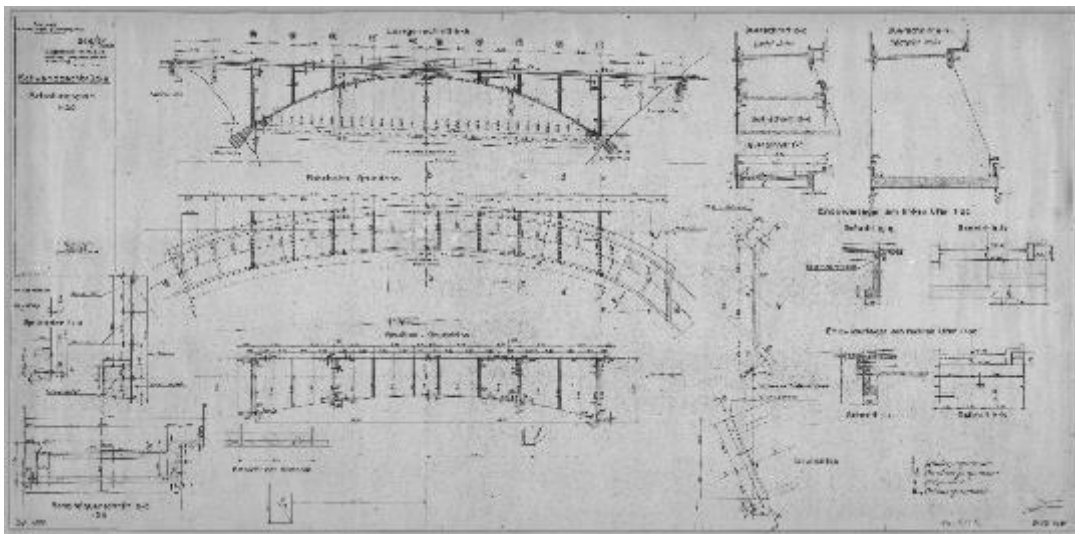


Figure 57. Bidimensional drawings of Schwandbach Bridge

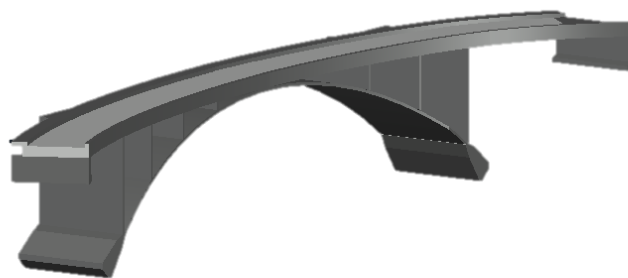


Figure 58. Representation of the 3D model of Schwandbach Bridge

	Volume [m ³]	Density [kg/m ³]	Mass [t]
Concrete	205.9	2 300	473.5
Steel	5.5	7 860	43.5
Timber	91.9	465	42.7

Table 37. Computed quantities of Schwandbach Bridge

Analysis

	ID	ECC
Building construction concrete (without rebars)	01.002	0.099
Reinforcement Steel	06.003	0.682
Solid spruce/pine/larch, chamber-dried, planed	07.011	0.143

Table 38. Coefficients for Schwandbach's GWP

Multiplying the correspondent coefficient values with the above-computed material quantities it is possible to find the result of carbon emissions of Schwandbach bridge.

$$\text{GWP} = 0.099 \text{ CO}_2\text{e/kg} \cdot 437.5 \cdot 10^3 \text{ kg} + 0.682 \text{ CO}_2\text{e/kg} \cdot 43.5 \cdot 10^3 \text{ kg} + 0.143 \text{ CO}_2\text{e/kg} \cdot 42.7 \cdot 10^3 \text{ kg} = 8.14 \cdot 10^4 \text{ kg CO}_2\text{e}$$

Equation 13. Computation of Schwandbach's GWP

Felsegg Bridge

Place	Year	Span	Width	Length	Rise	Ratio
Felsegg	1933	72.00 m	10.10 m	180.40 m	8.53 m	8.4
Hollow box 3 hinged arch						
Gravels and sands with light covering or clay-silt interlaying (deposits of current watercourses)						

Table 39. Characteristics of Felsegg Bridge [1]



Figure 59. Felsegg Bridge [43]



Figure 60. Geo-localisation of Felsegg Bridge to define its foundation soil [41]



Figure 61. Scaffolding of Felsegg Bridge [46]

Description

In this structure Maillart chose to reuse some of the techniques which were already present in Salginatobel bridge and some new methods too. The Felsegg bridge has a 68-metre span and features for the first time two parallel arches, both three-hinged. Like the Salginatobel Bridge, the Felsegg bridge's abutment hinges have a X-shape of reinforced concrete (invented by Freyssinet). This solution was more economical than steel hinges [3]. So, on one hand for the first time he designed the arch not continuous, but as the combination of two parallel structures. On the other hand, he tried to achieve the perfection of the efficiency of the hinges through a different shape of the abutments. Both aspects gave as a result an efficient structure, as many other times.

Volumes

Felsegg bridge is made on reinforced concrete, but there are no data available about the detail distribution of the rebars themselves. Thus, it is necessary to follow another strategy to compute the effect of steel on the GWP. It is chosen to adapt the same considerations already made for Zuoz Bridge. In fact, considering its structural scheme (hollow box 3 hinged arch) it is possible to assume that the amount of rebars is the same, in proportion, as the other structures built on the same way. For every one of the hollow-box three hinged arches is. Indeed, computed the ratio between the mass of steel and the volume of concrete. As already explained, this ratio is very useful in the bridge construction field, also in the present days, because it relates two different materials in a unique value, without considering the actual placement of the rebars. For this static scheme the ratio should be between 50 and 100. Since the analysed structures have an average value of 62.2, it is chosen to use the same number for the computation of the steel amount of Felsegg Bridge too.

As for the all other bridges the drawings are available from the original documents [1] stored in the ETH Archives, in Zurich. The boundaries of the structure are shown in the following figure (Figure 62) produced to compute the volumes.



Figure 62. Representation of the 3D model of Felsegg Bridge

	Volume [m ³]	Density [kg/m ³]	Mass [t]
Concrete	2222.0	2 300	5 110.6
Steel	$62.2 \cdot 2222.0 = 17.6$	7 860	138.2
Timber	370.0	465	172.0

Table 40. Computed quantities of Felsegg Bridge

Analysis

	ID	ECC
Building construction concrete (without rebars)	01.002	0.099
Reinforcement Steel	06.003	0.682
Solid spruce/pine/larch, chamber-dried, planed	07.011	0.143

Table 41. Coefficients for Felsegg's GWP

Multiplying the correspondent coefficient values with the above-computed material quantities it is possible to find the result of carbon emissions of Felsegg bridge.

$$\text{GWP} = 0.099 \text{ CO}_2\text{e/kg} \cdot 5110.6 \cdot 10^3 \text{ kg} + 0.682 \text{ CO}_2\text{e/kg} \cdot 138.2 \cdot 10^3 \text{ kg} + 0.143 \text{ CO}_2\text{e/kg} \cdot 172.0 \cdot 10^3 \text{ kg} = 6.25 \cdot 10^5 \text{ kg CO}_2\text{e}$$

Equation 14. Computation of Felsegg's GWP

Birs Bridge

Place	Year	Span	Width	Length	Rise	Ratio
Liesberg	1935	-	5.54 m	35.40 m	-	-
Dolomitic limestone						
Rigid frame, continuous beam						

Table 42. Characteristics of Birs Bridge [1]



Figure 63. Birs Bridge [43]



Figure 64. Geo-localisation of Bris Bridge to define its foundation soil [41]

Description

Birs Bridge is interesting because of different aspects. The first one to be considered is that it is the only analysed bridge not to be a car road, but to be a railway path. This aspect influenced all the design and the construction process, and it is at the base of all the following differences.

First, its design had to face different loads. In fact, the variable loads considered movements of trains instead of cars. As a means of comparison, in the present European norms [52] the difference is given mostly in the combination of the variable loads. For road bridges there are different load schemes and the highest value which is possible to find is in the first combination and in the first lane (9 kN/m^2). Considering that the width of the bridge is 5.54 m the distributed load would have been almost 50 kN/m for an equivalent road bridge, with the same dimensions. However, the distributed load for a railway bridge is the triple of it (150 kN/m). This is due to the fact that railways have to be designed to bear even freight trains which can be very much heavier than road trucks.

Thus, another aspect which differentiate this bridge with respect to the others is the structural scheme. This aspect is again directly linked to the fact that it is a railway and not a road bridge. Maillart designed it as a rigid frame, with continuous beam in order to be able to resist to the above-mentioned kinds of loads. The result is completely different from the previous bridges since it is straight, and it does not have a supporting arch structure.

So, the amount of reinforcement is completely different too. In fact, it is consistently higher than the other structures, since the load is directly supported by horizontal beams and not transferred to the abutments continuously as it happens in the arch systems. The amount of reinforcement is also increased in the piers to avoid their collapse and to guarantee enough resistance.

Volumes

The interesting part related to steel and concrete of this bridge is that the amount of reinforcement is much bigger than the equivalent quantity in the other bridges. The computed ratio between kg of steel and cubic meter of concrete is 307.9. This value is almost 5 times the amount used in the other arch structures which have a correspondent ratio around 60 and 80. However, the result can be considered reliable and not due to computational mistakes. In fact, in the original drawings [1] there is a specific section called “Dosierung” in which it is reported that in the main beams, including bays, there are 300 kg per m^3 of concrete and in the pillars there are 350 kg per m^3 of concrete. Since the obtained ratio is related to the entire structure and it is within the range between the two mentioned values in the project, it is considered reliable.

However, this difference with respect to the other bridges is linked to the structural scheme Birs Bridge itself. Without a supporting arch it is, indeed, necessary a greater amount of steel reinforcement to guarantee the stability and the safety of the structure, as well as the correct transmission of loads.

The problem of this bridge is in the scaffolding. Among the original documents [1] there are not pieces of information about the design of it, so it is not possible to compute directly its volume and mass.

As for the all other bridges the drawings are available from the original documents [1] stored in the ETH Archives, in Zurich. The boundaries of the structure are shown in the following figure (Figure 16) produced to compute the volumes.



Figure 65. Representation of the 3D model of Birs Bridge

	Volume [m ³]	Density [kg/m ³]	Mass [t]
Concrete	105.9	2 300	243.5
Steel	4.1	7 860	32.6

Table 43. Computed quantities of Birs Bridge

Analysis

	ID	ECC
Building construction concrete (without rebars)	01.002	0.099
Reinforcement Steel	06.003	0.682

Table 44. Coefficients for Birs' GWP

Multiplying the correspondent coefficient values with the above-computed material quantities it is possible to find the result of carbon emissions of Birs bridge.

Since data about scaffoldings are not available it is followed the same procedure, already adopted for Ziegenbach and Schrähbach Bridge. In fact, it is computed the ratio between the GWP of the previous structures with and without the contribution of timber. It is found that the contribution of timber increases the

kg of equivalent CO₂ of a 4%. Then, it is chosen to add this percentage to the available result in order to have numbers with similar meaning and close enough to be compared.

$$\text{GWP} = 1.04 (0.099 \text{ CO}_2\text{e/kg} \cdot 243.5 \cdot 10^3 \text{ kg} + 0.682 \text{ CO}_2\text{e/kg} \cdot 32.6 \cdot 10^3 \text{ kg}) = 4.82 \cdot 10^4 \text{ kg CO}_2\text{e}$$

Equation 15. Computation of Birs' GWP

Vessy Bridge

Place	Year	Span	Width	Length	Rise	Ratio
Geneva	1936	56 m	10.40 m	74.88 m	4.32 m	13
Breccias and conglomerates, strongly cemented sandstones, partly with schistose structure with deposits of phyllites.						
Hollow box 3 hinges arch						

Table 45. Characteristics of Vessy Bridge [1]



Figure 66. Vessy Bridge [43]



Figure 67. Geo-localisation of Vessy Bridge to define its foundation soil [41]



Figure 68. Internal structure of Vessy bridge [53]

Description

The last analysed bridges could be seen just as the developments of three-hinged arches which culminated in the masterpiece at Vessy [32]. In this structure Maillart expressed again his revolutionary ideas: he introduced x-shaped cross walls between the deck and the arch, and he moved the two abutment hinges into the span. Moreover, he added a vertical cut at the centre hinge, emphasizing the arch's discontinuity [33]. The X shape of the walls (Figure 68) matches the distribution of the bending moments caused by temperature expansion of the deck. They can also be explained by the improved cross-diagonal view, which at the time was not yet covered by vegetation [39]. The aesthetical contribution, in this sense, is exceptional, at the point that this pattern of lines on X shapes resembles the painting *Doppelzelt*, by the Swiss artist Paul Klee [33].

Volumes

As already happened for other bridges, the quantity of materials is not computed from drawings, but directly from additional documents which are parts of the whole available project [1]. As far as both concrete and steel are concerned, their amounts are available due to the price list used to compute the final cost of the structure. In particular, the list is composed of the amount of the different used structural materials (m^3 for concrete and kg of steel), their generic position (foundation, structure, super-structure) and their cost.

The quantity of steel is also available from the so called "Eisenliste" which is an additional part of the whole project [1]. As in other situations, this document shows the position, the length and the mass of each steel rebars and respectively the total quantities. This datum is not really necessary, since the mass is already known from the price list, but it can be used as a reciprocal proof of the validity of the two documents. In fact, the two numbers are the same, so the data can be considered even more reliable.

The volume of timber is not present in the above-mentioned price list thus, it is computed as usual, so through a 3D model, starting from the paper original drawings [1]. The interesting aspect about the scaffolding is that,

as mentioned in the introduction part, Maillart tried to minimize the amount of the materials, not only through the design itself of the scaffolding, but also during the process of construction.

Looking at the shape it is possible to see that a horizontal beam divided the structure in an upper part and a bottom one. The bottom part is composed of several piles equally distanced of 2 m, along the entire development of the bridge's cross section which is 10 m. Their presence guaranteed the stability of the entire structure, so their placement was fixed and constant during the whole construction process.

In the other hand, the upper part was used to allow the actual construction of the cross section. The geometry of it, is composed of three consecutive hollow boxes, equal from each other, thus, the scaffolding used to support everyone of each part was actually moved after the construction of the previous one. This means that the same upper scaffolding was used to build the first hollow box, after that the second one and at last the third one.

The computed volume is, then, made of the complete bottom part and the movable upper part. Thus, as never happened before, the total volume is not coincident with the actual volume occupied during the construction process.

	Volume [m ³]	Density [kg/m ³]	Mass [t]
Concrete	697.8	2 300	1 605.0
Steel	6.2	7 860	48.4
Timber	65.3	465	30.3

Table 46. Computed quantities of Vessy Bridge

Analysis

	ID	ECC
Building construction concrete (without rebars)	01.002	0.099
Reinforcement Steel	06.003	0.682
Solid spruce/pine/larch, chamber-dried, planed	07.011	0.143

Table 47. Coefficients for Vessy's GWP

Multiplying the correspondent coefficient values with the above-computed material quantities it is possible to find the result of carbon emissions of Vessy bridge.

$$\text{GWP} = 0.099 \text{ CO}_2\text{e/kg} \cdot 1605.0 \cdot 10^3 \text{ kg} + 0.682 \text{ CO}_2\text{e/kg} \cdot 48.4 \cdot 10^3 \text{ kg} + 0.143 \text{ CO}_2\text{e/kg} \cdot 30.3 \cdot 10^3 \text{ kg} = 1.96 \cdot 10^5 \text{ kg CO}_2\text{e}$$

Equation 16. Computation of Vessy's GWP

Parallel catalogue: non Maillart's Bridges

Langwieser Bridge by Schürch

Place	Year	Span	Width	Length	Rise	Ratio
Langwieser	1914	100 m	3.70 m	284 m	42 m	2.4
Elastic arch and monolithic beam						
Silty sand, usually clayey, often with blocks or mixed with cobbles or blocks.						

Table 48. Characteristics of Langwieser Bridge [54]



Figure 69. Langwieser Bridge [54]



Figure 70. Geo-localisation of Langwieser Bridge to define its foundation soil [41]

Description

Langwieser Bridge is 284 m long and it is the biggest structure of the Rhätische Bahn (RhB). It is a cultural asset with national importance since it is one of the most famous bridges of Switzerland. It was also the first railway concrete bridge of these dimensions, at the time of its erection, the Langwieser Viaduct was the longest railway bridge in the world. It was built between 1912 and 1914 by the private society Chur-Arosa Bahn (ChA). The chief engineer of the entire construction, Gustav Bener, wanted to build as many bridges and walls as possible of the railway in natural and local stone. In fact, stone is a very common construction material in that zone due to the presence of the river Plessur which guaranteed enough for similar constructions. Thus, the iron and concrete structures should have been designed only where the stone was not possible to be used because of the instability of the banks of the rivers or the insufficient bearing capacity of the soil. The kind of soil was exactly the reason why Langwieser Viaduct was chosen to be built in concrete. The presence of sand and gravel was not enough to give good properties to the foundation soil and even with a great amount of stone, a bridge would have been very difficult to be built there. Due to the problems of transportation also iron was excluded, leaving concrete as the only possible alternative. The leading engineering for the design and the construction of the structure was Hermann Schürch. The static computations were done by the Strasburg technical office of Karl Arnstein while the construction supervisor in the building site was followed by the engineer J. Müller with others local personalities such as A. Zwygart e J. Fleury. The final proof of the efficiency of the bridge was given by the final loading test when the bridge had a deflection less than 1 mm even if it was loaded by a steam locomotive and three heavily loaded freight cars. The final cost was around 625 000 CHF, without considering the reinforcement and the spare superstructure [54].

Volumes

Even if the original drawings are not available there are enough data from online sources to deduce the amount of the used materials. In fact, it is known that during the construction 250 tons of reinforcement steel were used, as well as 7469 m³ of concrete. It is interesting to underline also that this amount of concrete was higher than the initial expected one. The designed quantity was 4861 m³ but the difference of 2608 m³ was due to the variety of foundations that were necessary to be built [54].

As far as the scaffolding is concerned, it is known that 800 m³ of timber were used in order to support the principal arch. As already happened for many bridges of the same period, the cast arch was used as supporting structure itself for the rest of the structure, in order to save materials for the scaffolding. That is why the only used timber was the one supporting the arch itself. The design was merit of the well-known carpenter Richard Coray who worked, as already mentioned, in some of the Maillart's projects too [54].

As explained in the outline part of the catalogue, it happened that Coray used the same scaffoldings for different structures in Fribourg [42], but those two bridges were not isolated cases because the same dynamic also happened for a structure of the same railway of Langwieser. For the Gründjitobel Viaduct, indeed, he used the same scaffolding as Halen Bridge in Kirchlindach, in Bern. Even if it is technically different, this last-

mentioned viaduct is considered the “little brother” of Langwieser one because it is the second longest bridge of the RhB with an arch span of 85 m and a total length of 139 m. However, it is known that for the Langwieser itself the scaffolding was only used ones.

	Volume [m ³]	Density [kg/m ³]	Mass [t]
Concrete	7 469.0	2 300	17 178.7
Steel	318.0	7 860	250.0
Timber	800.0	465	372.0

Table 49. Computed quantities of Langwieser Bridge

Analysis

The coefficients chosen for the computation of the embodied carbon, are the ones of KBOB. The same assumptions as the ones done for the Maillart's bridges are considered for this bridge. The main reason for this choice is that the bridge was designed in the same period as Maillart's one and in Switzerland as well. So, it is possible to presume that the construction materials were very similar, thus the following coefficients are selected:

	ID	ECC
Building construction concrete (without rebars)	01.002	0.099
Reinforcement Steel	06.003	0.682
Solid spruce/pine/larch, chamber-dried, planed	07.011	0.143

Table 50. Coefficients for Langwieser 's GWP

Multiplying the correspondent coefficient values with the above-computed material quantities it is possible to find the result of carbon emissions of Langwieser bridge.

$$\text{GWP} = 0.099 \text{ CO}_2\text{e/kg} \cdot 17178.7 \cdot 10^3 \text{ kg} + 0.682 \text{ CO}_2\text{e/kg} \cdot 250.0 \cdot 10^3 \text{ kg} + 0.143 \text{ CO}_2\text{e/kg} \cdot 372.0 \cdot 10^3 \text{ kg} = 1.92 \cdot 10^6 \text{ kg CO}_2\text{e}$$

Equation 17. Computation of Langwieser 's GWP

Tamina Bridge by LAP

Place	Year	Span	Width	Length	Rise	Ratio
Valens	2017	260 m	9.50 m	473 m	36.75 m	7.1
Hollow box arch and continuous beam						
Limestone often with marly interleaves						

Table 51. Characteristics of Tamina Bridge [55]



Figure 71. Tamina Bridge [55]



Figure 72. Geo-localisation of Tamina Bridge to define its foundation soil [41]

Description

Tamina Bridge is the largest arched bridge in Switzerland: it connects the two villages of Pfäfers and Valens, which were previously separated by the deep Tamina gorge. The whole bridge was designed in 2013 by the Leonhardt, Andrä und Partner's. The structure consists of an arch and a continuous beam, which is monolithically connected to the arch via horizontal element shafts and arched supports. The vertical elements are monolithically connected to the horizontal elements and superstructure, and are essentially designed as a rectangular, walk-on cross-section [56]. The superstructure is 417 m long, but including the abutments the total length is 473 m. The road width between the concrete barriers is 9.5 m. Moreover, most of the arch cross-section, roughly from the foundations to the short central columns, is a hollow box in order to save weight [57]. The rise is derived from available plan [58] and considering that the two edges of the arch are placed at two different altitudes so an inclined line connecting them is drawn. Then, a perpendicular line is added, from the middle point of the first one, until it reaches the lower part of the arch itself. The length of this second line perpendicular to the first one is considered the rise of the arch.

Therefore, the structural engineer originally intended the arc and superstructure to be designed as a cantilever. but at end, after some simulations the opted for designing only the arc as a cantilever, but building the superstructure using conventional supports erected on the arc. Thus, the arch is erected from both sides [55].

Volumes

In order to compute the volumes, complete original drawings or 3D models are not available. However, in some of the technical documents [59] there are data about the order of magnitude of the amount of the used materials. In fact, it is known that they installed a total of 14,000 cubic meters of concrete, 3,500 tons of reinforcement, 245 tons of pre-tensioned strands and 190 tension member anchorages. The total weight of the bridge is 35,000 tons. The building costs are 37 million Swiss francs. The concrete class used for the structure is C45/55, the retention cables are made by 7 to 24 single strands which have a steel grade of St 1680/1860 with a cross-section of 150 mm² and a tensile strength of 1860 N/mm² [55]. So, it is possible to derive the needed quantities, useful to compute, in the analysis part, the GWP. The strands and cables mentioned before, are part of the reinforcement steel because they are parts of the pre-compressed concrete. So, their masses are included in the reinforcement steel. In fact, the structure is divided in a prestressed concrete deck and a simple reinforced concrete arch. That is why the amount of the strands is specified.

As far as the scaffolding is concerned it is described that it was chosen to be used a ground-supported scaffolds. Conventional scaffolding for the arc and superstructure was eliminated from the outset due to the gorge depth of 200 meters [55]. Auxiliary pylons made of steel were installed on the side of the imposts' foundations and 820 t of steel on the Pfäfers side and 520 t of steel on the Valens side was used for the temporary towers [57]. Thus, for the scaffolding towers 1340 t of steel are used. The interesting aspect is that in this case, since it is a modern bridge the scaffolding is not built in timber as was usual in Maillart's construction.

	Volume [m ³]	Density [kg/m ³]	Mass [t]
Concrete	14 000.0	2 300	32 200.0
Steel	N/A	N/A	3 500.0
Timber	N/A	N/A	1 340.0

Table 52. Computed quantities of Tamina Bridge

Analysis

The coefficients chosen for the computation of the embodied carbon, are the ones of KBOB [2]. However, not always the same assumptions as before are done for them, because the materials are different from the past ones thus the followings are selected:

	ID	ECC
Building construction concrete (without rebars)	01.002	0.099
Reinforcement Steel	06.003	0.682
Steel profile, blank	06.012	0.734

Table 53. Coefficients for Tamina 's GWP

- Building construction concrete (without reinforcement)

The coefficient is the same as the one used in the previous analysis because it is just related to the construction concrete. As already explained in the outline part, it is the same as to the one of the present times, so it does not change from the value used for Maillart's bridges.

- Reinforcement steel

The same motivations can be used to explain why this coefficient is not different from the one used until now in the catalogue part. Since it is not possible to relate these coefficients to the year of the actual construction process, also for the reinforcement steel the value does not change.

- Steel profile, blank

This coefficient is chosen for the towers steel. In fact, the used material is assumed as the most common one for the present constructions. Since no other specifications are underlined in the technical documents [59] it is possible to think that there is nothing special in the material construction and so the ordinary steel is used.

Multiplying the correspondent coefficient values with the above-computed material quantities it is possible to find the result of carbon emissions of Tamina bridge.

$$\text{GWP} = 0.099 \text{ CO}_2\text{e/kg} \cdot 32\,200 \cdot 10^3 \text{ kg} + 0.682 \text{ CO}_2\text{e/kg} \cdot 3\,500 \cdot 10^3 \text{ kg} + 0.734 \text{ CO}_2\text{e/kg} \cdot 1\,340 \cdot 10^3 \text{ kg} = 6.56 \cdot 10^6 \text{ kg CO}_2\text{e}$$

Equation 18. Computation of Tamina's GWP

Analysis

Elaboration of data

The catalogue section presents the GWP values of all discussed bridges. Figure 74 shows all the obtained values of the 15 chosen bridges, in chronological order. However, these numbers are not comparable. In fact, the analysed structures have very different geometric characteristics: as it is possible to see in the catalogue they differ from length and width of the deck, and from span and rise of the arch. Every one of these aspects influences the total amount of material used in the construction process. That is why, it does not make sense to relate directly the absolute values of the GWP: the biggest bridges would seem to always have the highest impact and the other way around. The following discussion focuses on finding a way to normalise them. It develops different normalization criteria and, after that, highlights possible trends, where they exist, linked to geometrical or structural properties.

In fact, the aim of this part is to understand if there is an additional reason which leads the GWP value, apart from the material quantities.

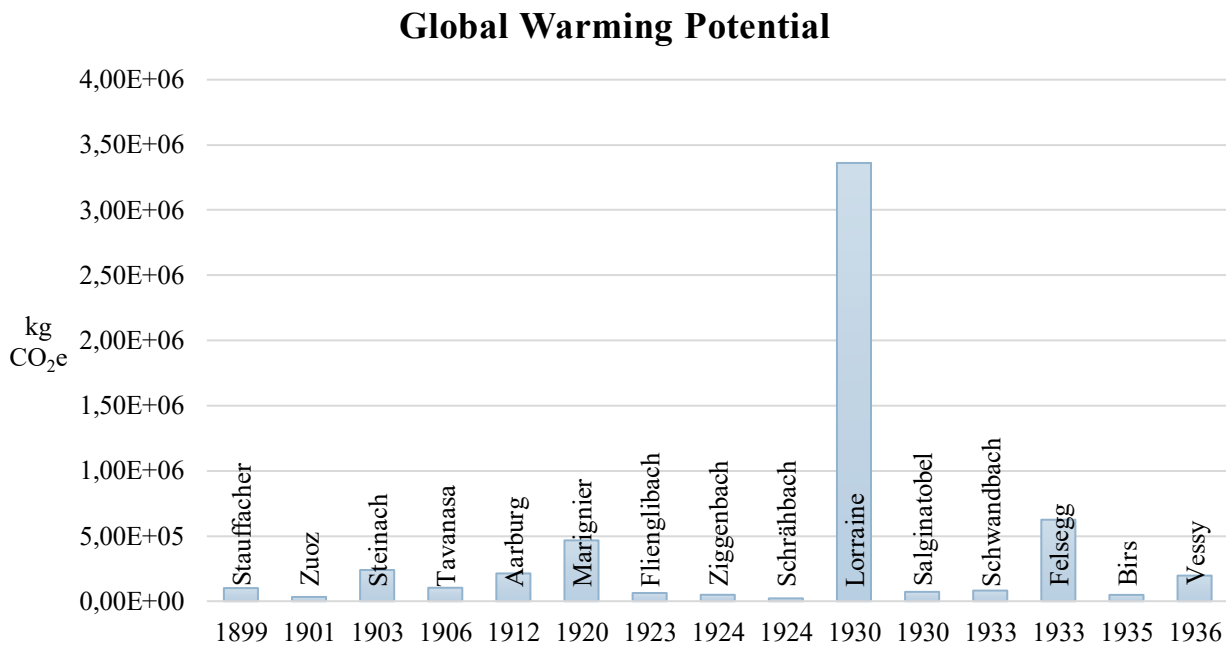


Figure 73. Absolute GWP of the analysed bridges

A first possibility is to correlate directly material quantities and the GWP. For this analysis it is chosen to initially exclude the contribution of timber. Since data about the scaffolding are not available for all the structures, comments on the impact of timber will be done afterwards in a specific section. Considering the other three construction materials, concrete, steel, and masonry, related to the existing bridge itself, it is possible to see that the kg of eq. carbon dioxide follows more or less the same shape of the material distribution (Figure 74). However, the distribution is not exactly the same. In fact, if the data of both quantities (materials

amount and GWP) are ordered with an increasing trend, the classification of bridges is not exactly the same in the two situations. In the cases where the amounts of used material are close to each other, the impact of steel ($ECC = 0.682$) and after that of timber ($ECC = 0.143$) influence more the final result and lead to a higher value of GWP with respect to a different bridge built with different amounts, but maybe higher kg of total materials.

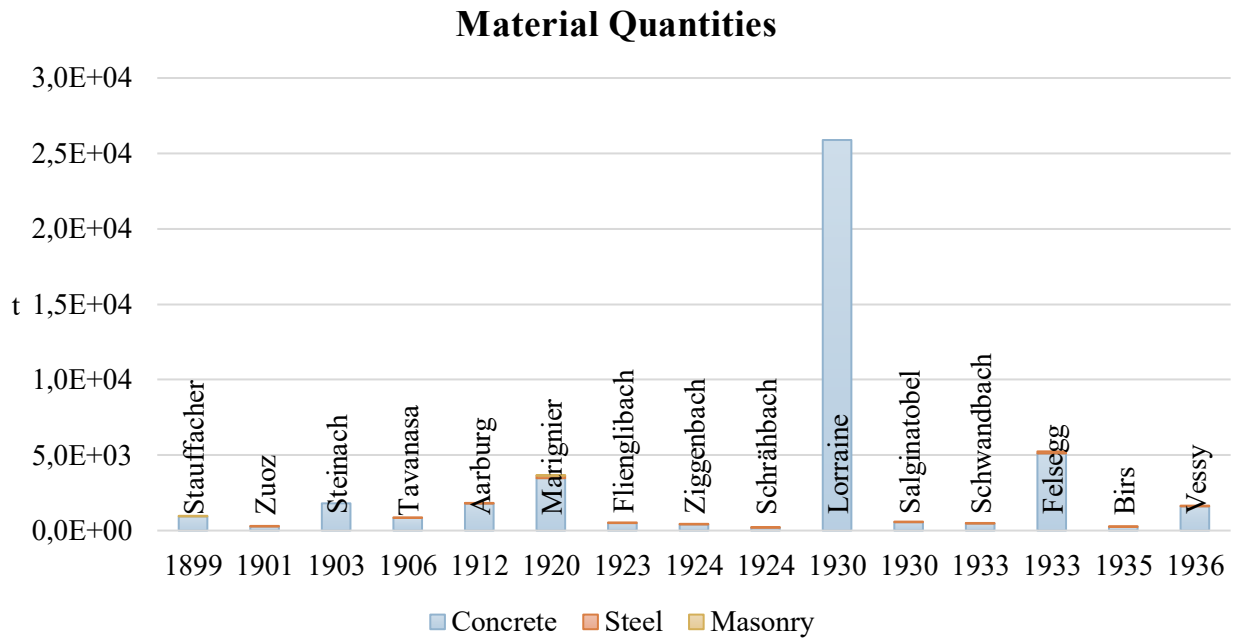


Figure 74. Material quantities of the analysed bridges

Since Lorraine Bridge is much bigger than the other ones it is even possible to exclude it from the figure to scale the data and see more clearly the amount of materials for the other structures (Figure 75).

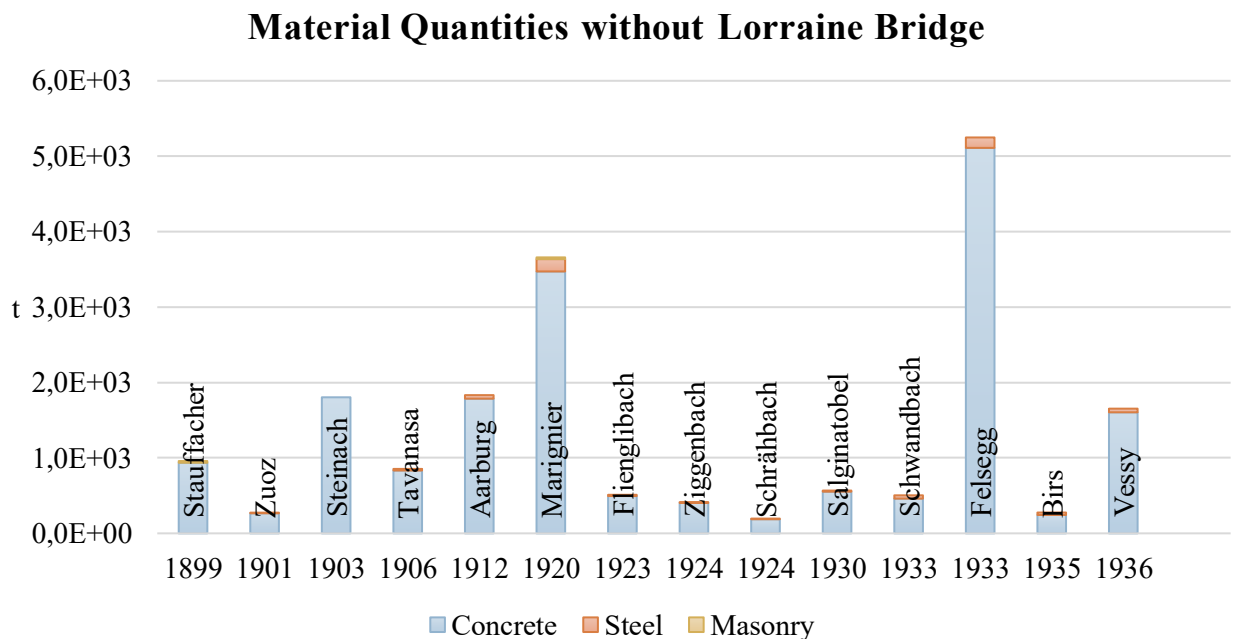


Figure 75. Material quantities of the analysed bridges apart from Lorraine Bridge

The influence of each material can be also seen explicating the total value of the GWP as the combination of the different materials, multiplied by the right coefficient. In fact, in this case (Figure 76), the contribution of every material on the final value of the GWP is more evident. It is also clear how the influence of concrete has less weight because of the small value of its coefficient compared to the contribution of steel which has a much higher impact, even if it usually has a considerably small mass for the same performance.

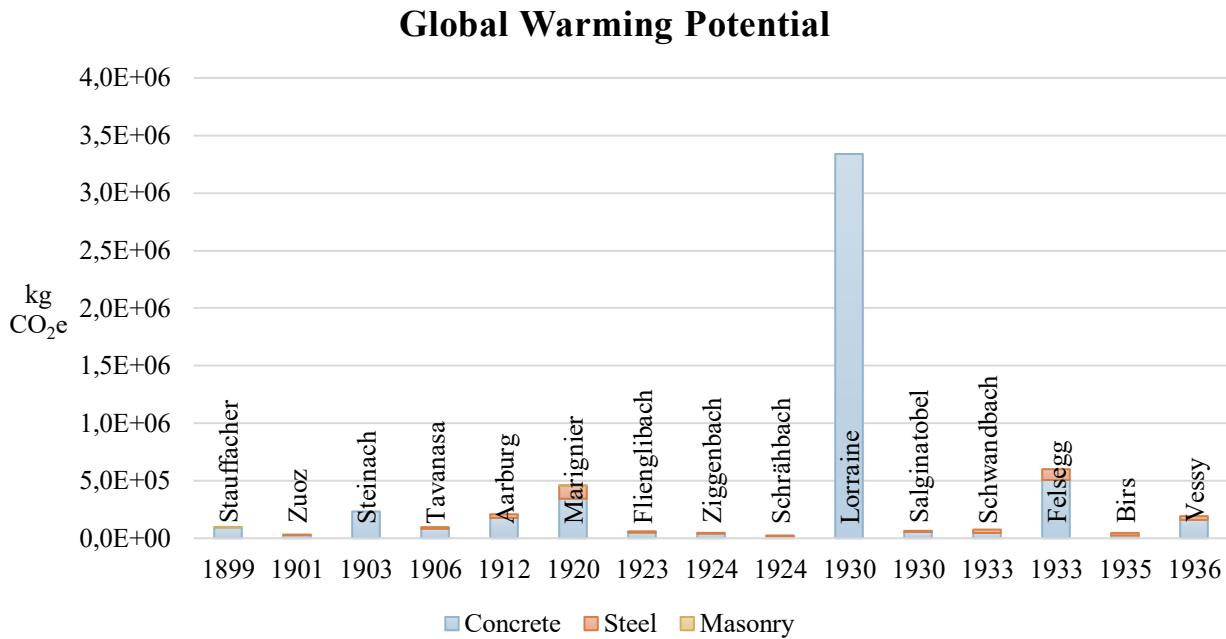


Figure 76. GWP, with the contribution of each material to the total GWP

Normalization criteria

Starting from the differences between all the 15 analysed structures, several normalisation strategies are used: the first one considers a 2D normalisation process, the second one a 1D normalisation process. After that a criterion is chosen to select the best normalisation procedure and to keep using the normalized data for the following clustering strategies.

Per deck area

In the first case the SMQ of each bridge are divided by its deck area (Figure 101, Appendix) so, the resulting GWP values are expressed in kg CO₂e per m² (Figure 102). They express, indeed, the carbon dioxide produced for every m² of the deck of the analysed bridge, according to the following formula.

$$GWP = \sum_{i=1}^n ECC_i \cdot \frac{SMQ_i}{L \cdot W}$$

Equation 19. Normalisation criterion of GWP per deck area

Where

GWP = Global Warming Potential (kg of CO₂e)

ECC = Embodied Carbon Coefficient (kg of CO₂e per kg of material)

SMQ = Structural Material Quantity (kg)

L= Length of the deck of the bridge (m)

W= Width of the deck of the bridge (m)

Comparing the contribution of different materials, after the normalisation, is even more interesting to visually have a perception of the weight each one has on the final normalised GWP value. Even in this case, all the bridges are considered, but the contribution of timber is excluded and discussed in the following section.

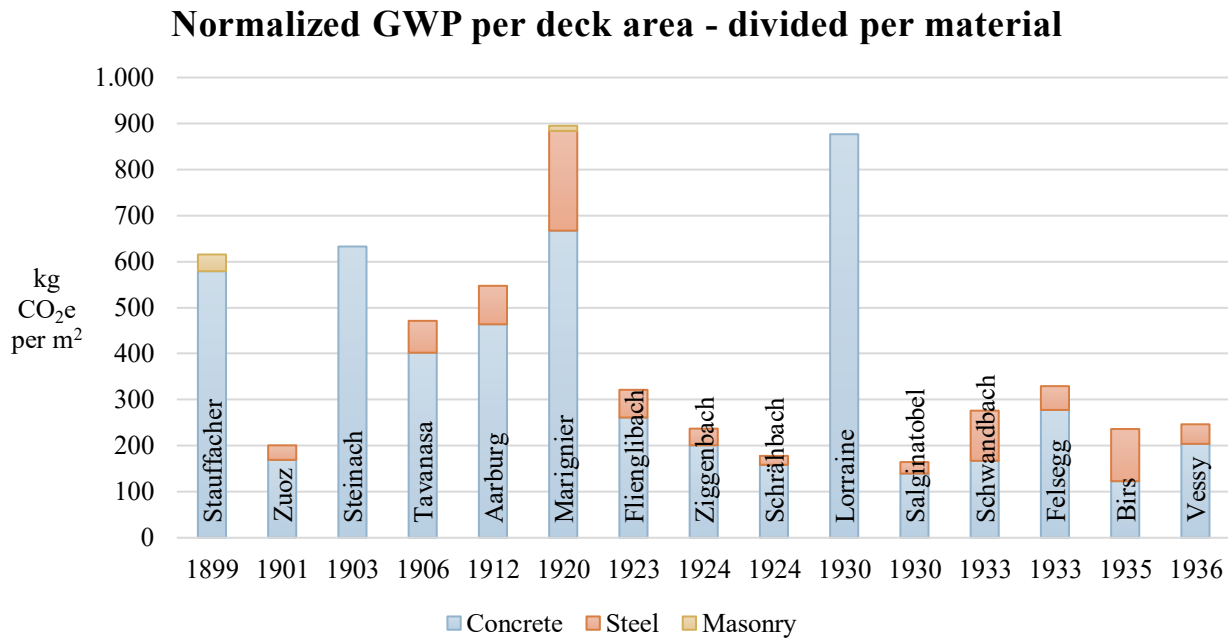


Figure 77. Normalised GWP per deck area, divided per material

Per span and per rise

A second possible normalisation procedures could be done according to singular geometrical properties, such as the span of the arch and its rise. The width and length of the deck could be other two possible one-dimensional quantities, available for the normalisation. However, they are excluded because they have already been used in the first normalisation strategy.

The only problem with the procedure based on the arch parameters is that it cannot be used for all the studied structures. In fact, the Birs bridge, for its geometrical configuration, is not supported by an arch. For this reason, the span and the rise cannot be used for it as references.

$$GWP = \sum_{i=1}^n ECC_i \cdot \frac{SMQ_i}{S}$$

Equation 20. Normalisation criterion of GWP per span

Where

GWP = Global Warming Potential (kg of CO₂e)

ECC = Embodied Carbon Coefficient (kg of CO₂e per kg of material)

SMQ = Structural Material Quantity (kg)

S= Span of the arch of the bridge (m)

$$GWP = \sum_{i=1}^n ECC_i \cdot \frac{SMQ_i}{R}$$

Equation 21. Normalisation criterion of GWP per rise

Where

GWP = Global Warming Potential (kg of CO₂e)

ECC = Embodied Carbon Coefficient (kg of CO₂e per kg of material)

SMQ = Structural Material Quantity (kg)

R= Rise of the arch of the bridge (m)

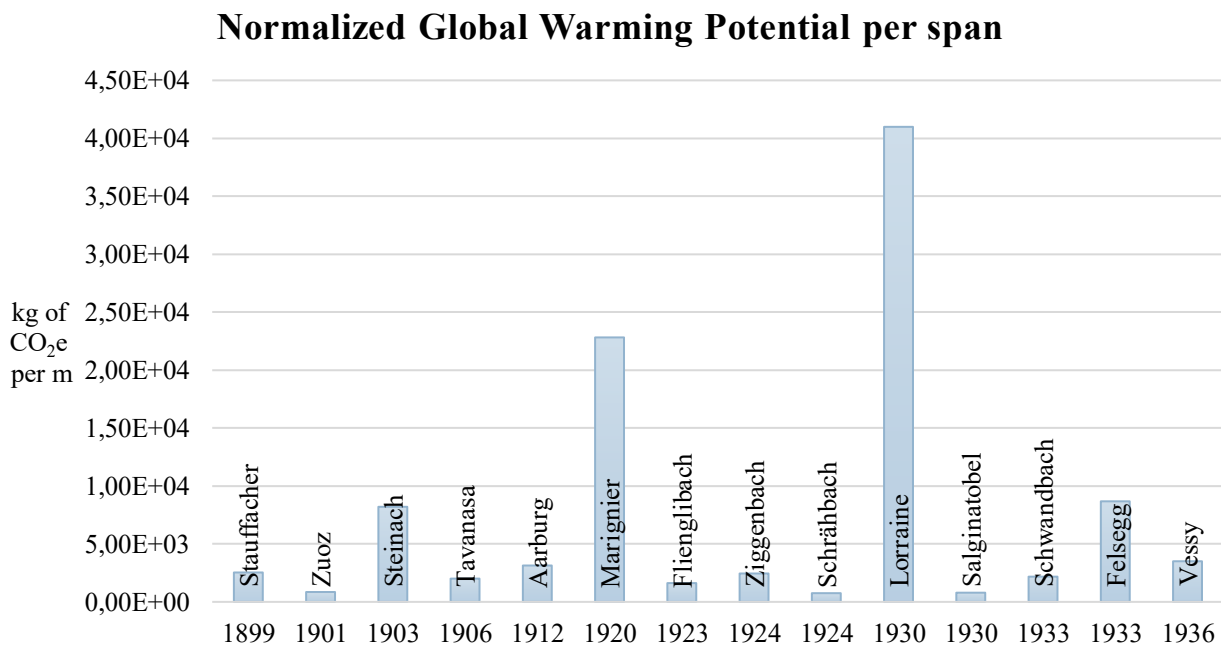


Figure 78. Normalised GWP per span

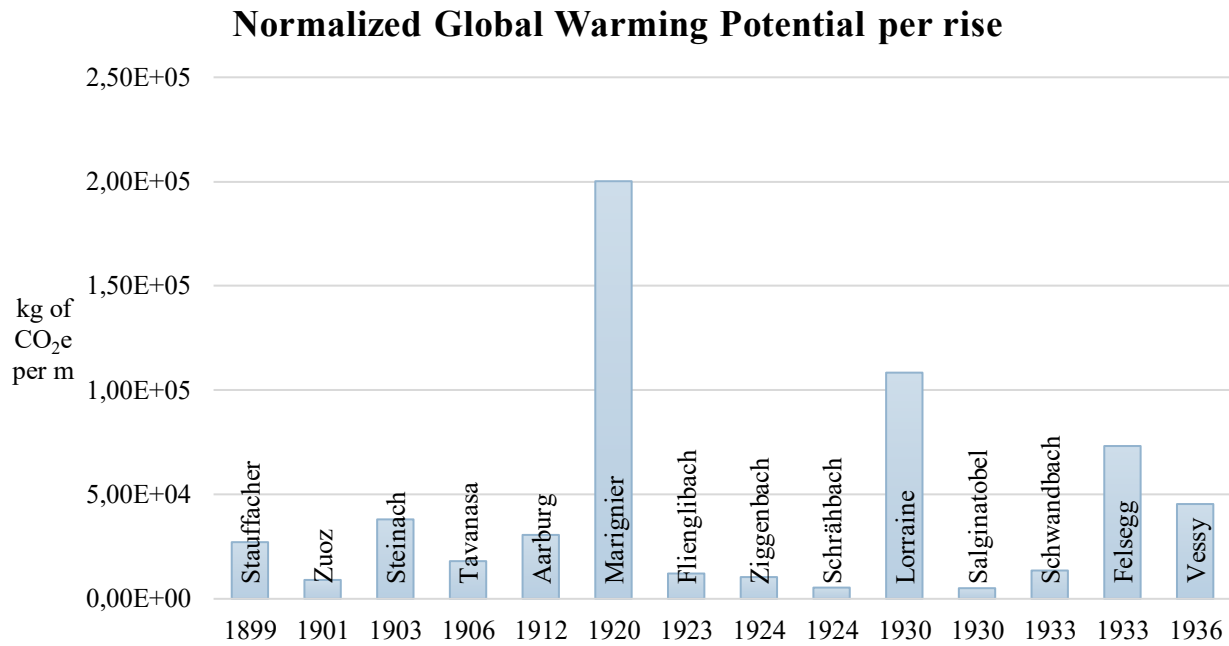


Figure 79. Normalised GWP per rise

Among all these three strategies, it is necessary to select a choice criterion to define the most performance normalisation procedure. It is possible to think that the first goal to achieve when data are normalised is to make them comparable and so to reduce the variation range in which the data themselves are distributed. In order to highlight this described performance of the different strategies, the following table (Table 54) is presented.

In fact, it shows the minimum and the maximum values of the absolute GWP of the 15 structures and their difference. Then, it shows the same variation range between the min and the max of the normalised procedure and among these, the one which has the smallest Δ is chosen as the best one. It is found that, according to this criterion, the worst technique is the normalisation per rise because the variation range of the data is reduced only by one order of magnitude with respect to the initial one, related to the absolute values of GWP. The best method is, instead, the choice of the deck area as unit. In this case the maximum and the minimum values differ much less than in all of the other cases. Moreover, this choice is even better from a physical and performance point of view since the deck is exactly what the bridge is used for.

	GWP (Absolute)	NGWP (deck area)	NGWP (span)	NGWP (rise)
Min	2,16E+04	1,82E+02	7,51E+02	5,10E+03
Max	3,36E+06	9,06E+02	4,10E+04	2,00E+05
Δ	3,34E+06	7,24E+02	4,02E+04	1,95E+05

Table 54. Variation ranges of GWP according to the different normalisation strategies

This is why this normalisation procedure is chosen as the best one and as the reference for the following clustering strategies.

Timber contribution

In this section, the goal is to include the data of the scaffolding for the structures for which they are available. This analysis is meant to quantify the impact of the scaffolding over the full structure. In the first graph (Figure 80) there are data related to the absolute GWP only due to timber and only of the structures for which the scaffolding was known. Then, in the second graph (Figure 81), to the same numbers are normalised according to the chosen method above described, so per deck area.

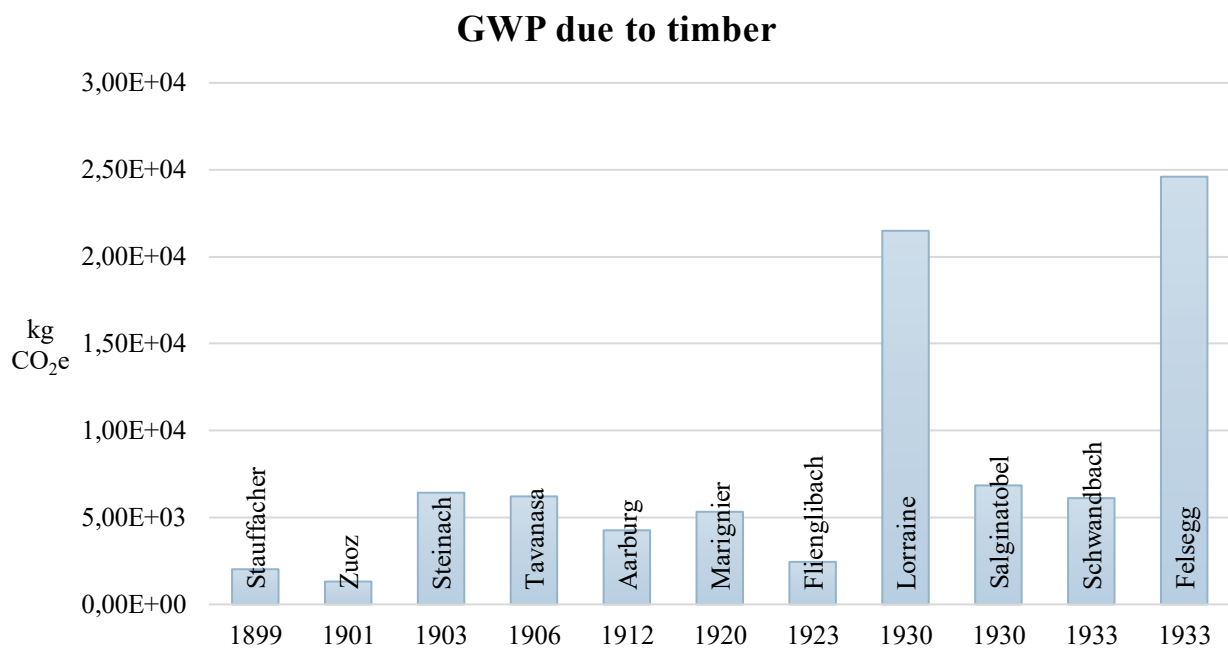


Figure 80. GWP due to timber

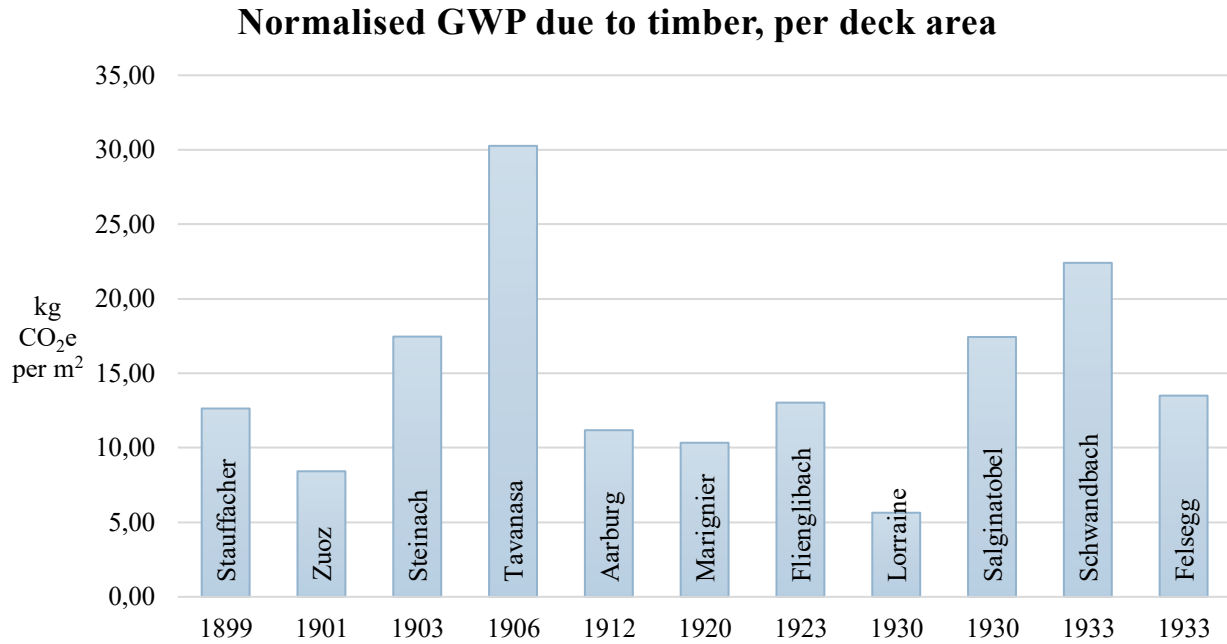


Figure 81. Normalised GWP due to timber, per deck area

The normalisation partly inverts the initial graph with the absolute values. While in Figure 80 the highest numbers are Lorraine's and Felsegg's ones, much bigger than all the ones related to the other structures, in Figure 81 Lorraine Bridge, after the normalisation, has the lowest value and Felsegg Bridge's values is lower than many other bridges. The normalisation anticipates also the trend of the following graph (Figure 82). In this last figure, indeed, the same structures are considered, and the environmental impact of their scaffoldings is compared with the total equivalent carbon emissions. The percentages represent exactly the ratio between the GWP due only to timber and the one produced considered also concrete, steel and masonry. The similarity between these two graphs lies mostly in the extremities. In both situations the minimum and the maximum values are mostly assumed by the same structures. The others assume numbers closely oscillating around the averages. In Figure 81 the average is 14 kg CO₂e/m², while in Figure 82 the medium value is 3.65%. In fact, in both Figure 81 and Figure 82, Lorraine remains the structure with the lowest relative impact (a bit more than 5 kg CO₂e/m² and less than 1%), Felsegg which had the second highest absolute GWP, stays among the average numbers while Tavanasa, Salginatobel and Schwandbach occupy the podium of the biggest normalised carbon equivalent emissions and percentages.

Even if these similarities are present among the extreme values, the relative "position" between a random couple of structures changes. Examples of this are the followings: in one graph Tavanasa has the highest kg CO₂e/m² while in the other has the third highest percentage. Same reverse opposite of Salginatobel Bridge. However, both bridges with Schwandbach remain the top ones with the highest normalised GWP and the timber's GWP.

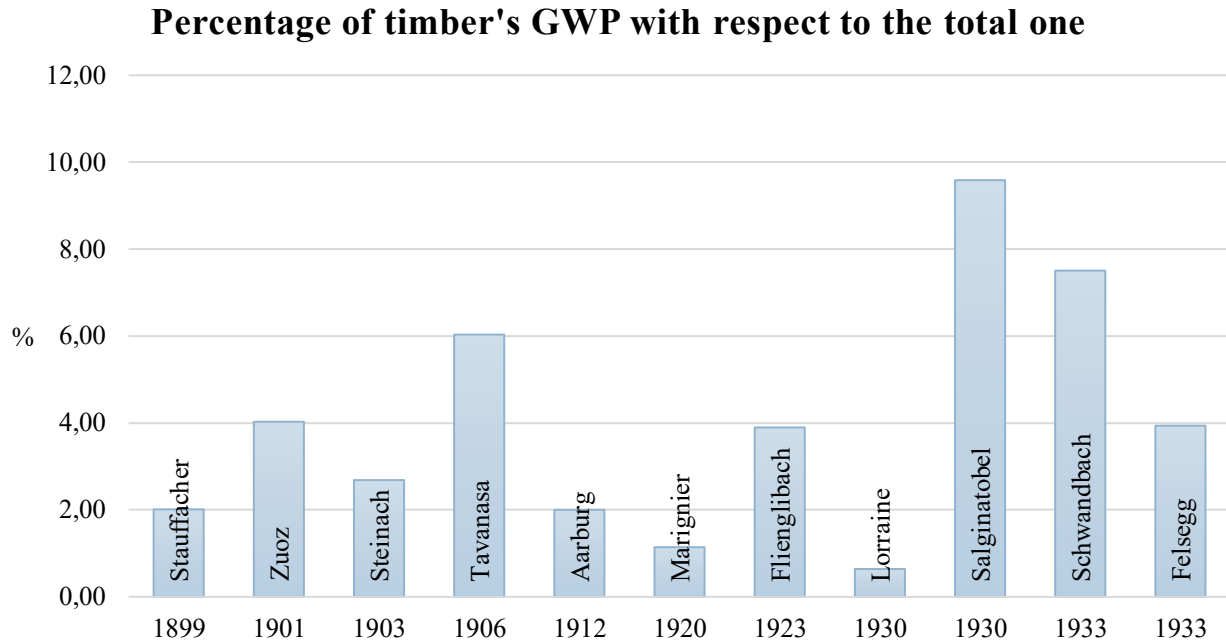


Figure 82. Percentage of GWP due to timber with respect to the total one

Clustering strategies

The first aspect that can easily and already be deducted from the normalisation procedures is that the GWP do not follow a temporal development. There is not a trend of increasing or decreasing values in the analysed bridges, so the goal of this section is to find if there are other parameters that influence carbon dioxide equivalent emissions of the construction processes. As already explained, from that point to the end, the used values of the GWP are not the absolute ones computed only from the combination of the SMQ and the ECC, in the catalogue, but are the ones obtained according to the normalisation strategy per deck area.

Moreover, as already mentioned in the catalogue outline, there are several criteria which can be used to classify these bridges and those same criteria can be also used to create clusters as well and verify if the similarities among them according to specific characteristics lead also to similar or meaningful values of GWP.

Structural classification

- Three hinged arches
- Massive Classical Arch bridges
- Deck arch bridges
- Deck-Stiffened arch bridges
- Rigid frame bridges
- Continuous girder bridges

Every one of these different static schemes corresponds to a different way to bear external loads. However, the following analysis does not follow exactly the same above-mentioned 6 classes. There are good examples of

the first four classes. The only needed clarification is that the massive classical arch bridges are considered the equivalent of concrete-block arches. However, the last two ones are exceptions. Within the 15 analysed bridges, no one of them is a rigid frame bridge or a continuous girder bridge. So, these two categories cannot be considered separately. The only example of them is Birs Bridge which is, indeed, a combination of the two. For this example, the two static configurations are couples together.

Moreover, the three hinged arches are distinguished according to the reinforcement and the characteristics of the cross section, separating, then, the hollow boxes from the unreinforced bridges. So, the final number of structural typologies is still six.

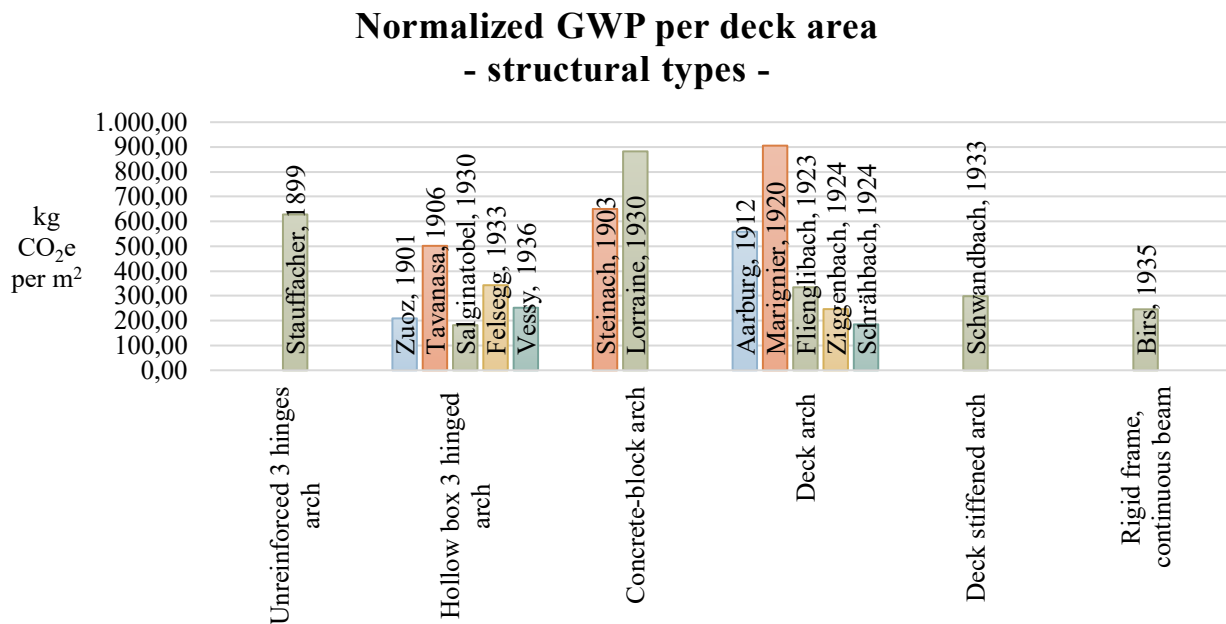


Figure 83. Normalised GWP per deck area, divided per structural type

Following this clustering method, it seems that the GWP of the same class of bridges does not follow any trend. The highest values are related to Marignier Bridge and Lorraine Bridge. But in neither of the two classes of these two bridges, the other structures have similar values. They have, instead much lower equivalent carbon emissions. The same evident differences are present in the hollow box three hinged arches class, where there is the bridge with the lowest value (Salginatobel Bridge): they have, indeed, an oscillating trend without any apparent link.

A possibility to well understand the differences between each structural class is to focus on steel. According to a different static scheme, a specific amount of reinforcement is needed. In fact, it is possible to analyse the amount of reinforcement (Figure 103, Appendix) and then divide it according to the same structural configurations above-mentioned (Figure 84). In both cases the numbers are referred to kg of steel per m³ of concrete. This ratio, as already explained in the Zuoz Bridge's analysis, is very useful in the construction field, also in present days, because it relates two different materials in a unique value, without considering the actual

placement of the rebars. In fact, it can give a general overview of the entire structure without distinguish cross section by cross section.

As expected, in the deck stiffened arches and for the combination of rigid frame and continuous beam, the amount of reinforcement steel is much higher than deck and three hinged arches.

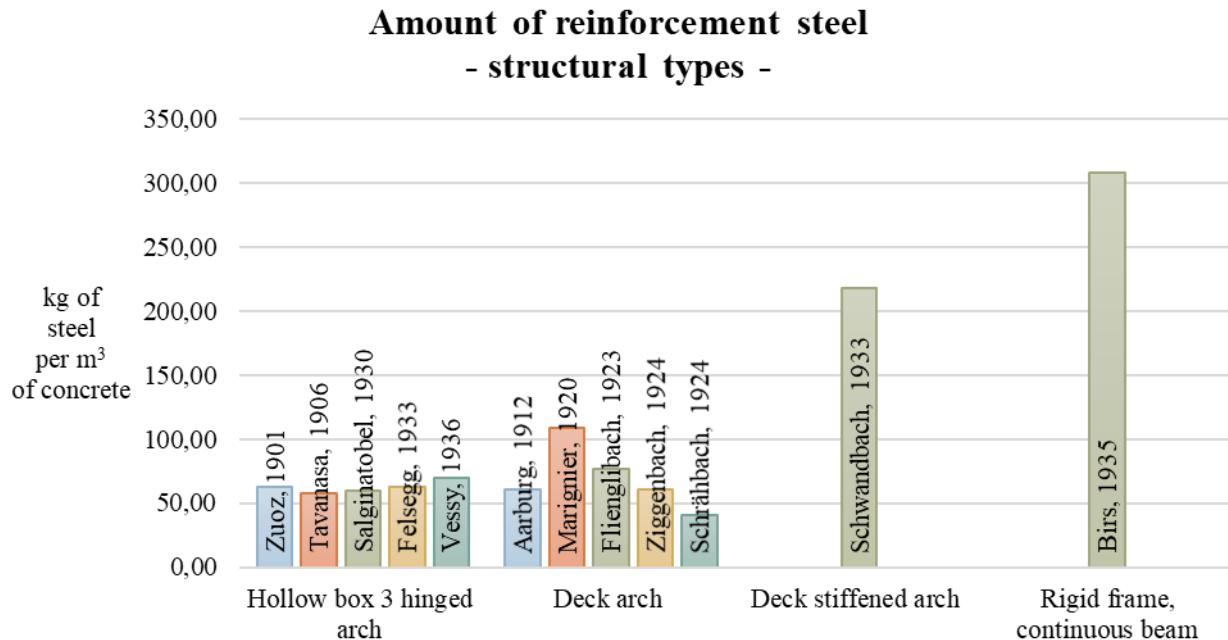


Figure 84. Amount of steel reinforcement, per structural type

Starting from the amount of reinforcement it is then possible to analyse the relative impact of GWP only due to steel with respect to the total GWP of each bridge. In fact, a similar graph to the one produced for timber (Figure 82) could be also useful for steel. The percentage values are produced at the same way. Directly dividing the amount of kg of equivalent carbon dioxide for the GWP of the whole structure lead to a knowledge about the impact of reinforcement over the full structure.

The percentage of the GWP only due to steel, with respect to the total one follows the same trend of the kg of steel with respect to m³ of concrete. It is possible to justify the similarities from a mathematical point of view: the ratio of the first graph is kg of steel over m³ of concrete; the ratio of the second one is GWP only due to steel over the GWP of the whole structure. In order to compare the two ratios, it is possible to think that the second one is similar to a scaled version of the first one according to specific assumption. If in the second ratio, the contribution of concrete is much higher than all the other materials, then it is true that it is the scaled version of the first one, using the ECC and the density to convert the quantities, from m³ to kg and then to GWP.

Moreover, it is very interesting to see how the percentage is much higher for steel than how it was for timber and how it achieves around 40% of the total impact both for Schwandbach and Birs Bridge.

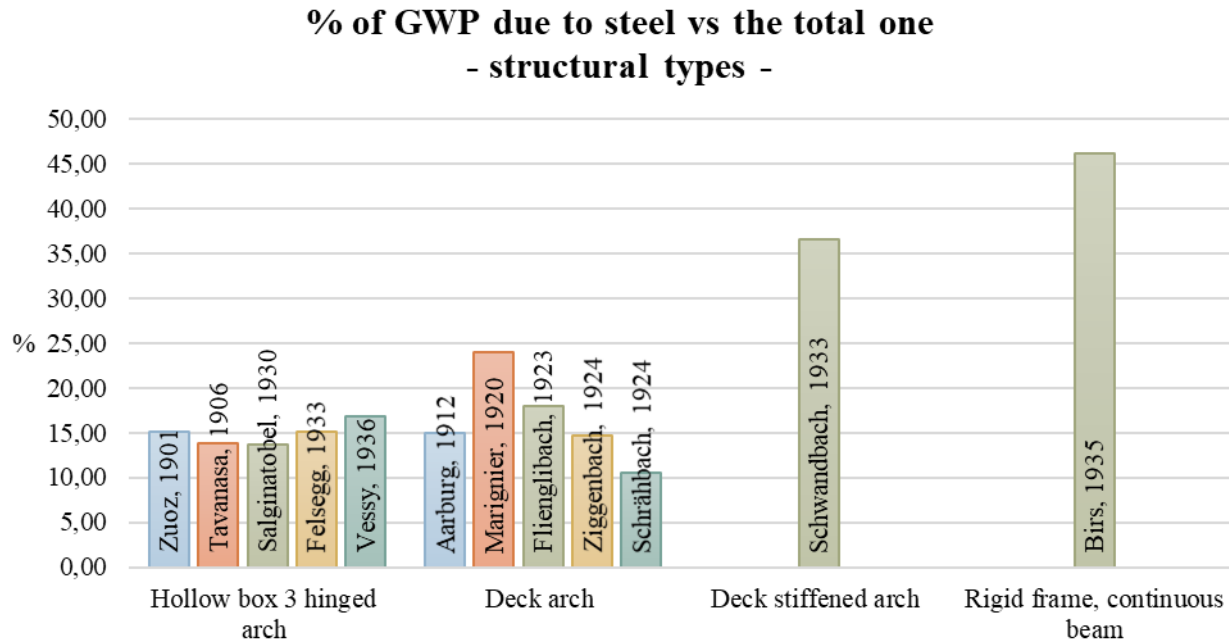


Figure 85. Percentage of GWP only due to steel over the total one, divided per structural types

Geometrical properties

- Span
- Rise
- Length
- Width
- Ratio between Span and Ratio

The classification through geometrical properties is done in order to understand the similarities between the different structures, if they exist, and to try to explain how their dimensions influence the GWP.

In every one of the following classifications it is chosen to create 4 classes which can divide the analysed bridges in non-empty sets. Moreover, the quantities which define the boundaries of these ranges are fixed considering that the classes should be spaced between regular intervals. Thus, they are divided as follow:

1. Span less than 30 m	1. Rise less than 4 m
2. Span between 30 m and 50 m	2. Rise between 4 m and 6 m
3. Span between 50 m and 80 m	3. Rise between 6 m and 8 m
4. Span bigger than 80 m	4. Rise bigger than 8 m
1. Length less than 40 m	1. Width less than 4 m
2. Length between 40 m and 70 m	2. Width between 4 m and 6 m
3. Length between 70 m and 100 m	3. Width between 6 m and 8 m
4. Length bigger than 100 m	4. Width bigger than 8 m

As already mentioned in the explanation of the second normalisation procedure, the span and the rise classification does not include Birs Bridge, which is not supported by an arch, so it cannot be considered a universal clustering method. However, these specific graphs are useful to find relationships between different structures.

If all the geometrical properties are considered, it is possible to find aspects which are common to all of them. Some of the structures, for example, are always in the same class no matter which geometrical parameter is considered for the clustering. The reasons for that is linked to the fact that some of them are much bigger or smaller than all the others. One of these is Schrärbach Bridge which is always in the first class because it is the smallest analysed structure as well as Lorraine Bridge which is always in the fourth one since it is the biggest chosen bridge. The interesting aspect is that this recurrent position is not valid only for the extreme structures, but also for the intermedium structures such as Flienglibach Bridge which is always in the second class.

However, it is also curious finding how, apart from specific and limited cases, the clustering according to different parameters do not gather the same structures. In every class of every graph, indeed, there are always different structures. Only few associations can be found as constant:

- Stauffacher Bridge and Schrärbach Bridge are always together in the first class apart from the graph related to the classification per span in which they are separated. In fact, Stauffacher is in the second class because it has a span bigger than 30 m, but smaller than 50 m.
- Lorraine Bridge and Felsegg Bridge follow the same kind of association because they are always together in the fourth class apart from the graph related to the classification per span in which they are separated. In fact, Felsegg Bridge is in the third class since it has a span within the range 50 and 80 m.
- The last association is between Flienglibach Bridge and Schwandbach Bridge which are always together in the second class apart from the graph related to the classification per rise in which they are separated. In fact, Schwandbach Bridge is in the third class since it has a rise bigger than 6 m, but smaller than 8 m.

This spread of data, is a hint of the fact that it is not easy or trivial to find relationships between a specific organisation of the structures and the linked carbon dioxide amounts. In fact, even if the geometrical properties are used to compute the GWP, they are not the reasons why it assumes that specific value instead of another one. Span, length, width and rise do not influence the GWP very conspicuously.

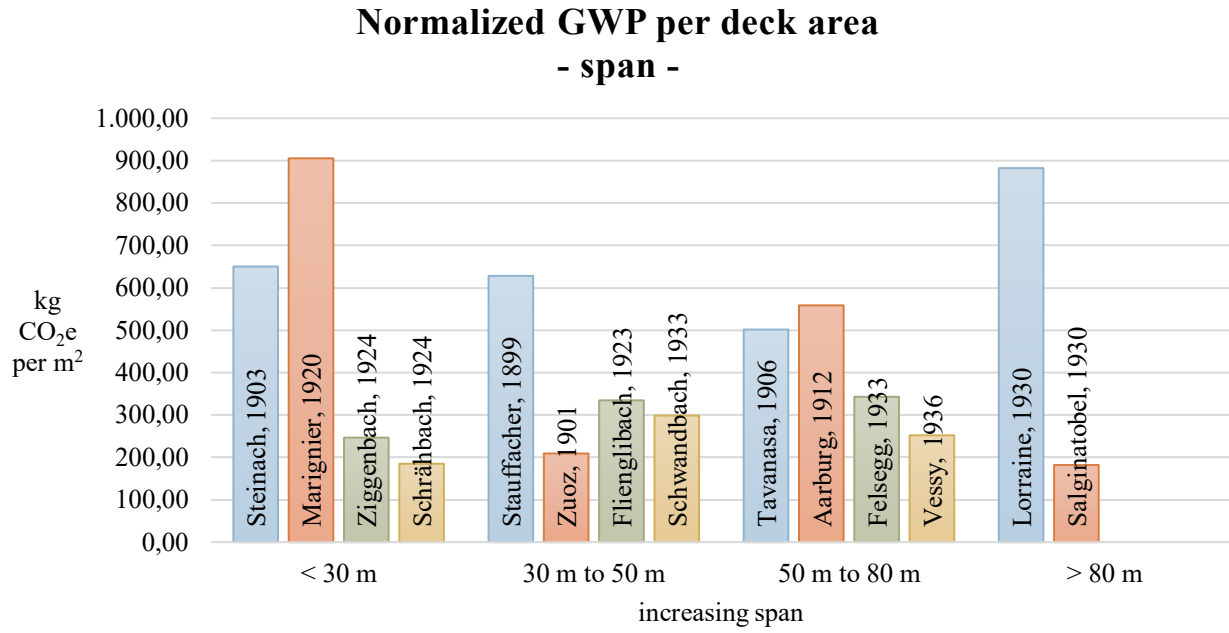


Figure 86. Normalised GWP per deck area, divided in categories of increasing span

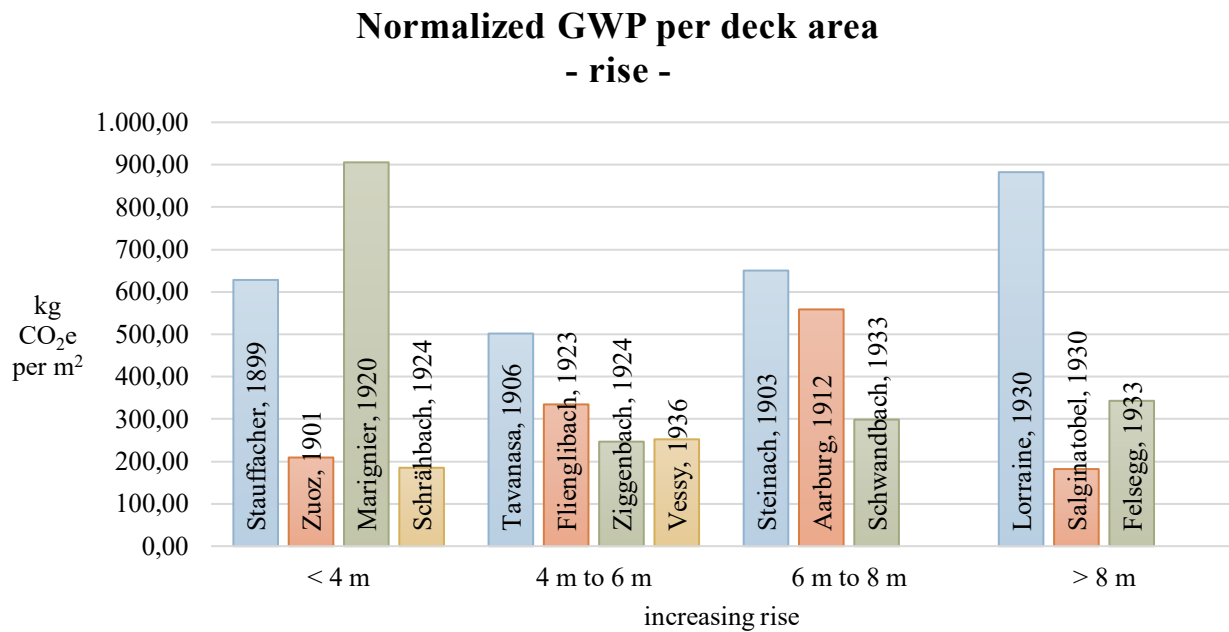


Figure 87. Normalised GWP per deck area, divided in categories of increasing rise

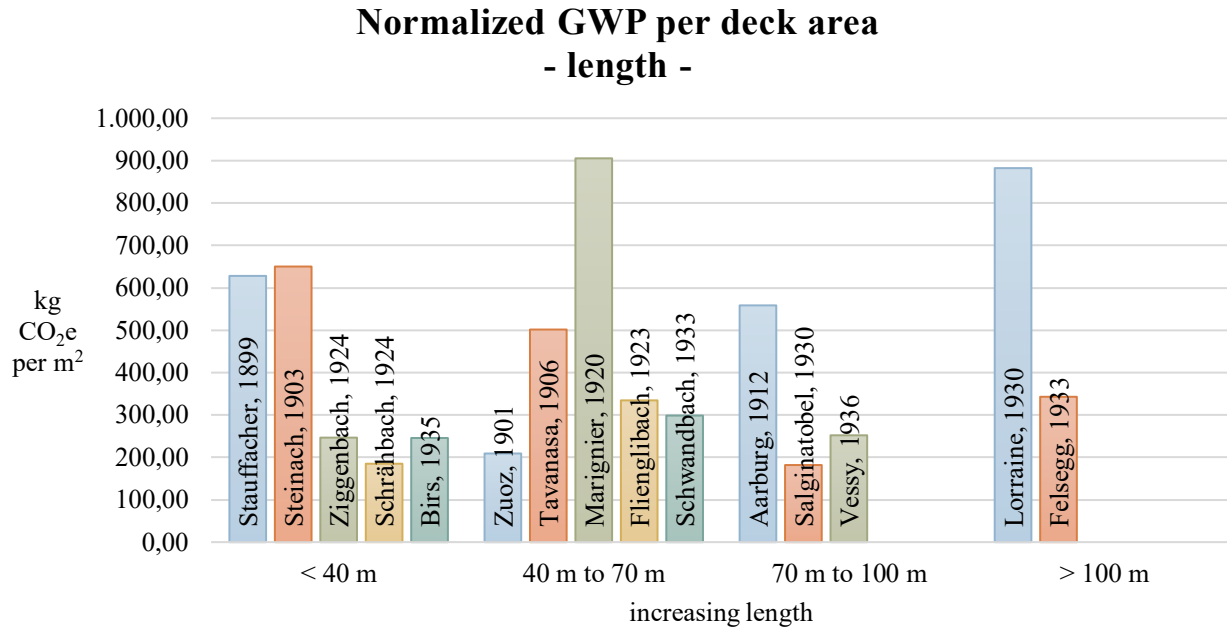


Figure 88. Normalised GWP per deck area, divided in categories of increasing length

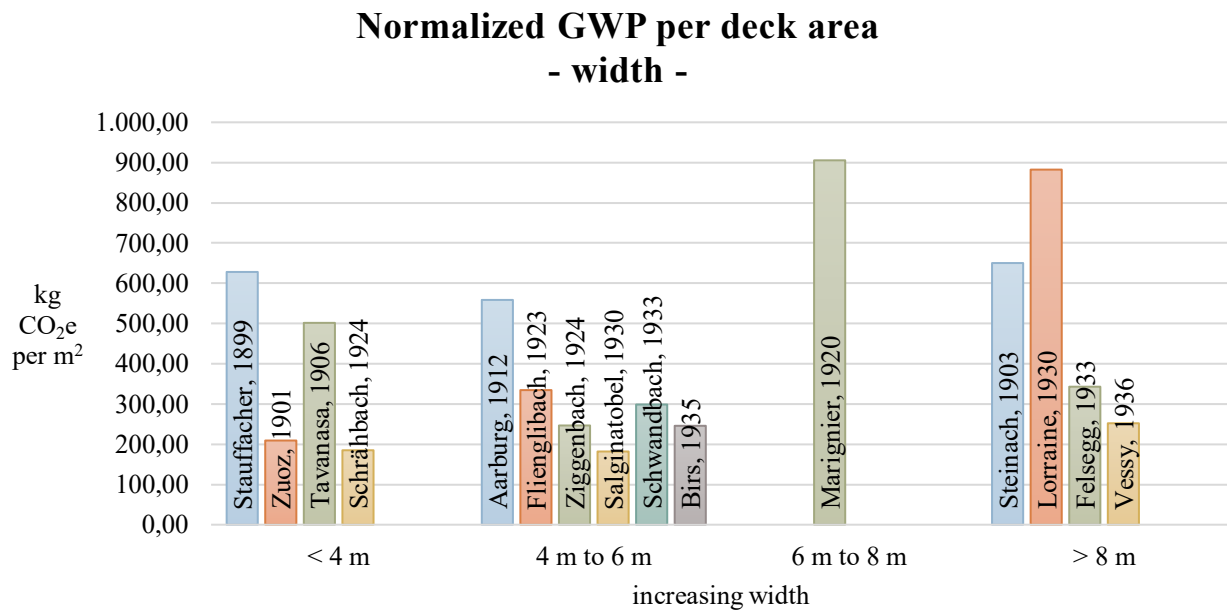


Figure 89. Normalised GWP per deck area, divided in categories of increasing width

A different analysis can be done for the graphs related to the span/rise ratio, linking them to the scaffoldings. The technique of designing the supporting timber structure is based on the fact that it should support the whole arch or only its first layer. So, it is possible to think that the amount of GWP due to its production, is directly linked to the parameter which expresses the geometrical evolution of the arch which is indeed the span/rise ratio. Thus, the data focused only on timber are recalled and clustered with the same technique as the following

one, according to an increasing span/rise ratio. The ratio itself is divided in four classes with the aim to try to distribute as much equally as possible the 15 structures.

1. Span/Rise ratio less than 6
2. Span/Rise ratio between 6 and 8
3. Span/Rise ratio between 8 and 10
4. Span/Rise ratio bigger than 10

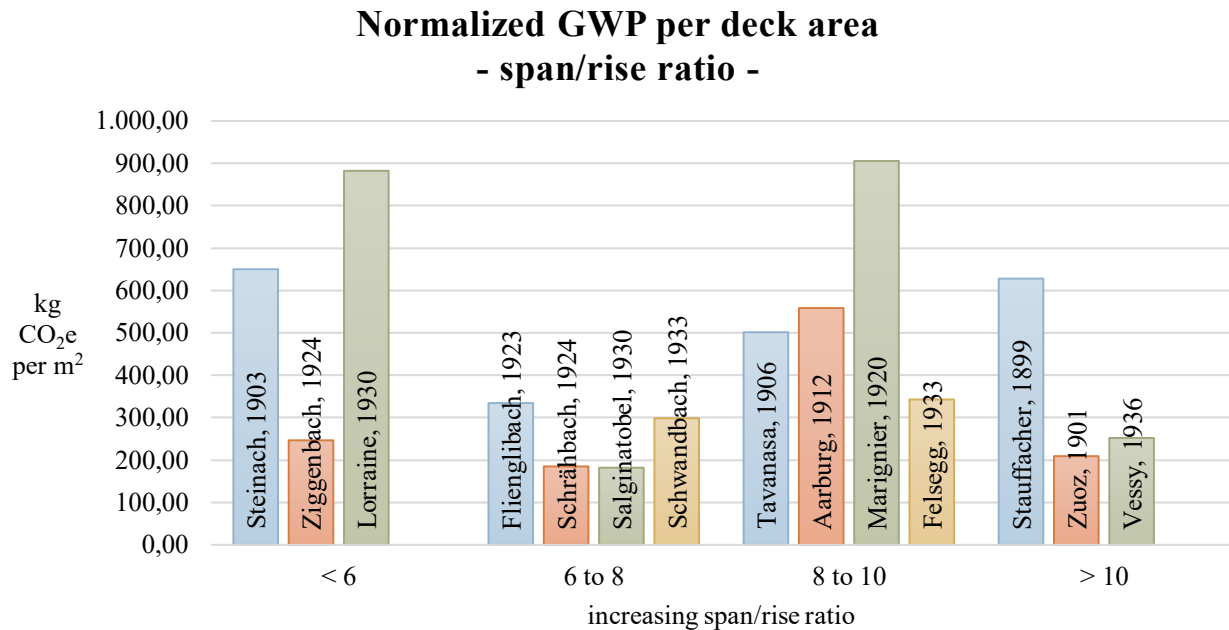


Figure 90. Normalised GWP per deck area, divided in categories of increasing span/rise ratio

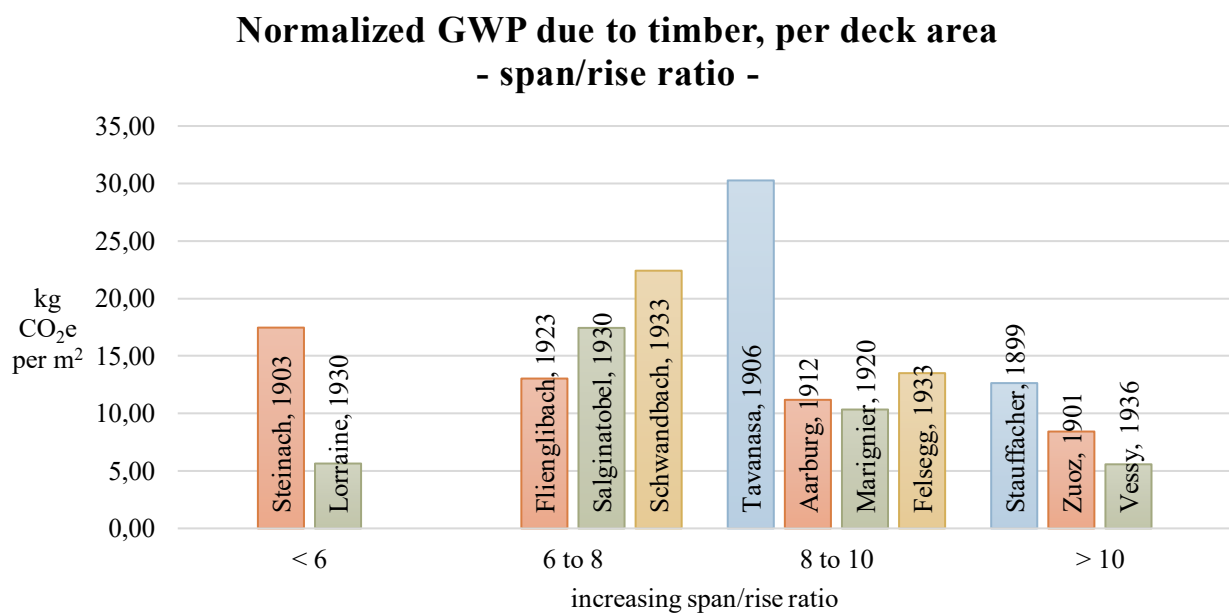


Figure 91. Normalised GWP due to timber per deck area, divided per increasing span/rise ratio

Looking at all the produced graphs (Figure 90 and Figure 91) it is firstly necessary to specify few things: Birs Bridge is again excluded because of its non-curved shape while Zigggenbach and Schrähbach Bridges need some additional specifications because they cannot be treated as the other structures. As already explained, data about the amount of timber used for their scaffoldings are not available, so the values of the normalised value of GWP are only computed through mathematical assumptions, but it would not be possible to extract from these results only the values of the GWP related timber because they would not be realistic numbers. Thus, in the graph of timber (Figure 91) these two bridges are excluded. Known that, it is possible to even try to couple the graph of the total normalized GWP with the normalized GWP only of the timber. However, even if the theoretic association seems a realistic possibility the graphs seem not to have a very strong numerical relation. Within the four classes of the two graphs there is not an evident trend.

However, some useful considerations can be done anyway. For quite small ratios (from 6 to 8) the bridges have the smallest and most similar GWP values on average, while in the other classes the values are much more oscillating. The highest average value is in the first class. This could mean that more the arches are closer to circles the higher value their GWP assumes. A semi arc would indeed assume a ratio exactly equal to 2. However, in the fourth class the biggest contribution from timber side is Tavanasa Bridge, while in the graphs related to the total amounts, the highest value is always Marignier's one. Thus, for this class it is assumed that there is not a direct link between the span over rise ratio and the GWP emitted because of the production of timber. Finally, the contribution of Schwandbach Bridge is always quite big than the other structures of its class. This could be explained by the fact that the gorge of the valley where the scaffolding was designed is very deep and so during its construction process a big additional part of timber, with respect to the other structures, was added in order to achieve the soil which was supposed to support it.

Environmental aspect

- Foundation soil

Through this final clustering method, the 15 bridges are gathered with respect to the soil in which their foundations are built. The classes are 6 and are distinguished according to the position of the structures. In fact, their place can be merged to the geotechnical map of Switzerland (Figure 92) in order to obtain details about the kind of soils. The legend of the map and the relative characteristics of each bridge are already mentioned in the previous catalogue part. A different soil implies different shapes of the foundations and so different amount of buried concrete. Thus, the present goal is to find if this characteristic influence or not the values of the GWP for the different structures.



Figure 92. Geotechnical map of Switzerland combined with the 15 positions of the chosen bridges

The following produced graph (Figure 93) is made always according to the same technique as the other ones produced in the previous sections of the “clustering strategies” chapter. So, considering the values obtained from the normalisation strategy and then gathering the bridges with the same characteristics. As far as the foundation soil is concerned 6 kinds are found as soils of the analysed bridges:

1. Breccias and conglomerates, strongly cemented sandstones, partly with schistose structure with deposits of phyllites. (*Breccias and conglomerates* called in the graph)
2. Gravels and sands with light covering or clay-silt interlaying (deposits of current watercourses). (*Gravels and sands* in the graph)
3. Conglomerates, few or quite cemented, always with banks of gravel and marl. (*Conglomerates, gravel and marl* in the graph)
4. Dolomitic limestone
5. Limestone often with marly interleaves (*Limestone* in the graph)
6. Marl with intercalations or conglomerates of soft sandstone (terrestrial and porous with limestone cement as an essential element) (*Marl with soft sandstone* in the graph)

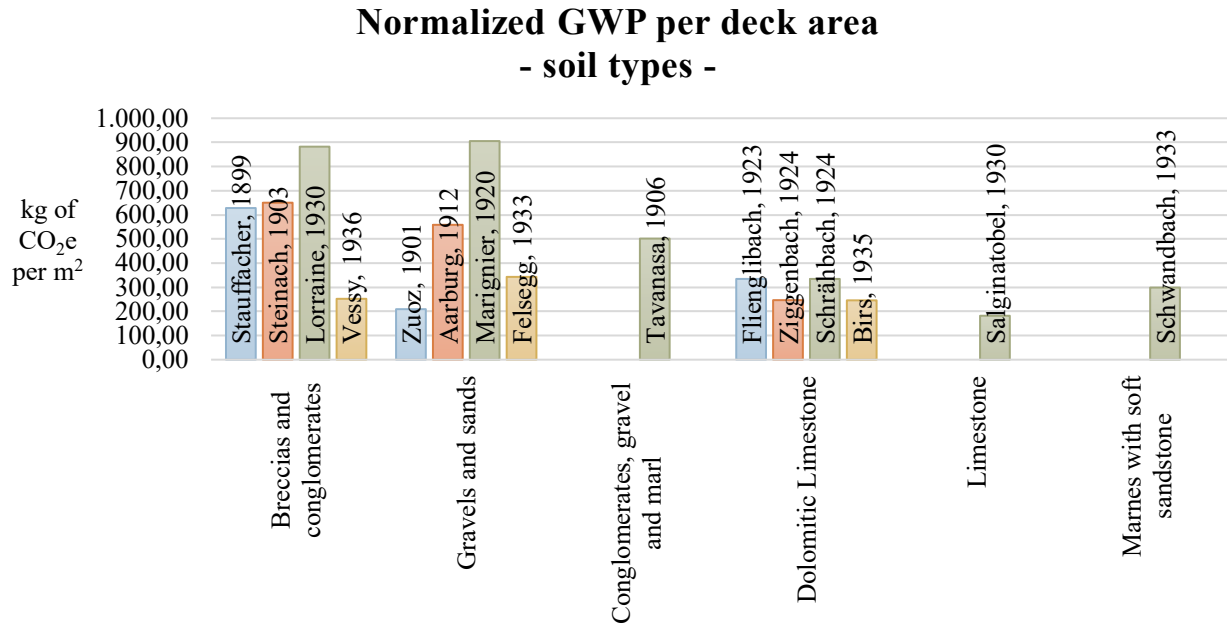


Figure 93. Normalised GWP per deck area, divided per soil type

The first impact is that the bridges in the last three classes have similar GWP values and smaller than the numbers in the first three classes which are much higher and much more oscillating. The similarities between these two macro groups, excluding Vessy and Zuoz which actually have values more similar to the last three classes bridges, could be thought to be probably explained by the shape of the foundations, and more than this by their dimensions.

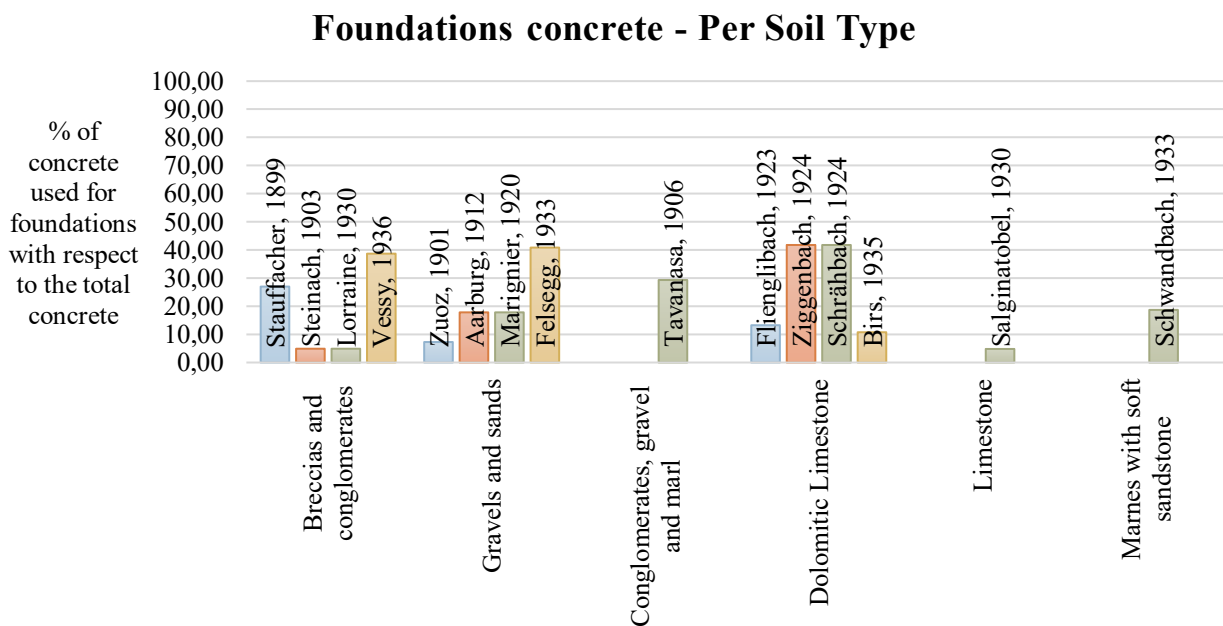


Figure 94. Percentage of foundations' concrete with respect to the total one, divided per soil type

Even if the same kind of soil usually implies the same shape of the foundations because the resistance is the same, for each bridge there are different loads, so different necessities. In Figure 93 there is, indeed, the representation of the volume of concrete used for the foundations, expressed in percentage, with respect to the total amount used for the whole structure. The shown trend does not follow the same path as the normalized GWP. The bridges in which the volume of concrete used for the foundations is highest are Zigggenbach (almost 42%), Felsegg (almost 41%) and Vessy (almost 39%) while, the average percentage is around 20%. On the contrary, according to the normalisation strategy the bridges with the highest GWP are Marignier, Lorraine, Steinach and Stauffacher. However, the distinction between the carbon emissions related to the first three classes of soils and the last three remains. In the Figure 93 for *Breccias and conglomerates*, *Gravels and sands* and *Conglomerates, gravel and marl* the average value of the normalized GWP (536,3 kg CO₂e/m² with a standard deviation of 58 kg CO₂e/m²) is bigger than the average of the other three classes of soil (244.5 kg CO₂e/m² with a standard deviation of 59 kg CO₂e/m²). The same happens in Figure 94: first three classes have an average (24.3% with a standard deviation of 4.6 %) higher than the last three ones (14.1 % with a standard deviation of 8%). In conclusion, the clustering strategy through the different soil types does not explain in a detailed way why some structures assume specific values of the equivalent carbon dioxide emissions, but among the two macro classes of soils the correlation is quite probable.

Maillart vs other engineers

The whole point of the analysis was to elaborate data in order to find the relationship between the transversal characteristics (structural, geometrical and environmental) of the 15 analysed bridges and the GWP values. However, as already explained in the introduction part, the goal is also to prove how much his advanced design method was also sustainable. The innovation found in the balance between structural efficiency, aesthetics and economic is not enough to prove the sustainability itself. An essential aspect is analysed when the investigation includes other bridges apart from Maillart's ones. This side of the analysis helps to have a more general overview in the bridges' construction world. In fact, considering these other examples, it is possible to find the differences with Maillart's structures and effectively give support to the thesis that his design's techniques were revolutionary also from the environmental point of view.

The two chosen structures are both made in reinforced concrete, but in very different periods. The first bridge, as already explained in the "Catalogue" part, is called Langwieser Bridge and was built in 1914, so in the same period while Maillart had just designed Aarburg Bridge and was moving from Switzerland to Russia, to find a new market where he could spend his abilities. Thus, Langwieser was built exactly with the same mechanical tools, theoretically knowledge about concrete and according to the same Swiss standards. As far as the standards are concerned, it is possible to specify that in that period the situation was still developing and there were no precise rules to follow during the design. There were no mandatory assessments such that the project was approved. In Switzerland there were only three documents as references: one related to bricks (*Normalisation des formats des briques*), a second one about iron and steel (*Classification des fers et aciers*)

and the last one related to bridges and railways (*Conditions standard pour les ponts et le matériel des chemins de fer*) [60]. However, nothing was about concrete which was still a construction material not well known. The modern standards appeared in 1988 when Switzerland agreed to adopt the European Standards. The writing of the first Eurocode started, indeed, in 1975 and was published in 1984 [61]. The other bridge chose as example is more modern. In fact, Tamina Bridge was built in 2017, with present tools and technologies. The application of modern standards is definitely an aspect that conditioned the whole procedure and the amount of materials.

These two bridges can be compared with the 15 Maillart's ones in terms of normalised GWP. The analysis allows a numerical comparison among the effective quantity of emitted equivalent carbon dioxide in the described situations. Moreover, there are common aspects which highlight similarities between Maillart's bridges and non-Maillart's ones which allow the analysis itself. The most evident one is the soil. Since all the chosen bridges are built in Switzerland, the foundations lie on the same terrain. Both two additional bridges are close to Salginatobel. Their positions are visible in the following explicative map of the 17 total analysed structures (Figure 95).

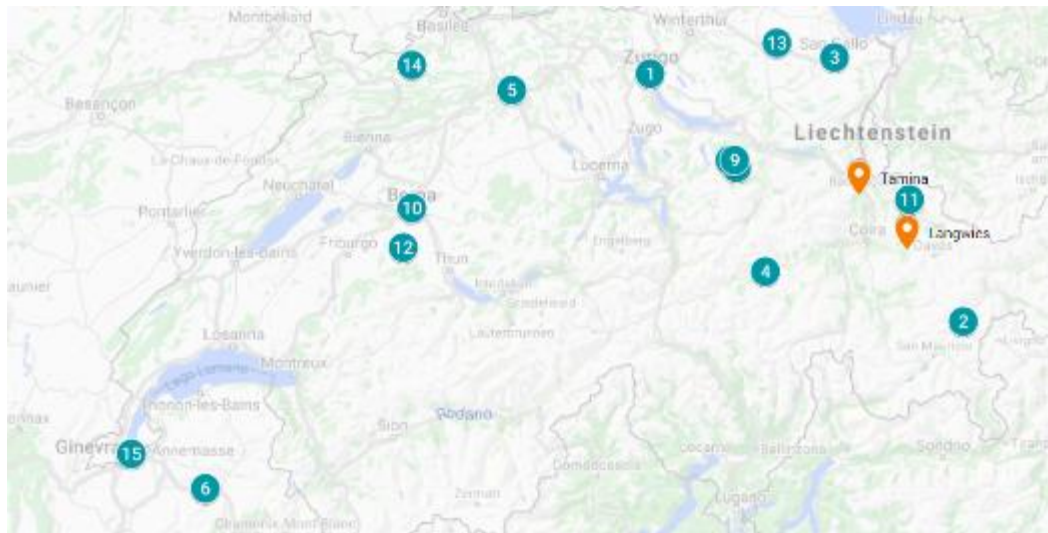


Figure 95. Positions of the 15 Maillart's bridges and of the two additional ones

Different is the case of the structural scheme: Langwieser Bridge is made of an elastic arch and a monolithic beam while Tamina Bridge is composed of a hollow box arch and a continuous beam. Both the solutions are different from the static schemes proper of the chosen Maillart's Bridges. However, they are both arch bridges so a massive common aspect that is proper to the analysed structures is the generic principle of how the loads are transferred from the deck to the foundations at the abutments, thanks to the presence of the arch itself.

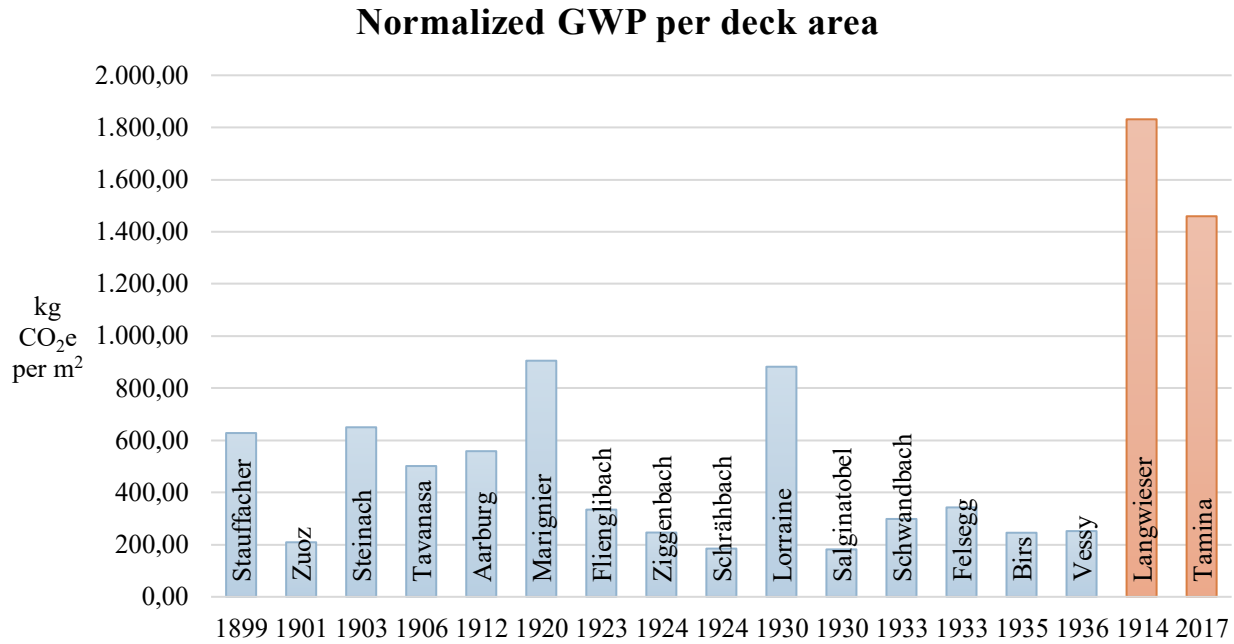


Figure 96. Normalised GWP per deck area, with the two additional ones

According to these results, the non-Maillart's structure have a higher impact. Even the modern Tamina Bridge is not comparable, in environmental efficiency, with Maillart's structures. This overview is an interesting prove for even the bridges that after the normalisation seem to have a very big carbon footprint. They have, indeed, a very good performance with respect to bridges designed by other engineers.

GWP compared with car and trees

Cars

An additional aspect is to find some realistic comparisons to understand practically what these numbers related to the equivalent carbon emissions mean. In particular it is chosen to focus on the carbon emitted by an average car and on the carbon absorbed by an average tree. In the same KBOB list [2] used for the selection of the ECC, there is a section dedicated to the transportations means. On average it is indicated the greenhouse gas emissions related to the operation phase of a passenger car per km. Moreover, it is possible to find data about the tons of carbon dioxide emitted per year too [62]. The data is not referred to a continuous use of the car, but again to an average use of the vehicle during the year.

The following graph (Figure 97) shows the km that an average car should travel to produce the same amount of equivalent carbon dioxide of each m² of the 17 analysed bridges. The same principle is valid for the other figure (Figure 98). This is the translation of the amount of time, expressed as fraction of years, needed to produce by a car the same amount necessary to build every unit area (m²) of the bridges.

Car	
kg CO ₂ e/year	kg CO ₂ e/km
4600	0,266

Table 55. Carbon emissions by cars

The impressive thing is that the production of carbon due to the usage of cars is not as small as expected. On average, each m² of Maillart's Bridges is equivalent to 1609.7 km produced by a generic car, so it is like a round trip between Lausanne and Barcelona. As well as it is necessary to use the car only for around 34 days (0.09 years), to emit, again, the average value of all Maillart's Bridges. As already explained, the above-mentioned days are not referred to a continuous usage of the car, but again to an average value per year. Including the two additional structures (Langwieser and Tamina) the medium values increase a bit but remain very similar to the ones mentioned (2148 km and 0.12 years or 45 days).

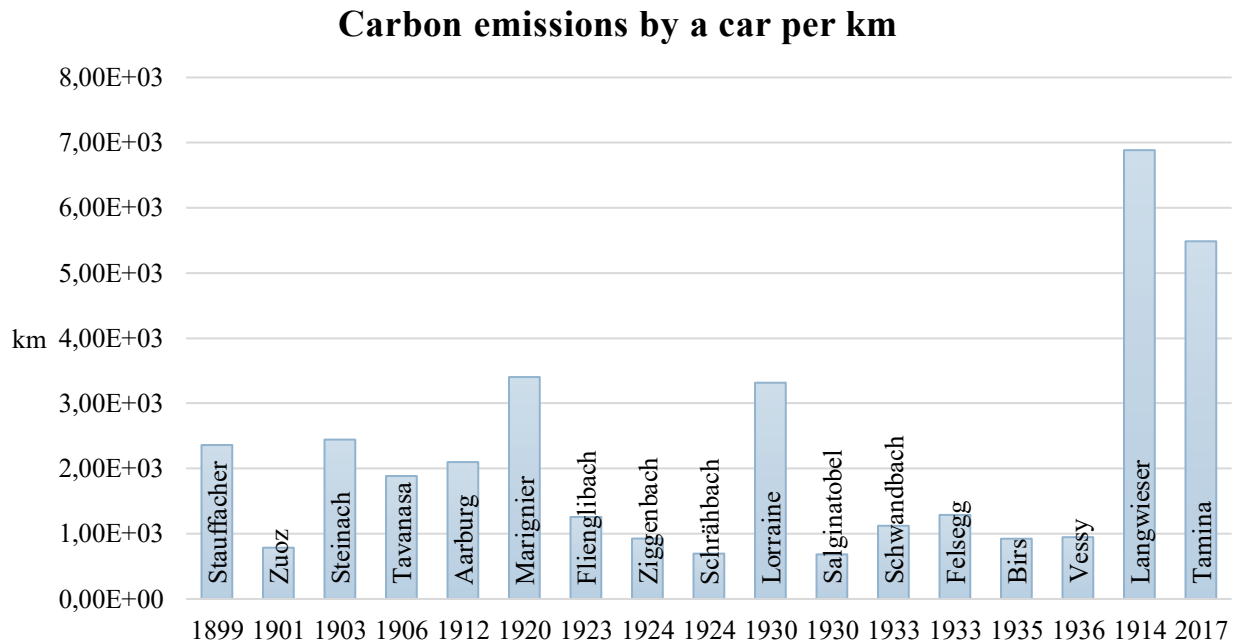


Figure 97. Translation of normalised GWP of the bridges into carbon emissions by a car per km

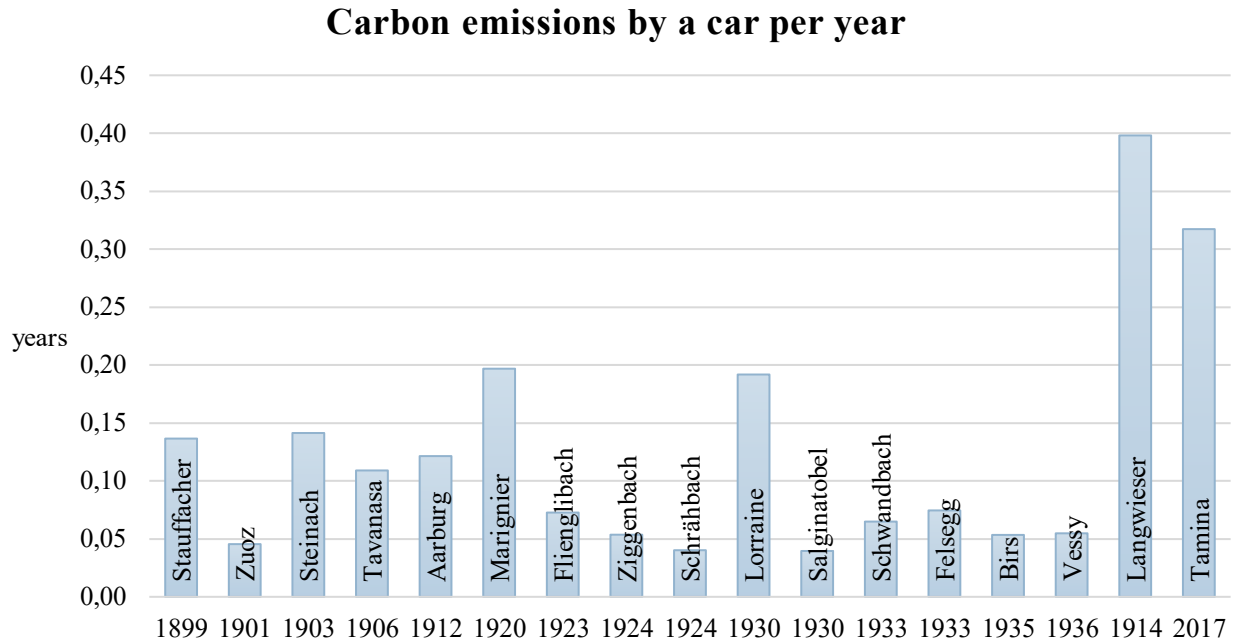


Figure 98. Translation of normalised GWP of the bridges into carbon emissions by a car per year

	Car		
	km	years	days
Maillart's bridges	1609,69	0,09	33,97
Non Maillart's bridges	6185,86	0,36	130,56
All bridges	2148,06	0,12	45,34

Table 56. Averages of the 2 previous graphs related to cars

Trees

Similar data can be found about absorption of carbon by one tree or by an acre of multiple trees. On average a tree can absorb between 10 and 20 kg CO₂e/year when it achieves the adulthood in an urban context, so when it is between 20 and 40 years old. But when it grows in a natural context the absorption increases up to 50 kg CO₂e/year. That is why it is chosen 20 kg CO₂e/year as a possible realistic value of a not well-known situation. However, since usually trees are not single, but they are placed in green areas, it is also used the data of the carbon absorption of an acre of trees [63]. The only aspect to highlight is that all the mentioned data are only indicative because for both cars and trees the values can vary a lot according to the kind of specific element it is considered. The chosen numbers are useful anyway to have a general overview and to better understand the previously analysed data of the normalised GWP per deck area.

Tree	Acre
kg CO ₂ e/year	kg CO ₂ e/year
20	2500

Table 57. Carbon absorption of trees

The figures (Figure 99 and Figure 100) are the translation of the amount of time, expressed as fraction of years, of how much a tree or an acre of trees should live in order to offset the embodied carbon of each m² of the bridges. The table (Table 58) expresses the averages of how long the life of a tree should be in order to absorb the same amount of carbon dioxide that Maillart's or non Maillart's bridges emit per m².

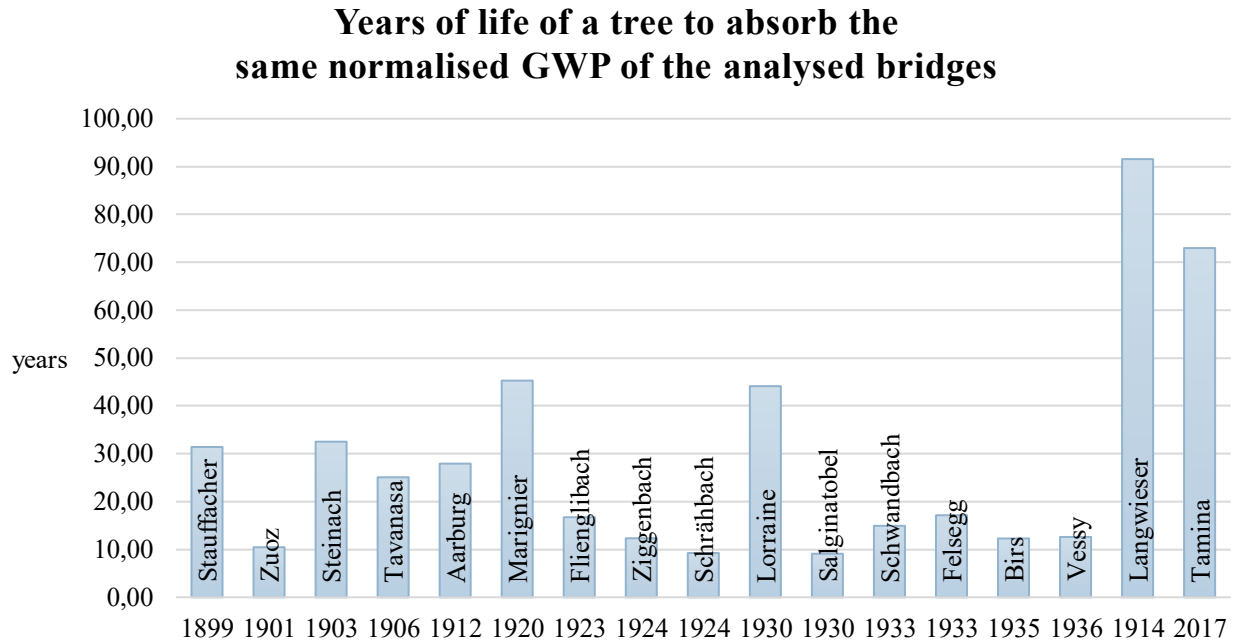


Figure 99. Translation of normalised GWP of the bridges into carbon absorption by a tree per year

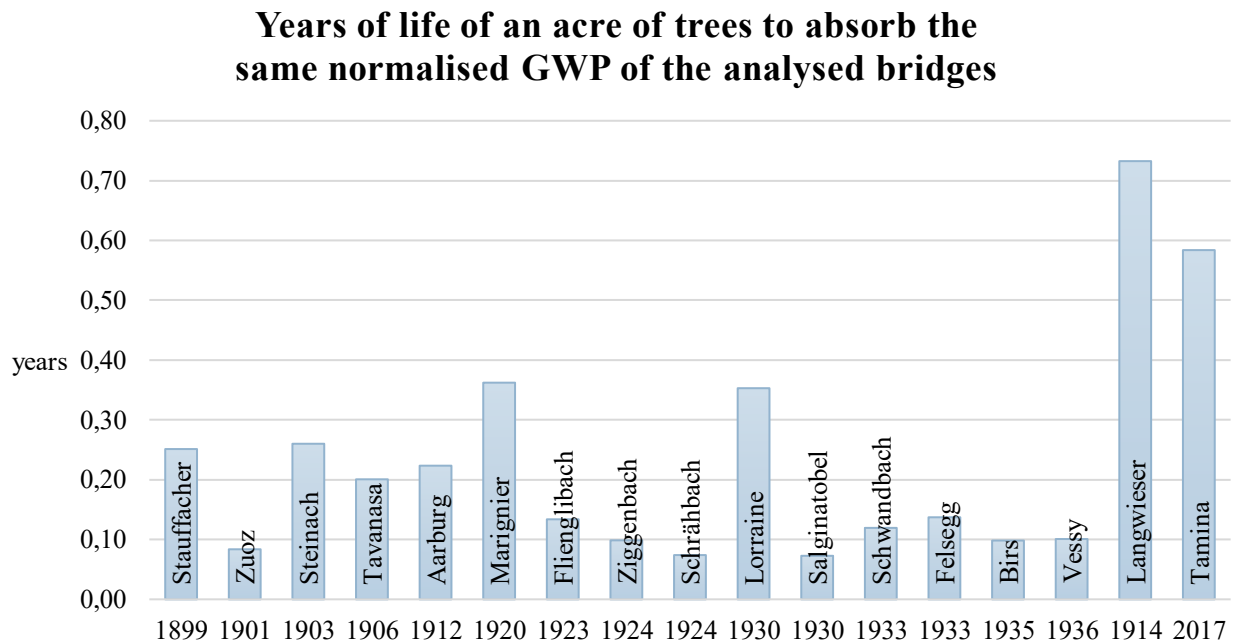


Figure 100. Translation of normalised GWP of the bridges into carbon absorption by an acre of trees per year

	Tree	Acre	
	years	years	days
Maillart's bridges	21,41	0,17	62,51
Non Maillart's bridges	82,27	0,66	240,23
All bridges	28,57	0,23	83,42

Table 58. Averages of the 2 previous graphs related to trees

Conclusions

At the end of the process of the analysis it is possible to summarise everything that has been done in the thesis and the most important results achieved. This thesis studied Maillart's legacy to investigate the sustainability of his structures. It is known, indeed, that his bridges are efficient, elegant and economically very competitive, but a numerical proof of the environmental impact of the same structures was missing. There are many aspects that characterised his way of thinking. Some of them can be found as clues of his educational path and of his teachers, such as the use of graphic statics to compute forces and to decide the best placement of materials. But others resulted from a slow growing process which lead him to experiment new shapes and new static configurations with materials (concrete and steel in reinforced concrete) which were not well-known at that time. His final shapes were distant from the traditional ones. His most famous and used static schemes (three hinged arches and deck-stiffened arches) were difficult to be accepted and explained by his contemporaries. All these reasons explained why his bridges were chosen. In fact, they were not only revolutionary in the 20th century, but they are also an inspiration for the present engineers who can learn from his genius mind.

To assess the sustainability of his bridges, LCA was used to calculate the GWP of the construction process through the combination of ECC and SMQ. 15 of his bridges are selected and analysed in chronological order. The ECC are found in the KBOB list [2] while the SMQ are computed from the original drawings [1], reworked in 3D models. The selected materials are concrete, steel, masonry and timber. The structures themselves were made of reinforced concrete which explains the necessity to compute concrete and steel quantities. Masonry was sometimes used to cover the internal structure and to give a traditional aspect to the bridge itself, while timber was used for the scaffoldings. The most important assumptions made during this computational process are related to the coefficients. The ECC are cradle-to-gate values. They are relative to the whole life of the materials, from the early production to the end of their life. Moreover, they are referred to the present time. Databases of past coefficients are not available. Thus, the computational process corresponds to the embodied carbon of the bridge if the bridge itself would have been built today. So, the CO_{2e} is not the actual embodied carbon of the bridge, effectively produced for its construction in the 20th century.

For every one of the bridges, the boundaries of the foundations and of the scaffoldings are highlighted according to the same original drawings [1], so the volumes and the GWP are computed. Parallel to this catalogue, other two structures are analysed at the same way. Langwieser Viaduct as an example of another arch bridge built in the same period of Maillart's one but by another engineer and Tamina Bridge as an example of a present arch bridge.

With the numerical data, collected in this way, then, three normalisation strategies are assumed in order to understand which unit is more valid as comparison among the 15 Maillart bridges and the 2 non-Maillart bridges. The possibilities were: deck area, span and rise. It resulted that the normalisation through the deck area reduces the variation range of the data much more than the other two strategies. Since the numbers are, then, closer, it is easier to speculate about possible and probable relationships among the data themselves.

As far as the scaffolding is concerned, a separate section is dedicated to timber. Complete data about the supporting structure is not available for every bridge. In particular, the missing data are the Ziegenbach, Schrähbach and Birs bridges. That is why a small chapter is dedicated only to the known wood centrings. The impact of the GWP due to timber is evaluated with respect to the GWP of the full structure.

The next step was to find correlations between the GWP results and the transversal characteristic of each structure. These parallel properties are related to the structural scheme, the geometry and the foundation soil. The structural schemes are distinguished among unreinforced three-hinged arches, hollow-box three-hinged arches, concrete-block arches, deck arches, deck-stiffened arches and rigid frame with continuous girder bridges. The geometrical properties are divided into span, rise, length, width and span over rise ratio. All the information mentioned until this point, are found in the original drawings and the additional documents [1] available in the ETH Archive, in Zurich. Finally, the foundations soils are found in the geotechnical map of Switzerland [41] where the positions of the structures occupy six different categories of terrain: breccias and conglomerates, strongly cemented sandstones, partly with schistose structure with deposits of phyllites; gravels and sands with light covering or clay-silt interlaying (deposits of current watercourses); conglomerates, few or quite cemented, always with banks of gravel and marl; dolomitic limestone; limestone often with marly interleaves and marl with intercalations or conglomerates of soft sandstone (terrestrial and porous with limestone cement as an essential element). So, several categorizations are produced in order to gather the structures with the same qualities. At first with the same static scheme, then with similar geometrical properties and finally built in the same foundation soil. These visualizations are meant to understand if the values of the GWP are also correlate to specific aspects, in addition to the quantities of material through which they are computed.

The main results are related to the correlation of the structural scheme and the amount of steel and to the classification with respect to the kind of soil. In fact, it is found that the geometrical parameters do not influence the distribution of GWP very much. The bridges gathered according to similar span, rise, length or width do not have a significant trend, but they have very oscillating data within the same class. On the other hand, there is a clear relationship between the amount of steel of each structural scheme and the percentage of the GWP due to steel with respect to the total one. The same procedure as the one described for timber is followed and it is found that the amount of reinforcement (kg per m^3 of concrete) is higher for deck-stiffened bridges and rigid frame with continuous beams. Moreover, the distribution of the mass of steel with respect to the volume of concrete follows the same trend as the ratio of the steel's GWP over the total one, expressed in per cent. It is very interesting to see also how this percentage is much higher for steel than how it was for timber: it achieves even around 40% of the total impact both for Schwandbach and Birs Bridge. An additional goal is found in the gathering of GWP values according to the six above-mentioned kinds of soils. In this case the main distinction is between the first three classes and the last three. If the GWP normalised per deck area and divided per soil type is compared with the percentage of concrete used for the foundations with respect to the total one, it is found that the two graphs have similar trends. In the first group of soils the averages are almost the double of the averages of the second group of terrains, always with a small standard deviation to prove that

the data do not oscillate much from the medium values. Thus, the clustering strategy through the different soil types does not explain in a detailed way why some structures assume specific values of the equivalent carbon dioxide emissions, but among the two macro classes of soils the correlation is quite probable. A possible future contribution, in this sense, could be done to understand why these two groups exist. A more detailed geotechnical analysis could explain why some classes of soils lead to more similar GWP values than others. Moreover, why the similarities are proper to those specific two groups composed like that and not by other terrains.

The final part of the thesis is, then, focused on the comparison with the two other mentioned structures which are counter examples because designed by different engineering from Maillart. It is found that both have a lower sustainable performance than all the chosen Maillart's bridges. Their normalised GWP is almost the double of the values assumed by the bridges with the highest values: Marignier has the biggest value which is equal to 905.51 kg CO₂e/m² while to Tamina Bridge and Langwieser correspond respectively 1459.52 kg CO₂e/m² and 1831.35 kg CO₂e/m². Moreover, to give an additional and more realistic meaning to all the values just mentioned, related to the normalised GWP per deck area, some comparisons are performed. It is chosen to translate the kg of equivalent carbon dioxide per m² of deck into the km that an average car should travel to emit the same amount of CO₂ or, similarly, to the years that an average car should be used to achieve the same goal. Therefore, the absorption of carbon dioxide of a tree or an acre of tree is compared too, to understand how many trees would need to be planted to offset the embodied carbon of the bridges.

As far as the general thesis is concerned, some suggestions for future contributions can be provided too. The first aspect that can make a real difference is to increment the number of analysed bridges. It is known that Maillart designed 47 bridges [32], listed in the following table (Table 59). Since only 15 structures were chosen, increasing their number will also lead to a more complete overview of the evolution of the carbon footprint. When the sample is denser it could be possible to find patterns and relationships among aspects that were excluded or even not noticed above.

Name	Place	Year
Pampigny	Le Veyron Brook	1896
Stauffacher Bridge	Zurich	1899
Zurich	Hadlaub Street	1901
Zuoz Bridge	Zuoz	1901
Steinach Bridge	Saint Gallen	1903
Billwil Bridge	Billwill	1904
Tavanasa Bridge	Danis-Tavanas	1906
Aach	Railroad	1907
Wattwill	Thur River	1909
Whylen	Underwasser Canal	1910
Laufenbrücke	Laufenburg	1911
Aarburg Bridge	Olten	1912
August-Wyhlen	Rhine River	1912

Rheinfelden Bridge	Rheinfelden	1912
Muota Bridge	Ibach	1913
Marignier Bridge	Marignier	1920
Flienglibach Bridge	Innerthal	1923
Ziggenbach Bridge	Innerthal	1924
Schrähhbach Bridge	Innerthal	1924
Chatelard	Eau-noire	1924
Grand Fey Viaduct	Fribourg	1925
Valtschielbach	Donath	1926
Lorraine Bridge	Bern	1930
Salginatobel Bridge	Schiers, Schuders	1930
Landquart River Bridge	Klosters-Serneus	1930
Spitalbrügg Bridge	Adelboden	1931
Ladholz Bridge	Frutigen	1931
Schangnau	Hombach	1931
Schangnau	Luterstalden Brook	1931
Felsegg Bridge	Felsegg - Nessental	1932
Rossgaben Bridge	Schwarzenburg	1932
Traubach Bridge	Habkern	1932
Bolbach Bridge	Habkern	1932
Schwandbach Bridge	Hinterfultigen	1933
Thur river	Felsegg	1933
Aare River	Innertkirchen	1934
Töss Footbridge	Winterthur	1933
Birs Bridge	Liesberg	1935
Huttwill	Railroad	1935
Twannbach Bridge	Twann	1936
Vessy Bridge	Geneva	1936
Grundlischwand	Luttschine River	1937
Weissensteinstrasse Bridge	Berne	1938
Wiler	Gadmerwasser	1938
Laubegg	Simme River	1940
Seestattstrasse Bridge	Altendorf	1939
Churerstrasse Bridge	Alterndorf, Lachen	1940
Garstatt Bridge	Garstatt	1939

Table 59. List of all the bridges designed by Maillart

Following the same principle, it could be also useful to increase the number of non-Maillart's bridges used as comparisons. The two chosen structures are selected among many options and without a specific reason apart from the presence of an arch structure and the use of concrete as construction material. However, maybe it is interesting to see if other famous personalities in the civil engineering sector, both past and present have been able to design similar environmentally friendly bridges. Starting from finding that, an additional aspect could

also be evaluating the common aspects among all of them and Maillart. Understanding the keys to designing efficient, elegant, economical, and sustainable structures should be the goal of every engineer and learning from both positive and negative past and present examples is a possible beginning point to elaborate a personal strategy to achieve similar and maybe even better results.

Appendix

Name	Place	Year	Structural scheme	Length	Span
\	\	\	\	m	m
Stauffacher	Zurich	1899	Unreinforced 3 hinges arch	40,00	39,60
Zuoz	Zuoz	1901	Hollow box 3 hinged arch	41,00	38,25
Steinach	Saint Gallen	1903	Concrete-block arch	36,78	29,15
Tavanasa	Danis-Tavanasa	1906	Hollow box 3 hinged arch	57,00	51,25
Aarburg	Olten	1912	Deck arch	71,92	67,83
Marignier	Marignier	1920	Deck arch	66,90	20,44
Flienglibach	Innerthal	1923	Deck arch	40,76	38,70
Ziggenbach	Innerthal	1924	Deck arch	37,50	20,00
Schrähhbach	Innerthal	1924	Deck arch	30,00	28,80
Lorraine	Bern	1930	Concrete-block arch	178,00	82,00
Salginatobel	Schiers	1930	Hollow box 3 hinged arch	90,00	90,00
Schwandbach	Hinterfultigen	1933	Deck stiffened arch	55,65	37,40
Felsegg	Felsegg	1933	Hollow box 3 hinged arch	180,40	72,00
Birs	Liesberg	1935	Rigid frame, continuous beam	35,40	-
Vessy	Geneva	1936	Hollow box 3 hinged arch	74,88	56,00

Table 60. Summary of the information of the chosen bridges, first part

Name	Width	Rise	Span/Rise	Area (LW)	Soil
\	m	m	\	m ²	\
Stauffacher	4,00	3,70	10,7	160,0	Breccias and conglomerates
Zuoz	3,80	3,60	10,6	155,8	Gravels and sands
Steinach	10,00	6,28	4,6	367,8	Breccias and conglomerates
Tavanasa	3,60	5,70	9,0	205,2	Conglomerates, gravel and marl
Aarburg	5,30	6,95	9,8	381,2	Gravels and sands
Marignier	7,70	2,33	8,8	515,1	Gravels and sands
Flienglibach	4,60	5,17	7,5	187,5	Dolomitic limestone
Ziggenbach	5,30	4,70	4,3	198,8	Dolomitic limestone
Schrähhbach	3,90	4,02	7,2	117,0	Dolomitic limestone
Lorraine	21,40	31,00	2,6	3809,2	Breccias and conglomerates
Salginatobel	4,36	14,00	6,4	392,4	Limestone
Schwandbach	4,90	6,00	6,2	272,7	Marl with soft sandstone
Felsegg	10,10	8,53	8,4	1822,0	Gravels and sands
Birs	5,54	-	-	196,1	Dolomitic limestone
Vessy	10,40	4,32	13,0	778,8	Breccias and conglomerates

Table 61. Summary of the information of the chosen bridges, second part

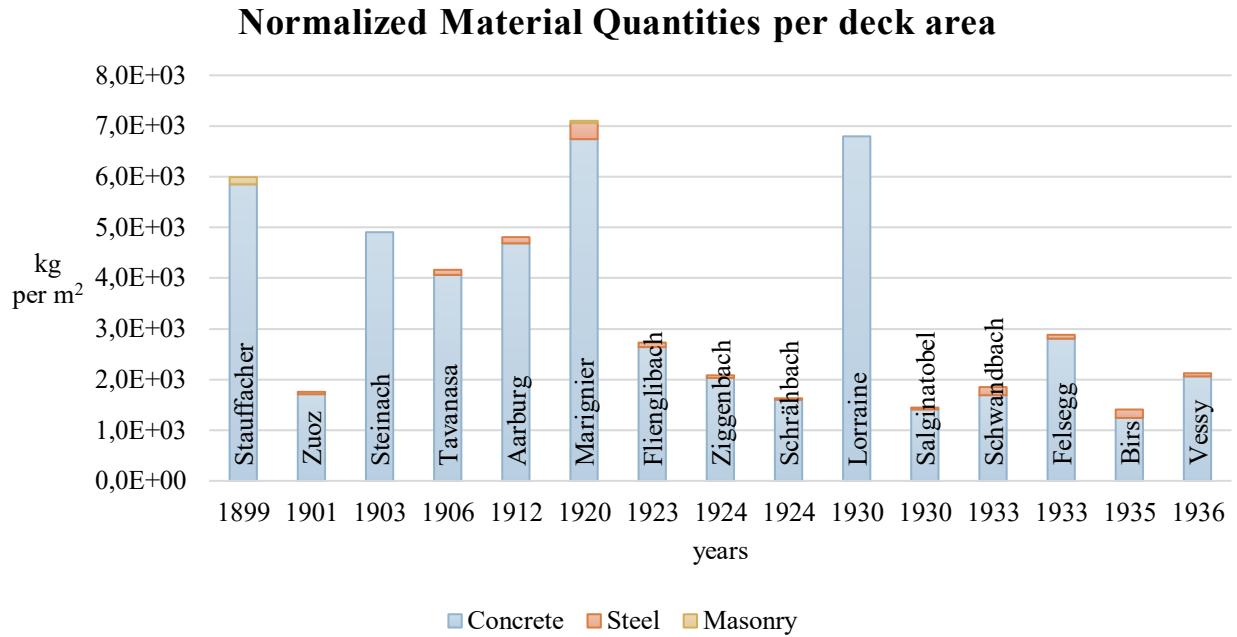


Figure 101. Normalized Material Quantities per deck area

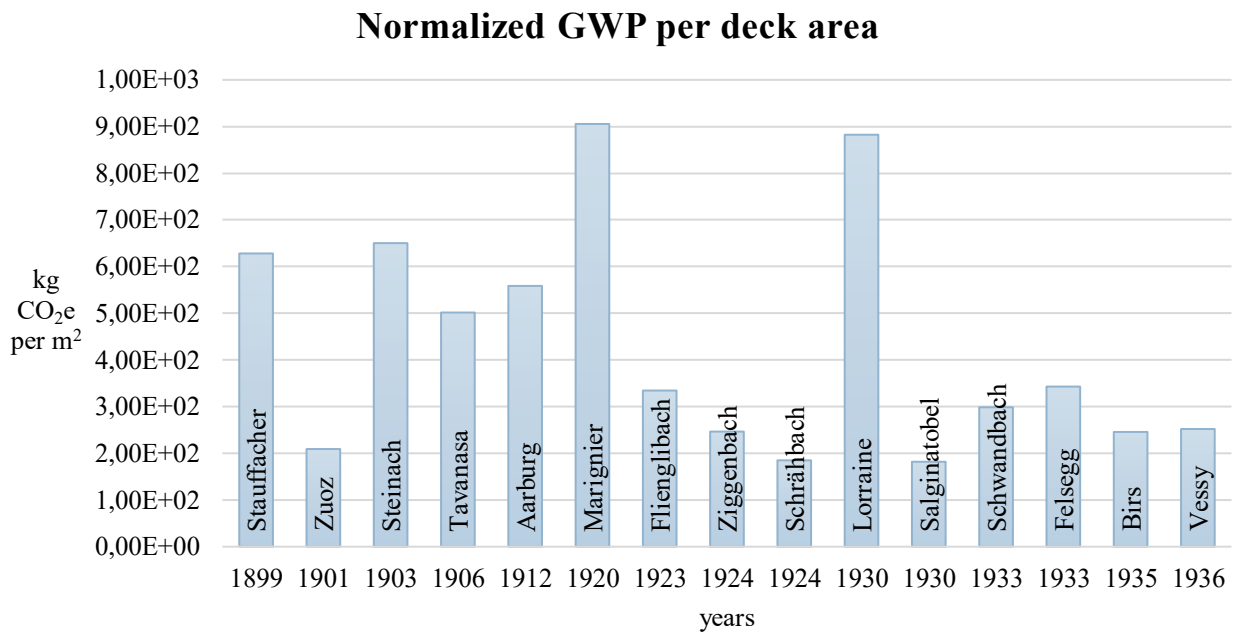


Figure 102. Normalised GWP per deck area

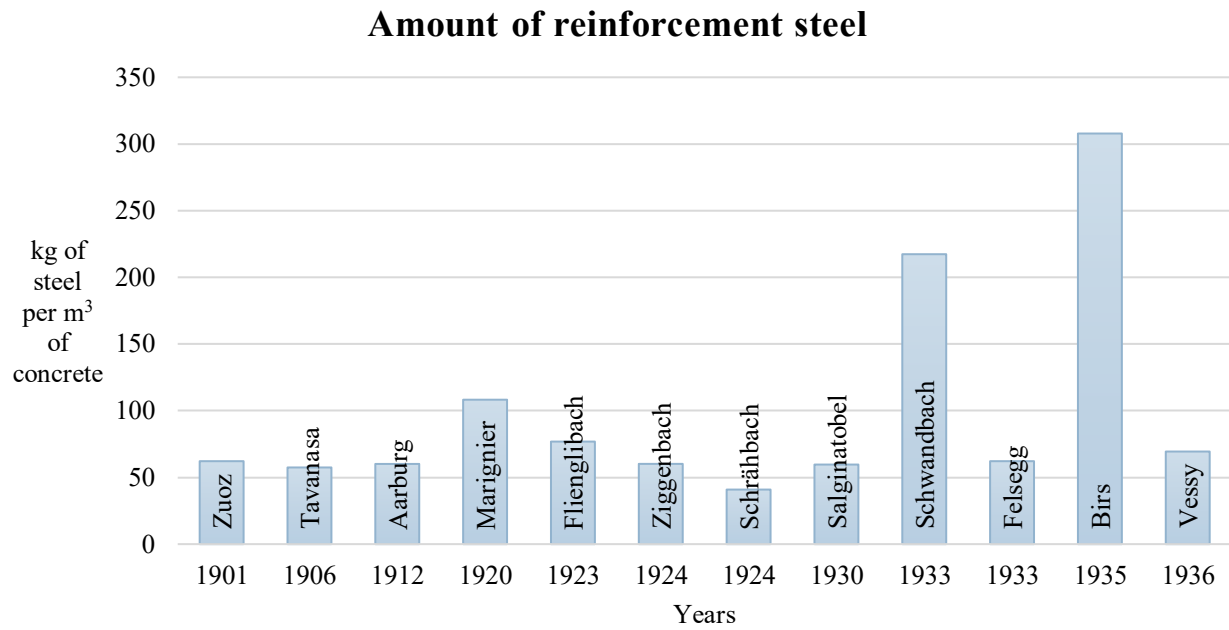


Figure 103. Amount of reinforcement steel

Indexes

Tables

Table 1. Densities of concrete and steel.....	25
Table 2. ECC used to compute the GWP	26
Table 3. Characteristics of Stauffacher Bridge [1]	27
Table 4. Computed quantities of Stauffacher's Bridge	29
Table 5. Coefficients for Stauffacher's GWP	29
Table 6. Characteristics of Zuoz Bridge [1]	30
Table 7. Computed quantities of Zuoz's Bridge.....	33
Table 8. Coefficients for Zuoz's GWP	33
Table 9. Characteristics of Steinach Bridge [1]	34
Table 10. Computed quantities of Steinach's Bridge	36
Table 11. Coefficients for Steinach's GWP	37
Table 12. Characteristics of Tavanasa Bridge [1].....	38
Table 13. Computed quantities of Tavanasa's Bridge	40
Table 14. Coefficients for Tavanasa's GWP	41
Table 15. Characteristics of Aarburg Bridge [1]	42
Table 16. Computed quantities of Aarburg Bridge.....	45
Table 17. Coefficients for Aarburg's GWP.....	45
Table 18. Characteristics of Marignier Bridge [1].....	46
Table 19. Computed quantities of Marignier Bridge	48
Table 20. Coefficients for Marignier's GWP	48
Table 21. Characteristics of Flienglibach Bridge [1]	49
Table 22. Computed quantities of Flienglibach Bridge	52
Table 23. Coefficients for Flienglibach's GWP	52
Table 24. Characteristics of Zigggenbach Bridge [1]	53
Table 25. Computed quantities of Zigggenbach Bridge	55
Table 26. Coefficients for Zigggenbach's GWP	55
Table 27. Characteristics of Schrähbach Bridge [1]	56
Table 28. Computed quantities of Schrähbach Bridge.....	58
Table 29. Coefficients for Schrähbach's GWP	59
Table 30. Characteristics of Lorraine Bridge [1]	60
Table 31. Computed quantities of Lorraine Bridge	63
Table 32. Coefficients for Lorraine's GWP	63
Table 33. Characteristics of Salginatobel Bridge [1]	64
Table 34. Computed quantities of Salginatobel Bridge	66

Table 35. Coefficients for Salginatobel's GWP	67
Table 36. Characteristics of Schwandbach Bridge [1]	68
Table 37. Computed quantities of Schwandbach Bridge	71
Table 38. Coefficients for Schwandbach's GWP	71
Table 39. Characteristics of Felsegg Bridge [1]	72
Table 40. Computed quantities of Felsegg Bridge	74
Table 41. Coefficients for Felsegg's GWP	74
Table 42. Characteristics of Birs Bridge [1].....	75
Table 43. Computed quantities of Birs Bridge	77
Table 44. Coefficients for Birs' GWP	77
Table 45. Characteristics of Vessy Bridge [1].....	79
Table 46. Computed quantities of Vessy Bridge	81
Table 47. Coefficients for Vessy's GWP	81
Table 48. Characteristics of Langwieser Bridge [54]	82
Table 49. Computed quantities of Langwieser Bridge.....	84
Table 50. Coefficients for Langwieser 's GWP.....	84
Table 51. Characteristics of Tamina Bridge [55]	85
Table 52. Computed quantities of Tamina Bridge.....	87
Table 53. Coefficients for Tamina 's GWP	87
Table 54. Variation ranges of GWP according to the different normalisation strategies.....	93
Table 55. Carbon emissions by cars	110
Table 56. Averages of the 2 previous graphs related to cars.....	111
Table 57. Carbon absorption of trees	111
Table 58. Averages of the 2 previous graphs related to trees	113
Table 59. List of all the bridges designed by Maillart	117
Table 60. Summary of the information of the chosen bridges, first part	119
Table 61. Summary of the information of the chosen bridges, second part	119

Figures

Figure 1. Steps of LCA [5].....	7
Figure 2. Schwandbach Bridge [31]	11
Figure 3. Salginatobel Bridge's scaffolding [31]	11
Figure 4. Legend of the geotechnical map of Switzerland, page 1 [41]	20
Figure 5. Legend of the geotechnical map of Switzerland, page 2 [41]	21
Figure 6. Legend of the geotechnical map of Switzerland, page 3 [41]	22
Figure 7. Legend of the geotechnical map of Switzerland, page 4 [41]	23
Figure 8. Legend of the geotechnical map of Switzerland, page 5 [41]	24
Figure 9. Stauffacher Bridge [43]	27
Figure 10. Geo-localisation of Stauffacher Bridge to define its foundation soil [41].....	27
Figure 11. Scaffolding of Stauffacher Bridge [44]	28
Figure 12. Representation of the 3D model of Stauffacher Bridge	29
Figure 13. Zuoz Bridge [43].....	30
Figure 14. Geo-localisation of Zuoz Bridge to define its foundation soil [41]	30
Figure 15. Scaffolding of Zuoz Bridge [46].....	32
Figure 16. Cross sections of Zuoz Bridge	33
Figure 17. Steinach Bridge [43]	34
Figure 18. Steinach Bridge [43]	34
Figure 19. Geo-localisation of Steinach Bridge to define its foundation soil [41]	35
Figure 20. Longitudinal view of Steinach Bridge.....	36
Figure 21. Representation of the 3D model of Steinach Bridge.....	36
Figure 22. Tavanasa Bridge [44]	38
Figure 23. Geo-localisation of Tavanasa Bridge to define its foundation soil [41].....	38
Figure 24. Scaffolding of Tavanasa Bridge [46]	39
Figure 25. Representation of the 3D model of Tavanasa Bridge.....	40
Figure 26. Aarburg Bridge when it was originally built [47].....	42
Figure 27. Aarburg Bridge at present time [43]	42
Figure 28. Geo-localisation of Aarburg Bridge to define its foundation soil [41].....	43
Figure 29. Part of the transversal section of Aarburg Bridge	44
Figure 30. Representation of the 3D model of Aarburg Bridge	44
Figure 31. Marignier Bridge [43]	46
Figure 32. Geo-localisation of Marignier Bridge to define its foundation soil [49].....	46
Figure 33. Representation of the 3D model of Marignier Bridge.....	47
Figure 34. Flienglibach Bridge [43]	49
Figure 35. Geo-localisation of Flienglibach Bridge to define its foundation soil [41]	49
Figure 36. Scaffolding of Flienglibach Bridge [46].....	50

Figure 37. Representation of the 3D model of Flienglibach Bridge	51
Figure 38. Ziggenbach Bridge [43].....	53
Figure 39. Geo-localisation of Ziggenbach Bridge to define its foundation soil [41]	53
Figure 40. Representation of the 3D model of Ziggenbach Bridge	54
Figure 41. Schrärbach Bridge [43].....	56
Figure 42. Geo-localisation of Schrärbach Bridge to define its foundation soil [41]	56
Figure 43. Bidimensional drawings of Schrärbach Bridge.....	58
Figure 44. Representation of the 3D model of Schrärbach Bridge	58
Figure 45. Lorraine Bridge [43]	60
Figure 46. Geo-localisation of Lorraine Bridge to define its foundation soil [41]	60
Figure 47. Scaffolding of Lorraine Bridge [50].....	61
Figure 48. Bidimensional drawings of Lorraine Bridge	62
Figure 49. Representation of the 3D model of Lorraine Bridge.....	62
Figure 50. Salginatobel Bridge [43]	64
Figure 51. Geo-localisation of Salginatobel Bridge to define its foundation soil [41]	64
Figure 52. Scaffolding of Salginatobel Bridge [46].....	65
Figure 53. Representation of the plan of Salginatobel Bridge.....	66
Figure 54. Schwandbach Bridge [43]	68
Figure 55. Geo-localisation of Schwandbach Bridge to define its foundation soil [41]	68
Figure 56. Scaffolding of Schwandbach Bridge [46]	69
Figure 57. Bidimensional drawings of Schwandbach Bridge	70
Figure 58. Representation of the 3D model of Schwandbach Bridge.....	70
Figure 59. Felsegg Bridge [43].....	72
Figure 60. Geo-localisation of Felsegg Bridge to define its foundation soil [41]	72
Figure 61. Scaffolding of Felsegg Bridge [46].....	73
Figure 62. Representation of the 3D model of Felsegg Bridge	74
Figure 63. Birs Bridge [43]	75
Figure 64. Geo-localisation of Birs Bridge to define its foundation soil [41]	75
Figure 65. Representation of the 3D model of Birs Bridge.....	77
Figure 66. Vessy Bridge [43]	79
Figure 67. Geo-localisation of Vessy Bridge to define its foundation soil [41]	79
Figure 68. Internal structure of Vessy bridge [53].....	80
Figure 69. Langwieser Bridge [54].....	82
Figure 70. Geo-localisation of Langwieser Bridge to define its foundation soil [41]	82
Figure 71. Tamina Bridge [55]	85
Figure 72. Geo-localisation of Tamina Bridge to define its foundation soil [41]	85
Figure 73. Absolute GWP of the analysed bridges.....	88

Figure 74. Material quantities of the analysed bridges	89
Figure 75. Material quantities of the analysed bridges apart from Lorraine Bridge.....	89
Figure 76. GWP, with the contribution of each material to the total GWP	90
Figure 77. Normalised GWP per deck area, divided per material	91
Figure 78. Normalised GWP per span	92
Figure 79. Normalised GWP per rise.....	93
Figure 80. GWP due to timber	94
Figure 81. Normalised GWP due to timber, per deck area	95
Figure 82. Percentage of GWP due to timber with respect to the total one	96
Figure 83. Normalised GWP per deck area, divided per structural type.....	97
Figure 84. Amount of steel reinforcement, per structural type.....	98
Figure 85. Percentage of GWP only due to steel over the total one, divided per structural types.....	99
Figure 86. Normalised GWP per deck area, divided in categories of increasing span	101
Figure 87. Normalised GWP per deck area, divided in categories of increasing rise.....	101
Figure 88. Normalised GWP per deck area, divided in categories of increasing length.....	102
Figure 89. Normalised GWP per deck area, divided in categories of increasing width	102
Figure 90. Normalised GWP per deck area, divided in categories of increasing span/rise ratio.....	103
Figure 91. Normalised GWP due to timber per deck area, divided per increasing span/rise ratio	103
Figure 92. Geotechnical map of Switzerland combined with the 15 positions of the chosen bridges	105
Figure 93. Normalised GWP per deck area, divided per soil type	106
Figure 94. Percentage of foundations' concrete with respect to the total one, divided per soil type	106
Figure 95. Positions of the 15 Maillart's bridges and of the two additional ones	108
Figure 96. Normalised GWP per deck area, with the two additional ones	109
Figure 97. Translation of normalised GWP of the bridges into carbon emissions by a car per km	110
Figure 98. Translation of normalised GWP of the bridges into carbon emissions by a car per year.....	111
Figure 99. Translation of normalised GWP of the bridges into carbon absorption by a tree per year.....	112
Figure 100. Translation of normalised GWP of the bridges into carbon absorption by an acre of trees per year	112
Figure 101. Normalized Material Quantities per deck area	120
Figure 102. Normalised GWP per deck area.....	120
Figure 103. Amount of reinforcement steel	121

Equations

Equation 1. Cradle-to-gate GWP [8]	8
Equation 2. Computation of Stauffacher's GWP	29
Equation 3. Computation of Zuoz's GWP	33
Equation 4. Computation of Steinach's GWP	37
Equation 5. Computation of Tavanasa's GWP	41
Equation 6. Computation of Aarburg's GWP	45
Equation 7. Computation of Marignier's GWP	48
Equation 8. Computation of Flienglibach's GWP	52
Equation 9. Computation of Zigggenbach's GWP	55
Equation 10. Computation of Schrähbach's GWP	59
Equation 11. Computation of Lorraine's GWP	63
Equation 12. Computation of Salginatobel's GWP	67
Equation 13. Computation of Schwandbach's GWP	71
Equation 14. Computation of Felsegg's GWP	74
Equation 15. Computation of Birs' GWP	78
Equation 16. Computation of Vessy's GWP	81
Equation 17. Computation of Langwieser 's GWP	84
Equation 18. Computation of Tamina's GWP	87
Equation 19. Normalisation criterion of GWP per deck area	90
Equation 20. Normalisation criterion of GWP per span	92
Equation 21. Normalisation criterion of GWP per rise	92

References

- [1] R. Maillart, *Pläne, Berechnungen, Photographien, Akten*, ETH-Bibliothek, Archives and Private Collections. Maillart collection HS 1085.
- [2] [Online]. Available: https://www.kbob.admin.ch/kbob/it/home/publikationen/nachhaltiges-bauen/oekobilanzdaten_baubereich.html. [Accessed 10 October 2018].
- [3] D. P. Billington, H. Shirley-Smith and al., *Bridge - Reinforced concrete - Maillart's innovations*, Encyclopaedia Britannica, 2019.
- [4] D. Zastavni, *Maillart's Design Methods and Sustainable Design*, vol. 96, I. Congress, Ed., Bangkok: 33rd Iabse International Symposium "Sustainable Infrastructure: Environmental Friendly, Safe and Resource Efficient", 2009, pp. 17-18.
- [5] *ISO 14040 LCA*.
- [6] C. Fivet and C. De Wolf, *Introduction & Overview*, Ecole Polytechnique Fédérale de Lausanne, Building Design in the Circular Economy, 2018.
- [7] R. J. Bianquis, *Assessment methodology for environmental impact of bridges*, MIT, Ed., Boston: Department of civil and environmental engineering, 2015.
- [8] C. De Wolf, *Low Carbon Pathways for Structural Design*, MIT, Ed., Boston: Department of Architecture, 2017.
- [9] [Online]. Available: <https://www.epa.gov/ghgemissions/understanding-global-warming-potentials>. [Accessed 23 May 2019].
- [10] T. C. E. Dequitt, *Life Cycle Assessment of a Norwegian Bridge*, D. o. C. a. T. Engineering, Ed., Norwegian University of Science and Technology, 2015.
- [11] G. Du, *Life cycle assessment of bridges, model development and case studies*, Stockholm: KTH Architecture and the Built Environment In G. Du, Life cycle assessment of bridges, model development and case studies, 2015.
- [12] C. Zhang, *Environmental evaluation of FRP in UK highway bridge deck replacement applications based on a comparative LCA study*, Advanced Materials Research In Dequitt, T. C. E. Life Cycle Assessment of a Norwegian Bridge, 2011, pp. 374-377:43–48.
- [13] J. Hammervold e et al., *Environmental life-cycle assessment of bridges*, Journal of Bridge Engineering In Dequitt, T. C. E. Life Cycle Assessment of a Norwegian Bridge, 2011.

- [14] Z. Lounis e e. al., *Towards sustainable design of highway bridges*, National Research Council of Canada In Dequit, T. C. E. Life Cycle Assessment of a Norwigan Bridge, 2010.
- [15] L. Bouhaya, L. Le Roy e A. Feraille-Fresnet, *Simplified environmental study on innovative bridge structure*, Environ. Sci. Technol. In Dequit, T. C. E. Life Cycle Assessment of a Norwigan Bridge, 2009, p. 2066–2071.
- [16] H. Gervásio e L. S. Da Silva, *Comparative life-cycle analysis of steel-concrete composite bridges*, Structure and Infrastructure Engineering, 2008, p. 251–269.
- [17] D. Collings, *An environmental comparison of bridge forms*, vol. 159, Bridge Engineering. Issue BE4 In Dequit, T. C. E. Life Cycle Assessment of a Norwigan Bridge, 2006.
- [18] MEEDDM, *Analyse du cycle de vie d'un pont en béton*, In Dequit, T. C. E. Life Cycle Assessment of a Norwigan Bridge, 2006.
- [19] K. Steele, *Environmental sustainability for bridge management.*, Bridge Management 5 In Dequit, T. C. E. Life Cycle Assessment of a Norwigan Bridge, 2005.
- [20] G. A. Keoleian, A. Kendall, J. E. Dettling, V. M. Smith, R. F. Chandler, M. Lepech e V. C. Li, *Life cycle modelling of concrete bridge design: Comparison of engineered cementitious composite link slabs and conventional steel expansion joints. Jour*, vol. 51, Journal of Infrastructure Systems, ASCE In Dequit, T. C. E. Life Cycle Assessment of a Norwigan Bridge, 2005.
- [21] Martin, *Concrete bridges in sustainable development*, Proceedings of the ICE In Dequit, T. C. E. Life Cycle Assessment of a Norwigan Bridge, 2004.
- [22] Y. Itoh e e. al., *Using CO2 emission quantities in bridge life cycle analysis*, vol. 25, Engineering Structures In Dequit, T. C. E. Life Cycle Assessment of a Norwigan Bridge, 2003, p. 565–577.
- [23] A. Horvath e e. al., *Steel versus steel-reinforced concrete bridges: Environmental assessment*, Journal of Infrastructure Systems, ASCE In Dequit, T. C. E. Life Cycle Assessment of a Norwigan Bridge, 1998.
- [24] J. Widman., *Environmental impact assessment of steel bridges*, vol. 46, Journal of Constructional Steel Research, Elsevier In Dequit, T. C. E. Life Cycle Assessment of a Norwigan Bridge, 1998, p. 291–293.
- [25] G. Du, M. Safi, L. L. Pettersson e R. Karoumi, *Life cycle assessment as a decision support tool for bridge procurement: environmental impact comparison among five design proposals*, vol. 1, International Journal of Life Cycle Assessment In G. Du, Life cycle assessment of bridges, model development and case studies, 2014.

- [26] M. Safi, G. Du, R. Karoumi e H. Sundquist, *Holistic approach to sustainable bridge procurement considering LCC, LCA, User-cost and Aesthetics*, 2015.
- [27] G. Du, L. L. Pettersson e R. Karoumi, *Life cycle environmental impact of two commonly used short span bridges in Sweden*, In G. Du, *Life cycle assessment of bridges, model development and case studies*, 2015.
- [28] G. Du e R. Karoumi, *Environmental life cycle assessment comparison between two bridge types: reinforced concrete bridge and steel composite bridge*, 3rd International conference on Sustainable Construction materials and Technologies (SCMT3) In G. Du, *Life cycle assessment of bridges, model development and case studies*, 2013.
- [29] G. Du e R. Karoumi, *Environmental comparison of two bridge alternative designs*, Stockholm: fib symposium Stockholm, Concrete Structure for Sustainable Community In G. Du, *Life cycle assessment of bridges, model development and case studies*, 2012, pp. 353-356.
- [30] G. Du, *A literature review of life cycle assessment for bridge infrastructure*, Malta: COST Action C25: Sustainability of Constructions: An Integrated Approach to Life-time Structural Engineering In G. Du, *Life cycle assessment of bridges, model development and case studies*, 2010.
- [31] [Online]. Available: <https://www.atlasofplaces.com/architecture/>. [Accessed 19 June 2019].
- [32] D. P. Billington, *Robert Maillart's Bridges: The art of engineering*, Princeton - N.J.: Princeton University Press, 1979.
- [33] D. Billington, *The revolutionary Bridges of Robert Maillart*, vol. 283, Scientific American, a division of Nature America, Inc., 2000.
- [34] D. Zastavni, *What Ideas Does Maillart's ighty-Year-Old Approach Give Us About How A Concrete Structure Could Be Designed in the 21st Century*, Valencia: Association for Shell and Spatial Structures (Iass) Symposium, 2009.
- [35] D. Zastavni, *Maillart's Practices for Structural Design [ETH- Bibliothek's Virtual Exhibition]*, Louvain-la-Neuve: Université catholique de Louvain, 2012.
- [36] D. Zastavni, *What Was Truly Innovative About Maillart's Designs Using Reinfroced Concrete?*, Proceedings of The Thrid International Congress on Contruction History, 2009.
- [37] C. Fivet and D. Zastavni, *Purely Geometrical Considerations Durign the Design of Bridges in th Early 20th Century - The case of R. Maillart*, First ed., vol. 3, Chicago: 5th International Congress on Construction History. In B. Bowen, D. Friedman, T. Leslie and J. Ochsendorf Proceedings, 2015, pp. 637-644.

- [38] E. P. G. Bruun, *Robert Maillart: The Evolution of Reinforced Concrete Bridge Forms*, Calgary, Alberta: 9th International Conference on Short and Medium Span Bridges, 2014.
- [39] J. Schlaich, *The Bridges of Robert Maillart.*, vol. 15, Concrete International, 1993, pp. 30-36.
- [40] M. Laffranchi and P. Marti, *Robert Maillart's Curved Concrete Arch Bridges*, Journal of Structural Engineering 123(10), 1997, pp. 1280-1286.
- [41] [Online]. Available: <https://map.geo.admin.ch/>. [Accessed 10 October 2018].
- [42] J. Brutting and et al., *The reuse of loading-bearing components.*, IOP Conference Series: Earth and Environmental Science, 2019.
- [43] [Online]. Available: <https://structurae.net/>. [Accessed 10 October 2018].
- [44] R. Sangree e e. al., *Robert Maillart and the Origins of Reinforced Concrete*, Johns Hopkins University - University of Massachusetts, Perspectives on the evolution of structures (9th lecture), 2018.
- [45] W. Ritter, *Consultation on the Design of Stauffacher Bridge in Zürich*, PMA In Billington, B. P., Robert Maillart's Bridges: The Art of engineering, 1898, p. 1.
- [46] [Online]. Available: <http://www.swiss-timber-bridges.ch/>. [Accessed 10 October 2018].
- [47] M. Garlock, *Aarburg Bridge*, edX, The Art of structural Engineering: Bridges In Dequit, T. C. E. Life Cycle Assessment of a Norwigan Bridge, 2018.
- [48] [Online]. Available: <http://scihi.org/robert-maillart-structural-reinforced-concrete/>. [Accessed 23 May 2019].
- [49] [Online]. Available: <https://www.geoportail.gouv.fr/donnees/cartes-geologiques>. [Accessed 8 March 2019].
- [50] [Online]. Available: <https://www.bern.ch/politik-und-verwaltung/stadtverwaltung/tvs/tiefbauamt/150-jahre-tab/historische-aufnahmen#bildergalerie>. [Accessed 23 May 2019].
- [51] D. Zastavni and C. Fivet, *Robert Maillart's Key Methods from Salginatobel Bridge Design Process (1928)*, Journal of the international association for Shell and Spatial structures: J. Iass, 2012.
- [52] *Norme Tecnica per le Costruzioni - D.M.*, 2008.
- [53] [Online]. Available: <https://www.pinterest.ch>. [Accessed 23 May 2019].
- [54] [Online]. Available: https://de.wikipedia.org/w/index.php?title=Langwieser_Viadukt&oldid=184206005. [Accessed 23 May 2019].

- [55] [Online]. Available: https://www.nemetschek.com/en/collaboration-par-excellence/tamina-bridge/?tx_news_pi1%5Bcontroller%5D=News&tx_news_pi1%5Baction%5D=detail. [Accessed 23 May 2019].
- [56] [Online]. Available: <https://blog.allplan.com/en/tamina-bridge>. [Accessed 23 May 2019].
- [57] H. Haug, *Leap of faith*, Bd&e. Issue 86, 2017.
- [58] H. Haug e F. Striebel, *Taminabrücke: Bauausführung der größten Bogenbrücke in der Schweiz*, vol. 95, Bautechnik, 2018, pp. 157-166.
- [59] V. Angelmaier, *The Tamina Canyon crossing near Pfäfers*, 2017.
- [60] [Online]. Available: <http://www.sia.ch/it/la-sia/la-sia/storia/>. [Accessed 23 May 2019].
- [61] [Online]. Available: <https://eurocodes.jrc.ec.europa.eu/showpage.php?id=12>. [Accessed 23 May 2019].
- [62] [Online]. Available: <https://www.epa.gov/greenvehicles/greenhouse-gas-emissions-typical-passenger-vehicle>. [Accessed 23 May 2019].
- [63] [Online]. Available: <http://urbanforestrynetwork.org/benefits/air%20quality.htm>. [Accessed 23 May 2019].
- [64] R. Maillart, *Report for a bridge over the Inn near Zuoz designed as an arch bridge of reinforced concrete*, In Billington, D. P., Robert Maillart's bridges: The art of engineering ed., Zürich: PMA, 1900, p. 2.
- [65] E. Mörsch, *Concrete-Steel Construction*, In Billington, D. P., Robert Maillart's bridges: The Art of Engineering ed., Engineering News Pub. Co. 1910., 1902, p. 279.
- [66] D. Zastavni, *The Structural Design of Maillart's Chiasso Shed (1924): A Graphic Procedure*, vol. 18, Structural Engineering International , 2008, pp. 247-252.
- [67] Allplan Engineering, *An exciting path across the gorge: the Tamina Bridge in the Canto of St. Gallen*, 2017.
- [68] F. Giovannardi, *Robert Maillart e l'emancipazione del C.A.*, 2017.
- [69] [Online]. Available: <https://www.carbondeqo.com/>. [Accessed 10 October 2018].
- [70] [Online]. Available: <https://www.kbob.admin.ch/>. [Accessed 10 October 2018].
- [71] [Online]. Available: <https://www.reteclima.it/l-albero-mangia-la-co2/>. [Accessed 23 May 2019].
- [72] [Online]. Available: https://en.wikipedia.org/wiki/Clastic_rock#Sedimentary_breccias. [Accessed 19 June 2019].

